FRANCISCO JAVIER VEGA PIEDRAS

HYDROMETALLURGICAL APPROACH FOR RECOVERY OF PGMS FROM SPENT AUTOMOBILE CATALYTIC CONVERTERS

MESTRADO ERASMUS MUNDUS EM INOVAÇÃO QUÍMICA E REGULAMENTAÇÃO

ERASMUS MUNDUS MASTER'S IN CHEMICAL INNOVATION AND REGULATION

Trabalho efetuado sob a orientação de / Work supervised by:

ANA PAULA PAIVA PhD
MARIA CLARA COSTA PhD

Faculdade de Ciências e Tecnologia
2019

Declaration of Authorship,

Hereby, I declare I am the author of this work, which is original and unpublished. Authors and works consulted are properly cited in the text and listed in the list of references included.

_____

Francisco Javier Vega Piedras

ACKNOWLEDGMENTS

First and foremost, I would like to express my deepest gratitude to Professor Ana Paula Paiva for her guidance, knowledge, and patience through all this process. A special gratitude note should be given to Dr. Carlos Nogueira, from the Laboratório Nacional de Energia e Geologia, because he was a fundamental pillar during the first stage of my project; he allowed me to work by his side, and together with his institution, helped me to learn more about hydrometallurgy and leaching techniques, in which he is an expert. To both I am very grateful for allowing me to develop my own vision of where I would like to lead the research, thus, giving me the opportunity to expand my knowledge regarding air pollution and critical raw materials regulations. Their mentorship was a key role in expanding my knowledge horizons and growing as a scientist, they answered all my raising questions and guided me down the right path.

I would also like to express my gratitude to the University of Barcelona and the University of Lisbon for being my home during the last two years; also my gratitude to Professor Maria Clara Costa, from the University of Algarve, for the opportunity of letting me come to Lisbon to perform my work.

To Rosalia, my mother, all of this is only possible because of you. Thank you for the gift of life, for your support during all these years and for all your love; to Joaquín, my father, thank you for all your support and guidance. To Sher, for being not only my sister but also my best friend, confidant, and conscience whenever I needed it. My special and loving thanks to Thomas, my heartmate, thank you for being in my life and for all you give me every day, you are the way in which the universe told me how happiness looks like. You guys are the best family somebody could have.

To my family and friends in Mexico, for all your support, love and encouragement, and for keeping a place in your lives for me, despite time and distance. My individual mention to Ale, Rosa and Andie, thank you for these 12 years together and for many more to come. Also, to my ChIR-mates, special shout out to Kateryna and Maciej, I was so lucky meeting you guys, and that we could share so many memories together. This would have not been the same without you, I am pretty sure there will be much more of us in the future.

A special mention to Cris, Rafa and all my Brazilian friends, you not only taught me the Portuguese language but also made me love Brazil already. And in general, to all and every single person I met during this journey for making me love, laugh, enjoy, grow and find my home on this other side of the world; all of you made these last two years one of the best times in my entire life.

Finally, my deepest gratitude to the European Commission, which through the EMMC-ChIR study grant helped me to accomplish one of my dreams in life.

Me das tanto, Vida.
Francisco Javier V. Piedras, Lisboa, 2019.

ABSTRACT

The recovery of platinum-group metals (PGMs) from secondary sources, such as spent devices like automobile catalytic converters (ACC), has been gaining interest in the last decades due to their scarcity in the earth crust and their high demand. Their extended applications among different industries, together with their difficulty to be replaced by other materials, has created the urge to develop new technologies for PGMs recovery that can help with the supply requirements, while being environmentally friendlier than the existing processes. Hydrometallurgical techniques represent a possible strategy to recover PGMs and avoid the high energy consumption of smelting processes in pyrometallurgical plants.

In this study, a hydrometallurgical approach was adopted, starting with a leaching step for the solubilization of the metals into an aqueous phase, employing the use of an oxidizing agent for the formation of metal chlorocomplexes, thus facilitating their dissolution; after this, the recovery of PGMs was intended by using a solvent extraction (SX) step with appropriate extractants, to transfer the selected metals into a more purified aqueous phase, from which the PGMs recovery and transformation into forms with commercial interest would be easier.

Two spent ACCs were collected (H98 and I95), and their initial metal compositions were evaluated by an X-ray fluorescence (XRF) analysis. Two different elemental compositions were found, leading to a separate treatment of each sample. In the first stage of the work, the leaching process, the most relevant variables such as temperature (°C), acid concentration (M), L/S ratio (L/kg), time (h), stirring (min^{-1}) and particle size (mm) were evaluated experimentally and through a factorial design methodology (FDM), to establish the individual and joint contributions of the relevant parameters to the leaching efficiency. As a result, the optimised conditions for the leaching of both catalyst samples were T= 60 ºC, [HCl]= 11.6M, L/S= 2L/kg, t= 3h, stirring= 250 min^{-1}, and particle sizes D_p=0.397mm and D_p=0.409mm for H98 and I95, respectively. The FDM treatment showed that time represented the most determinant parameter in terms of leaching efficiency for the H98 sample. For the I95, time, temperature, acid concentration, and the pair time-temperature

were the main interactions to be considered, according to the FDM, in order to obtain a higher efficiency of the leaching process.

For the second step, the SX, four commercial compounds and/or mixtures (tributyl phosphate (TBP), Cyanex® 471X, trioctylphosphine oxide (TOPO) and Adogen® 464), and one ionic liquid (Cyphos® 101), were employed as extractants, using toluene as diluent. The concentrations of each extractant were calculated according to the concentration of the targeted metals in the solutions.

The first part of the SX step was the development of a scheme for each sample using model solutions, prepared with the metals expected to be in higher concentrations in the real leaching solutions obtained.

The results achieved with the model solutions showed that the appropriate SX scheme, when using traditional extractants, would involve an approximate 6M HCl concentration for the aqueous phases and the use of TBP to remove Fe(III) in the first extraction, followed by an extraction with Cyanex® 471X to remove Pd(II). In the third extraction, TOPO could be used to remove Pt(IV), and the final extraction could be carried out with Adogen® 464 to remove Rh(III). The above loaded organic phases were subjected to a stripping procedure, to transfer the metals to new aqueous phases and to evaluate the reusability of the organic solutions. The stripping agents chosen were: a 0.1M HCl solution to strip Fe(III) from TBP, a stabilized 1M $Na_2S_2O_3$ solution to strip Pd(II) from Cyanex® 471X, and a 0.4M malonic acid solution to strip Pt(IV) from TOPO. Due to the low content of Rh(III) in the solutions, the decision of not stripping this metal from Adogen® 464 was taken.

Regarding the application of the ionic liquid Cyphos® 101 for the SX of the model solutions, it was found that Pd(II), Pt(IV) and Fe(III) were quantitatively extracted from both 3M and 6M HCl solutions. Two stripping agents were tested, e.g., a 0.1M KSCN to remove Pt(IV), and a 0.1M CH_4N_2S in 5% v/v HCl to strip Pd(II).

Finally, the SX schemes previously developed were tested in the real leaching solutions for each catalyst, and a completely different behavior was found. The extraction and stripping efficiencies were very low compared to the results from the model solutions. This unexpected behavior is attributed to the complexity of the real leaching solutions, to the

large number of metals involved that were not considered for the composition of the model solutions, and to possible interactions of the extractants with those unanalysed metals

Keywords:

PGMs, catalytic converters, hydrometallurgy, leaching, solvent extraction.

RESUMO

A recuperação de metais do grupo da platina (PGMs) de fontes secundárias, particularmente a partir dos dispositivos usados como conversores catalíticos em automóveis (ACC), tem vindo a ganhar expressão nas últimas décadas, devido à escassez destes metais na crosta terrestre e ao facto de serem muito solicitados. Para além dos ACCs, as aplicações dos PGMs estendem-se a diferentes áreas; por exemplo, os PGMs estão presentes na composição de catalisadores para processos petroquímicos e de refinação de petróleo, na indústria farmacêutica, sendo também frequentes em componentes da indústria eletrónica e em biomedicina, particularmente sob a forma de medicamentos para tratamento de cancro. Atendendo à dificuldade de serem substituídos por outros materiais, a utilização crescente dos PGMs potenciou o desenvolvimento de novas tecnologias para a sua recuperação a partir de materiais em fim de vida, e que, simultaneamente, contribuem para aumentar o seu suprimento global e que são usualmente mais amigáveis sob o ponto de vista ambiental do que a generalidade dos processos existentes. As técnicas hidrometalúrgicas representam uma possível estratégia para recuperar PGMs, pois são em geral mais “amigas do ambiente” e a sua utilização evita o alto consumo de energia dos processos de fundição típicos das instalações pirometalúrgicas.

Neste estudo adotou-se uma abordagem hidrometalúrgica. A investigação iniciou-se com uma etapa de lixiviação para a solubilização dos PGMs numa fase aquosa, empregando-se um agente oxidante para promover a formação de clorocomplexos metálicos, facilitando a sua dissolução; em sequência, a recuperação de PGMs foi planeada recorrendo à etapa de extração por solventes (SX), com extratantes apropriados, para transferir os metais selecionados para uma fase aquosa mais purificada, a partir da qual a recuperação e transformação dos PGMs em formas com interesse comercial seriam facilitadas.

Foram recolhidos dois ACCs usados (H98 e I95), e as suas composições metálicas iniciais foram avaliadas por uma análise de fluorescência de raios-X (XRF). Devido ao facto das duas composições elementares serem significativamente diferentes, procedeu-se a tratamentos separados para as duas amostras. Na primeira etapa do trabalho, as

variáveis mais relevantes para a eficiência do processo de lixiviação, tais como a temperatura (° C), concentração de ácido (M), relação L / S (L / kg), tempo (h), agitação (min^{-1}) e tamanho de partícula (mm) foram avaliadas experimentalmente e por meio de uma metodologia de planeamento fatorial (FDM), para estabelecer as contribuições individuais e conjuntas dos parâmetros relevantes. Teve-se como objetivo maximizar as concentrações de PGMs em solução mas, simultaneamente, minimizar as concentrações dos metais considerados como principais contaminantes no processo, nomeadamente, alumínio e cério. Como resultado, as condições otimizadas para a lixiviação das amostras de catalisador foram semelhantes para os dois casos, a saber: T= 60 ºC, [HCl]= 11,6M, L / S= 2L / kg, t= 3h, agitação= 250 min^{-1} e tamanhos de partícula D_p= 0,397 mm e D_p= 0,409 mm para H98 e I95, respetivamente. O tratamento com a metodologia FDM mostrou que o tempo representou ser o parâmetro mais determinante em termos de eficiência de lixiviação para a amostra H98. Para a amostra I95, o tempo, temperatura, concentração de ácido e o par tempo-temperatura foram as principais interações encontradas, que mostraram ser as mais influentes para se obter uma maior eficiência do processo de lixiviação, de acordo com o FDM.

Para o segundo passo, a etapa de SX, quatro compostos comerciais e / ou misturas (fosfato de tributilo (TBP), Cyanex® 471X, óxido de trioctilfosfina (TOPO) e Adogen® 464), e um líquido iónico (Cyphos® 101), foram testados como extratantes, utilizando-se tolueno como diluente. As concentrações usadas de cada extratante foram calculadas de acordo com a concentração dos metais alvo a recuperar nas respetivas soluções de lixiviação.

A primeira parte desta segunda etapa consistiu no desenvolvimento de um esquema de SX para cada amostra recorrendo a soluções modelo, que foram preparadas com os metais que se espera estarem em concentrações mais altas nas soluções de lixiviação reais obtidas, ou seja, os PGMs e também os principais contaminantes: Al(III), Ce(III) e Fe(III).

Os resultados obtidos com as soluções modelo mostraram que o esquema SX mais apropriado, ao usar extratantes tradicionais, envolveria uma concentração aproximada de 6M HCl para as fases aquosas e o uso de TBP para remover Fe(III) na primeira

extração, seguindo-se uma extração com Cyanex® 471X para remover o Pd(II). Na terceira extração, o TOPO poderia ser usado para remover Pt(IV), e a extração final poderia ser realizada com Adogen® 464 para remover o Rh(III). As fases orgânicas carregadas acima obtidas foram em seguida submetidas a um processo de reextração, para transferir os metais para novas fases aquosas e para avaliar a capacidade de reutilização das soluções orgânicas. Os agentes de reextração escolhidos foram: uma solução 0,1M de HCl para remover o Fe(III) do TBP, uma solução estabilizada de $Na_2S_2O_3$ 1M para remover o Pd(II) do Cyanex® 471X, e uma solução de ácido malónico 0,4M para remover a Pt(IV) do TOPO. Devido ao baixo conteúdo de Rh(III) nas soluções, foi tomada a decisão de não se testar a reextração deste metal do Adogen® 464.

Em relação ao teste do líquido iónico Cyphos® 101 para a SX das soluções modelo, verificou-se que o Pd(II), a Pt(IV) e o Fe(III) foram quantitativamente extraídos das soluções de HCl 3M e 6M. Foram testados dois agentes de reextração, nomeadamente, KSCN 0,1 M para remover a Pt(IV) e CH_4N_2S 0,1 M em HCl a 5% v/v para retirar o Pd(II).

Finalmente, os esquemas SX previamente desenvolvidos foram testados nas soluções de lixiviação reais, em separado para cada catalisador, tendo-se verificado comportamentos completamente diferentes relativamente aos anteriormente conseguidos. Com efeito, as eficiências de extração e de reextração dos PGMs foram muito baixas quando comparadas com os resultados obtidos para as soluções modelo. Estes comportamentos inesperados são atribuídos à complexidade das soluções de lixiviação reais, ao grande número de metais envolvidos que não foram considerados para a composição das soluções modelo (por exemplo, neodímio, lantânio, cálcio, magnésio, zinco, zircónio) e às possíveis interações dos extratantes com esses metais não analisados.

Palavras-chave:

PGMs, catalisadores, hidrometalurgia, lixiviação, extração por solventes.

Todo tiene su tiempo y todo lo que se quiere,

debajo del cielo encuentra su hora.

Eclesiastés 3:1

The cure for everything is always salty water:

the tears, the sweat or the sea.

- *Karen Blixen*

No podem escriure en l'aigua, no podem tallar l'aigua.

La naturaleza de l'aigua és fluir, és així com hauríem

de tractar la vida.

- *Joan Anderson, un any al costat del Mar*

"O que hoje não sabemos, amanhã saberemos"

- *Garcia de Orta (1563), FCUL*

TABLE OF CONTENTS

LIST OF TABLES

LIST OF FIGURES

LIST OF ABBREVIATIONS

%E: Percentage of extraction

A/O: Aqueous/organic volume ratio

ACC: Automobile catalyst converter

ANOVA: Analysis of variance

B.S.: Bottleneck screening

CAA: Clean air act

CARB: California air resources board

CL: Confidence level

CLP: Classification, labelling and packaging information

CRM: Critical raw materials

CRML: Critical raw material list

DF: Degrees of freedom

DI: Direct ignition

DRC: Democratic republic of Congo

E.I.: Economic importance

E.R.: Export restrictions

E_a: Activation energy

EC: European Commission

ECC: European consumer centres

EI: Economic Importance

EOL-RIR: End-of-life recycling input rate

EPA: Environmental protection agency

EU: European Union

FDM: Factorial design methodology

H98: Spent automobile catalyst converter from a Honda Civic model 1998

HCHO: Formaldehyde

HCs: Unburned hydrocarbons

I.R.: Import reliance

I95: Spent automobile catalyst converter from a Seat Ibiza model 1995

ICE: Internal combustion engines

ICP-AES: Inductively coupled plasma-atomic emission spectrometry

ILs: Ionic liquids

L/S: Liquid-solid ratio

LLE: Liquid-liquid extraction

MS: Mean square

NAAQS: National ambient air quality standards

NMHC: Non-methane hydrocarbon emissions

NMOG: Non-methane organic gases

NO_x: Nitrogen oxides

NRMM: Non-road mobile machinery

PGMs: Platinum group metals

R.I.R.: End of life-recycling input rate

RMI: Raw materials initiative

rpm: Revolutions per minute

S.R.: Supply risk

SS: Sum of squares

SX: Solvent extraction

TBP: Tributyl phosphate

TOPO: Trioctylphosphine oxide

TWC: Three-way catalytic converter

US: United States of America

VOCs: Volatile organic compounds

XRF: X-ray fluorescence

AIMS OF THE STUDY

The main objective of the present work is the development of a hydrometallurgical methodology for the recovery of platinum group metals (PGMs), namely Pt, Pd and Rh, from secondary sources, such as spent automobile catalysts, using hydrochloric acid in the leaching step and adequate extractants for the solvent extraction stage.

The above-mentioned methodology will be assessed, in terms of its recovery efficiency, as a contribution to a possible alternative for increasing the Recycling Input Rate of PGMs described in the Critical Raw Material List (CRML) of the European Union (EU) in 2017; therefore, a brief explanation of the CRM's methodology is presented, for a clearer understanding of the urge of recycling PGMs.

BOUNDARIES OF THE STUDY

This study is conducted within the boundaries of the hydrometallurgy knowledge disclosed in the literature, using HCl media for the leaching step, with an evaluation of the effects caused by the different leaching parameters on the efficiency of the process, such as liquid/ solid ratios, temperature, acid concentration, and particle size.

The selection of the extractant agent in the solvent extraction step will be done among commercial compounds found in the market, to facilitate the industrial applicability of this methodology.

INTRODUCTION

1. INTRODUCTION

1.1 Background of the study

1.1.1 Automobile industry: a brief historical description

The story of the motor vehicles is big and vast, with its first attempts during the 15th century, with the sketches of the first motor-engine impulse vehicle by Leonardo Da Vinci (Motorfull, 2007), and being consecrated in 1886, when the German engineer Karl Benz patented the first motor vehicle that constituted the beginning of the modern automobile industry. This latter invention involved a mono-cylindrical engine of 4 strokes and achieved a maximum speed of 16 km/h (Autocosmos, 2017).

The 20th century brought countless developments and established the industry as one of the most important and solid businesses worldwide. Having a healthy automobile industry became the flag of development, wellness, and growth for a country. Cars turned to be not only a transportation mean but also an article of personal expression (Gao et al. 2014). This made vehicles grow exponentially in popularity, an example of this is the over 32 million car units sold worldwide before the Great Depression of 1929, with the US as the producer of 90% of them, and with a national ratio of 1 car per 4.87 citizens (Science, 1929). The car industry has experienced a continuous annual growth rate of about 3% and placed over one billion vehicles on worldwide roads by 2010 (Sousanis, 2011). Vehicles are distributed inequality around the globe, with a bigger concentration in the developed countries (Gao et al. 2014) as can be appreciated in Figure 1.1.

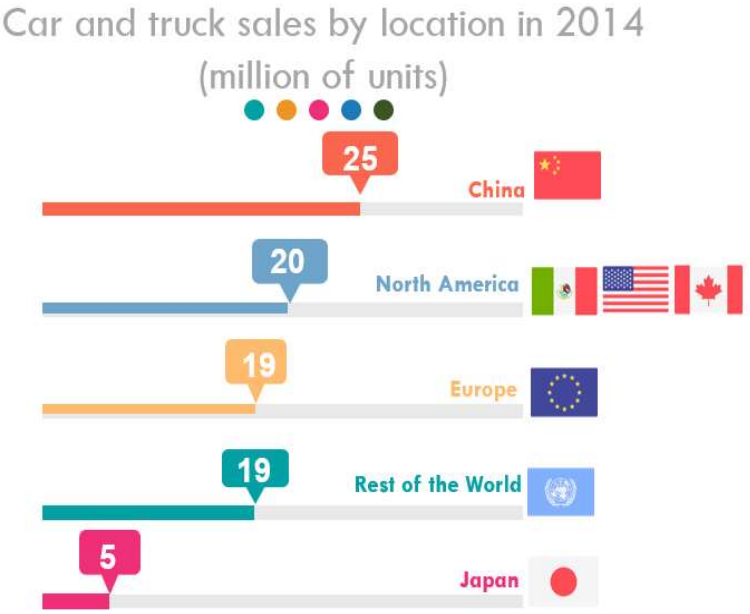

Figure 1.1 Car and truck sales by location in 2014, own drawing.

Aside from the notorious economic development, a big concentration of vehicles also reflects other factors such as high consumption of resources, need of fuel, dependence on roadway networks, parking spaces, and most importantly, a high concentration of air pollutants and exhaust gases that can enhance the greenhouse effect and bring public health problems in those zones.

To mitigate the negative effects of vehicles, the governments around the globe have specific air-pollution regulations regarding the emissions from vehicles. These regulations are based on strict emission limits; to comply with them, car manufacturers rely on a specific device, the automobile catalytic converter (ACC). ACCs transform the exhaust gases into less harmful emissions. This task implies the use of specific chemical elements, such as the platinum group metals (PGMs) for the transformation of the air pollutants.

1.2 Regulatory framework

This section describes and compares the US and EU regulations for the emissions of air pollutants from vehicles. The description is made based on the emission limits that car manufacturers should meet to guarantee a low impact in the air quality.

1.2.1 United States' regulatory framework in air pollution

To talk about the European regulatory framework in air pollution as we know it today, it is necessary to discuss the pioneer regulation system developed by the US government through their Clean Air Acts (CAA) (U.S. Environmental Protection Agency, 1999) and their amendments over time. The most important dates and facts of this system are shown in the timeline of Figure 1.2.

This system recognizes seven principal air pollutants to be controlled, together with their major emission sources (Table 1.1) (U.S. Environmental Protection Agency, 1999):

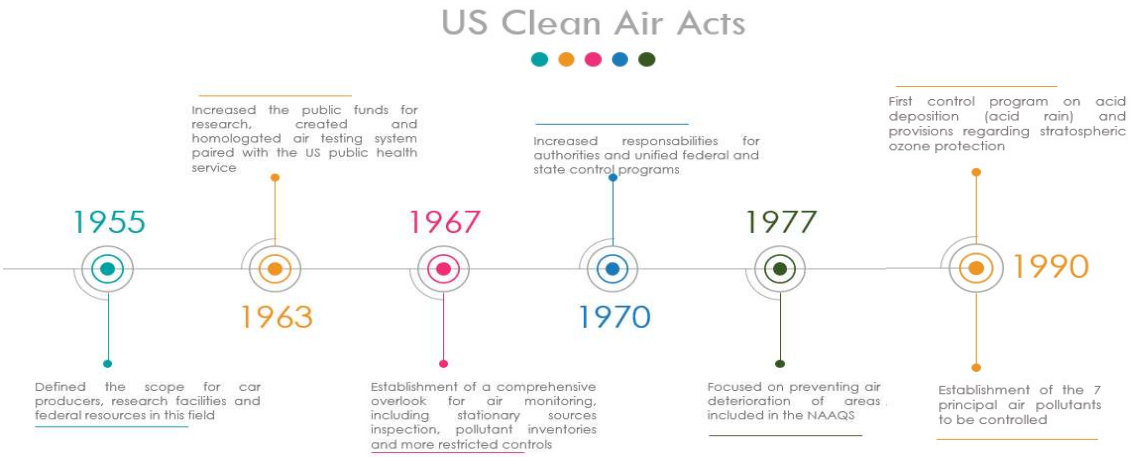

Figure 1.2 Timeline of the US Clean Air Acts, own drawing.

1. Volatile organic compounds (VOCs)
2. Unburned hydrocarbons (HCs)
3. NO_x, nitrogen oxides
4. SO_2, sulfur dioxide, responsible for the acid rain
5. CO, carbon monoxide
6. Primary PM_{10}, particulate matter with a diameter of 10 micros or less, and
7. Primary $PM_{2.5}$, fine particulate matter

Table 1.1 Major emission sources in the US

Source Category	Examples
Industrial point sources	Boilers, cement kilns, heaters and turbines
Utilities	Facilities to produce electricity
Non-road engines/vehicles	Aircraft, construction equipment, garden tools, locomotives, marine engines
Motor Vehicles	Buses, cars, trucks, and engines that operate in roads and/or highways
Area sources	Agricultural tools, dry cleaners, open burning of wastes and wildfires

In 1990, an emissions calculation and projections for 2000 and 2010 were performed for the five emission sources. The contributions and projections[1] from motor vehicles are shown in Table 1.2 (U.S. Environmental Protection Agency, 1999).

Table 1.2 Motor vehicle emission contributions for the 1990 CAA		
Pollutant	**1990 base-year (thousand tons)**	**2000 projection (thousand tons)**
VOC	6,800	7,300
NO_X	7,400	9,100
SO_2	570	770
CO	62,00	66,00
Primary PM_{10}	360	300
Primary $PM_{2.5}$	290	230

The 1990 CAA established the emissions limits for internal combustion engines (ICE) under average driving conditions (cold start, after the engine ignites for 8h; hot start and a combination of urban and highway roads) as follows:

- Non-methane hydrocarbon emissions (NMHC): 0.125 g/mile,
- CO emissions: 1.7 g/mile,
- NO_x emissions: 0.2 g/ mile,
- Catalyst durability: at least 100,000 miles.

To complete the American regulatory framework, in 1999, the California Air Resources Board (CARB) introduced the following classification of vehicles and emission limits for vehicles to be sold in California:

- Tier 1 (progressively Tier 2 and Tier 3)
- TLEV: Transitional Low Emission Vehicles
- LEV: Low Emission Vehicles
- ULEV: Ultra Low Emission Vehicles
- SULEV: Super Ultra Low Emission Vehicles, and
- ZEV: Zero Emission Vehicles

[1] In the EPA report, emissions projection for 2010 are not given; therefore, they are also not shown in this table.

Table 1.3 provides a comparison between the emission limits from the CAA and the CARB after 1999 (DieselNet, 2013b).

Table 1.3 CARB emission limits according to the vehicle category										
Category	**50,000 miles/5 years (g/mile)**					**100,00 miles / 10 years (g/mile)**				
	NMOG	**CO**	**NOx**	**PM**	**HCHO**	**NMOG**	**CO**	**NOx**	**PM**	**HCHO**
Tier 1	0.25	3.4	0.4	0.08	-	0.31	4.2	0.6	-	-
TLEV	0.125	3.4	0.4	-	0.015	0.156	4.2	0.6	0.08	0.018
LEV	0.075	3.4	0.2	-	0.15	0.090	4.2	0.3	0.08	0.018
ULEV	0.040	1.7	0.2	-	0.008	0.055	2.1	0.3	0.04	0.011

Together, CARB and CAA requirements represent the basis for the other international air pollution politics and influenced the development of the European regulatory framework in air pollution.

1.2.2 European Union's regulatory framework in air pollution

After the establishment of the American system, and to solve the resistance from certain European countries towards the dispositions of the ACCs, in 1992, the Directive 91/441/ECC and Directive 93/59/ECC (DieselNet, 2018) were established as the basis of the European regulatory framework in air pollution.

The five types of ICEs contributing to air pollution recognized within the European system, and that should be monitored constantly and considered in the control standards are (DieselNet, 2013a):

- Cars and light trucks,
- Heavy-duty trucks and bus engines,
- Engines for non-road mobile machinery (NRMM) and the non-road spark ignited engines,
- Stationary engines (such as for power generation), and
- Two- and three-wheel vehicles.

The present study is focused on the category “cars and light trucks”, from which a further explanation is found in Annex I. For this type of engine, the Directive 70/220/EEC of March 1970 established the EU standards[2]. The emission limits established in this document are given in Table 1.4 (DieselNet, 2018).

Table 1.4 Euro standards for cars and light trucks

Standard	Directive	Date	CO	HC	NOx	PM[3]	PN[4]
			g/km				#/km
Euro 1	Directive 91/441/CEE	31/12/1992	2.72 (3.16)	-	-	-	-
Euro 2	Directive 94/12/CE	01/01/1997	2.2	-	-	-	-
Euro 3	Directive 98/69/CE	01/01/2001	2.30	0.20	0.15	-	-
Euro 4	Directive 98/69/CE	01/01/2007	1.0	0.10	0.08	-	-
Euro 5	Regulation 715/2007	01/01/2011	1.0	0.10 [d]	0.06	0.005 [e]	-
Euro 6	Regulation 715/2007	01/09/2015	1.0	0.10 [d]	0.06	0.005 [e]	$6x10^{11}$ [e]

Notes:
d. and NMHC = 0.068 g/km
e. applicable only to vehicles using DI engines

1.2.3 US and EU air pollution legislations: a comparison

The American and European systems are different, yet they share the same principles. For comparison it should be considered that the US and the EU are two different legal and political entities, legislating with different interests, and with different needs. The most remarkable differences are given in the chart of Figure 1.3 (Nesbit et al., 2016).

[2] Applicable for vehicles M, M1, M2, N1 and N2 with a mass less than 2610kg (Euro 5/6). For further details refer to Annex I.
[3] PM referring to PM_{10} and $PM_{2.5}$.
[4] PN referring to Particle Number, particles per kilometre.

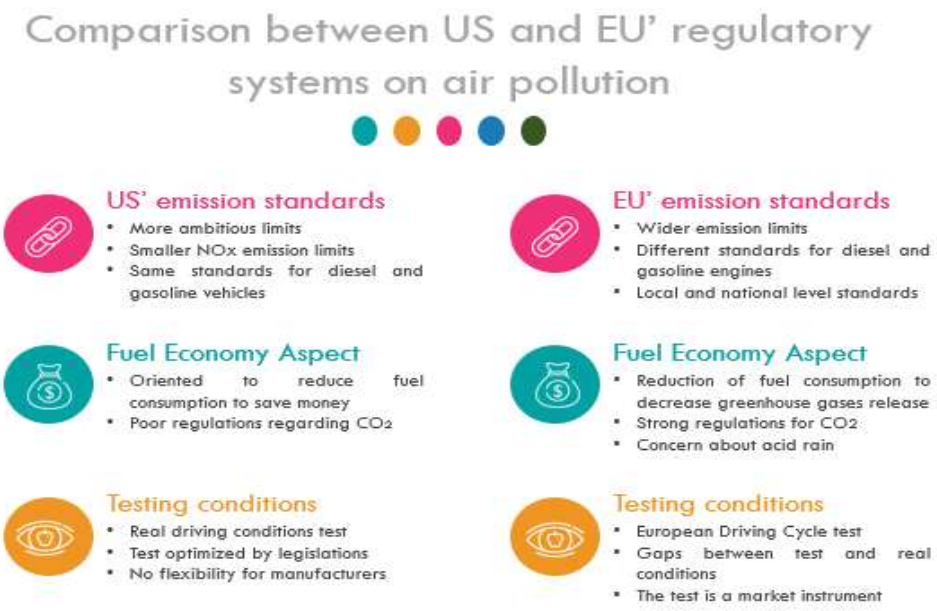

Figure 1.3 Comparative chart of US and EU regulatory frameworks, own drawing.

The differences shown are just a part of a complex context that holds responsibility in the environmental impact of emissions. A weaker system represents a higher amount of emissions each year, lower air quality, more concerns in human health, and an increase in the climate change effect.

The fulfillment of the previous standards is conditioned on how combustion gases are treated in the engine. This relies completely on the use of ACCs to accomplish the emission standards, and the transformation of air pollutants prior to their release into the atmosphere. In the way of thinking of the present work, it is of utmost importance the understanding of ACCs as part of the exhaust system. It is expected that this explanation will bring together all the pieces of the problematics assessed and will make the connection between the experimental methodology developed and the need to recycle and recover PGMs obvious.

1.3 Automobile catalyst converter: device description

In the automobile industry, ACCs are used to reduce the amounts of air pollutants from the engine (Mason, 1999). They consist in a closed metallic chamber containing a defined structure coated with catalytic particles of PGMs. Through this chamber, the exhaust gases will pass and will be transformed into less harmful gases prior to their release. Typically the device is situated at the exit point of the engine, as depicted in Figure 1.4 (Basics, 2013).

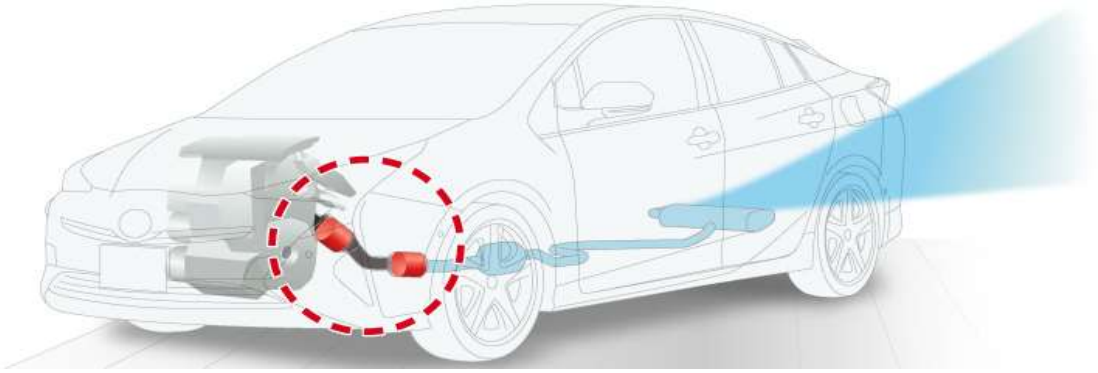

Figure 1.4 Representation of an ACC within the engine's exhaust system.

The pollutants transformation is initiated automatically due to the high operating temperature of the engine, dictated by a kinetically controlled rate. This transformation is established to occur through two mechanisms: the first one involves the **Pt/Pd active sites in charge of the oxidation reactions of CO and HCs into H_2O and CO_2**, and the second one deals with the **Rh active sites which are responsible for the reduction reactions of the NO_x into N_2 and O_2** (Mooney, 2007). These mechanisms are illustrated in Figures 1.5 and 1.6.

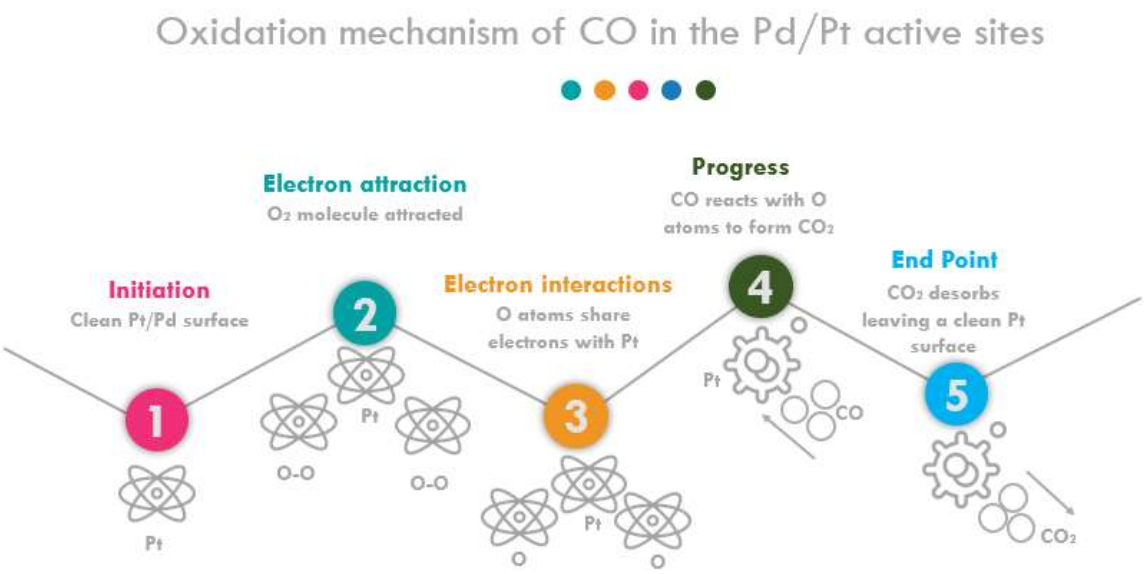

Figure 1.5 Oxidation mechanism of CO in the Pd/Pt active sites, own drawing.

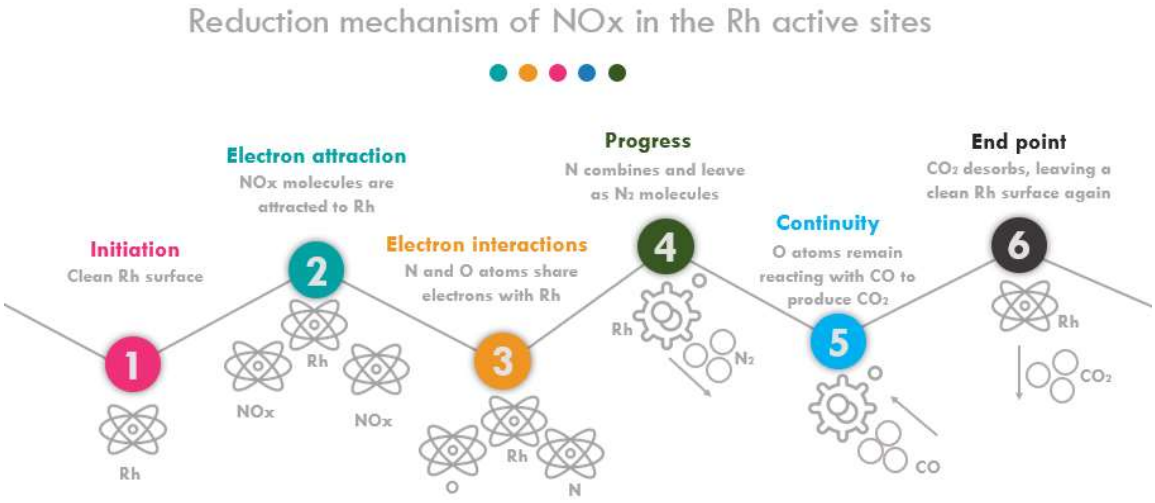

Figure 1.6 Reduction mechanism of NOx in the Rh active sites, own drawing.

Chemically speaking, the first mechanism, which is the oxidation of CO and HCs to CO_2 and H_2O, is represented in Eq. 1 and Eq. 2 (Fornalczyk and Saternus 2009).

$$C_nH_{2n+2} + \left(\frac{3n+1}{2}\right) O_2 \rightarrow nCO_2 + (n+1)H_2O \qquad \text{(Eq. 1)}$$

$$CO + \frac{1}{2}O_2 \rightarrow CO_2 \qquad \text{(Eq. 2)}$$

The second mechanism, meaning the reduction of NO_x to N_2, is explained by the reaction displayed in Eq. 3 (Fornalczyk and Saternus 2009).

$$NO_x + xCO \rightarrow \frac{1}{2}N_2 + xCO_2 \qquad (Eq.3)$$

The term NO_x comprises all the nitrogen oxides that can be formed depending on the interactions of the atoms, such as N_2O, N_2O_3, NO_2, NO, N_2O_5. Nevertheless, it is observed that NO_2 is the predominant compound in our studied process; therefore, its transformation occurs under Eq. 4 (Fornalczyk and Saternus 2009).

$$NO_2 + 2CO \rightarrow \frac{1}{2}N_2 + 2CO_2 \qquad (Eq.4)$$

To acquire the above transformation mechanisms, the catalytic properties of PGMs are combined with other technical features of the ACCs that were developed and improved over time, such as the type of structure in which the PGMs are deposited on. Pellets and honeycomb monoliths are the two most suitable micro-engineering structures for ACCs (Mason, 1999). The main characteristics of these structures can be described as follows:

- Alumina pellets (aluminum oxide, Al_2O_3) with a 3mm (0.125 in) diameter, with 10mm^2 of internal contact surface per unit, offering a total contact surface of ~500,000m^2 in 1L of the catalyst.
- Honeycomb-monoliths, consisting in up to 2,000 longitudinal pores with an average size of 1mm, manufactured with cordierite ($Mg_2Al_4Si_5O_{18}$), which is a cyclic six-membered ring silicate, with an Al-substituted ring cordierite group material (Minerals, 2016) used for its low thermal expansion.

The catalyst types analyzed in this work were of the honeycomb-monolithic ACC type; for this reason, the following sections offer a brief description of the development history of the device.

1.3.1 First generation: oxidation catalyst

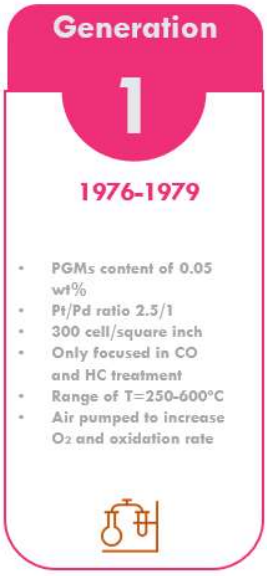

These catalysts were highly affected by sulfur dioxide impurities and tetraethyl lead traces present in gasoline; this caused the so-called "poisoning effect in the catalyst". This involves the formation of a low-activity alloy that produces a decrease in the performance of the device. The reaction for the formation of the alloy is presented in Eq. 5 (Chu, 2015).

$$Pd\ or\ Pt + Pb \xrightarrow{air,\ 900°C} PtPb\ or\ PdPb \qquad (Eq.5)$$

Pt showed to be slightly more tolerant towards Pb than Pd, but possibly it could form two kinds of alloys, Pt_2Pb and PtPb. These alloys increased the hardness of the catalyst, and when their content is over 30% the catalyst experiments fracture, leaving the surface ready to be oxidized by air (Atomistry, n.d.), potentiating the poisoning effect.

1.3.2 Second generation: NOx reduction

The addition of Rh required a stoichiometric air/fuel ratio (λ) to achieve the parallel conversion of all pollutants. For the recently developed three-way catalytic converter (TWC) the use of a ratio λ=1.0 was suggested; that is achieved by adding an O_2 sensor built up with zirconia (ZrO_2) electrodes and disposed among the honeycomb (Leroy et al., 2007).

This sensor allowed a greater tolerance towards Pb and Si poisoning, and together with a heat sensor propitiated the creation of the O_2 storage component, with the purpose of releasing or absorbing oxygen according to the λ perturbations. This storage component uses CeO_2 as redox compound according to Eq. 6 and Eq. 7 (Leroy et al. , 2007):

$$Rich\ stream: 2CeO_2 + CO \rightarrow Ce_2O_3 + CO_2 \qquad (Eq.6)$$

$$Lean\ stream: Ce_2O_3 + \frac{1}{2}O_2 \rightarrow 2CeO_2 \qquad (Eq.7)$$

1.3.3 Third generation

The concept of fuel economy (reduction in the amount of fuel used by the engine) changed the operation mechanism of the engine. This brought higher working temperatures, a new injection system and a decrease in the oxidant character of the working atmosphere, causing the deactivation of Rh due to undesired reactions with the Al-substrate. Inactive Rh-Al was extensively created. Fortunately, this reaction is partially reversible, as shown in Eq. 8 and 9 (Leroy et al., 2007).

$$Rh + \gamma - Al_2O_3 \xrightarrow{800°C,\ lean\ media} RhAl_2O_3 \qquad (Eq.8)$$

$$RhAl_2O_3 + H_2 \xrightarrow{rich\ media} Rh + \gamma - Al_2O_3 \qquad (Eq.9)$$

The deposition of Rh in less-active compounds such as ZrO_2 reduced the formation of inactive species and prevented the Rh segregation due to high-temperature and lean conditions.

1.3.4 Fourth generation: palladium TWC catalyst (the Mid-1990s)

After years of research, Ford® discovered that a Pd-only ACC would be able to deliver proper results, such as (Hepburn et al., 1994):

- reduction of 30% in the tailpipe of HCs
- 20% reduction of the tailpipe of CO
- 50% reduction in the emission of NO_x

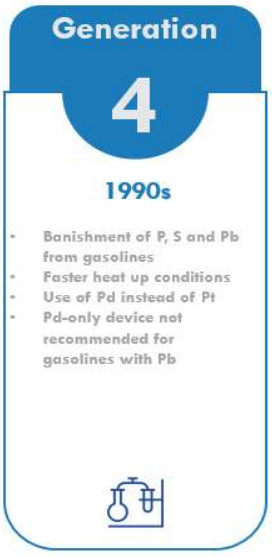

This device was not recommended for countries like Portugal or Eastern Europe where the Pb contained in their gasoline was about 0.64 g/L (Nriagu, 1990). This fact occurs because Pd is more susceptible to poisoning by Pb, affecting the NO_x conversion.

1.3.5 Three-way catalyst converter: the leading technology

The TWC technology established an air/fuel ratio equal to 14.65 to achieve the parallel conversion of all air pollutants at a time. Figure 1.7 (Mooney, 2007) illustrates the air/fuel ratio in terms of the % of conversion of the air pollutants.

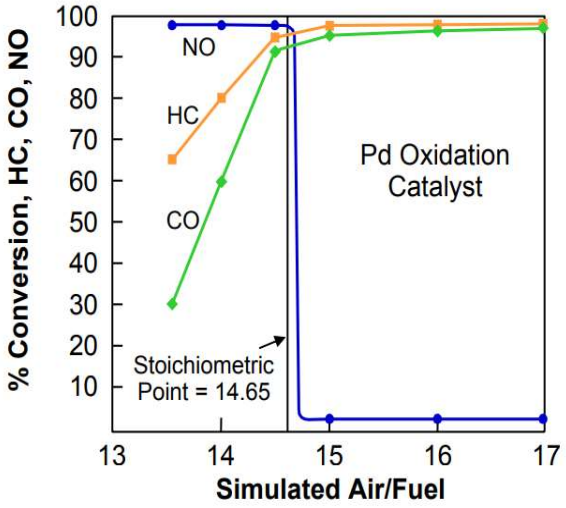

Figure 1.7 Stoichiometric ratio for parallel conversion, own drawing.

After this implementation, more technical features and improvements were added to the device. A summary of this evolution can be appreciated in Figure 1.8.

The use of ACCs has contributed to the disintegration of approximately 4 billion tons of HCs, 4 billion tons of NO_x and 40 billion tons of CO since their implantation. The ACCs also brought other indirect beneficial actions, like the removal of Pb from gasoline, decreasing its potential threat for human health (Pb is associated with negative mental health developments, high blood pressure, heart diseases and multiple organ damage (W.H.O., 2018)).

After the description of the operating principles of an ACC, the relevance of PGMs for air pollution regulations has become clear. Now the state of the art and the current global scenario for these metals will be addressed in sequence, for a deeper understanding of the need of recovering them from spent devices.

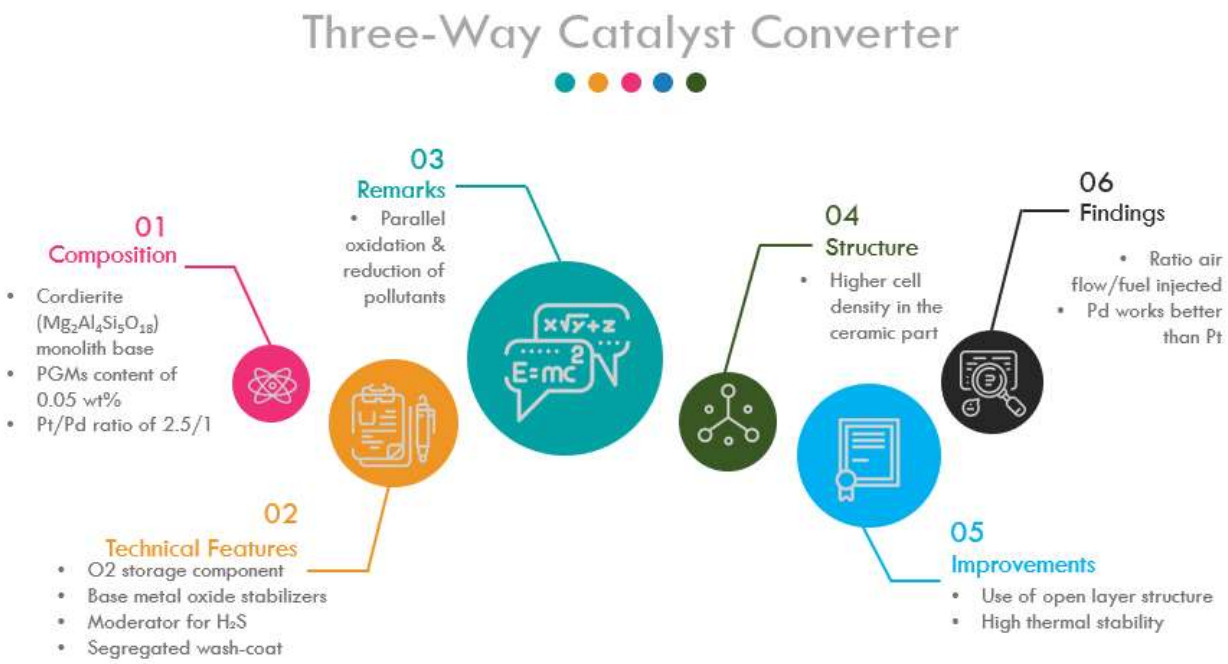

Figure 1.8 Outstanding features of the TWC, own drawing.

PLATINUM GROUP METALS

2. PLATINUM GROUP METALS

2.1 PGMs: properties and applications

The platinum group metals comprise six noble metals: **Ruthenium (Ru), Rhodium (Rh), Palladium (Pd), Osmium[5] (Os), Iridium (Ir) and Platinum (Pt)**. Found in the d-block of the periodic table, they are grouped together because they share similar properties, as it is shown in Table 2.1 (Balance, 2017).

Table 2.1 Physicochemical properties of PGMs

Name	Ruthenium	Rhodium	Palladium	Osmium	Iridium	Platinum
Symbol	Ru	Rh	Pd	Os	Ir	Pt
Atomic Number	44	45	46	76	77	78
Molecular weight	101.07	102.91	106.42	190.23	192.22	195.08
Density (g/cm^3)	12.45	12.41	12.01	22.61	22.65	21.45
Melting point (ºC)	2,310	1,960	1,554	3,050	2,443	7,769
Electrical resistivity (μΩ.cm)	6.80	4.33	9.93	8.12	4.71	9.85
Thermal conductivity (W/m.ºC)	105	150	76	87	148	73

These properties, together with their high tolerance for wear, tarnish, chemical attacks, temperature resistance and their high catalytic activity (alone or in alloys with other metals) (Panda et al., 2018; European Commission, 2017) provide PGMs with a high economic value in the manufacturing chain of many industries.

After 2015, the applications of PGMs were widespread among different industries, like jewelry, chemical manufacturing processes, petroleum and oil refining plants, medical devices, electronic products and automobile catalytic converters (Lonmin, 2015). The proportions of these metals destined to each industry are shown in Figure 2.1.

[5] Osmium was assessed in 2011 and 2014, however, it is excluded from the EU CRM's report of 2017 due to the lack of robust information.

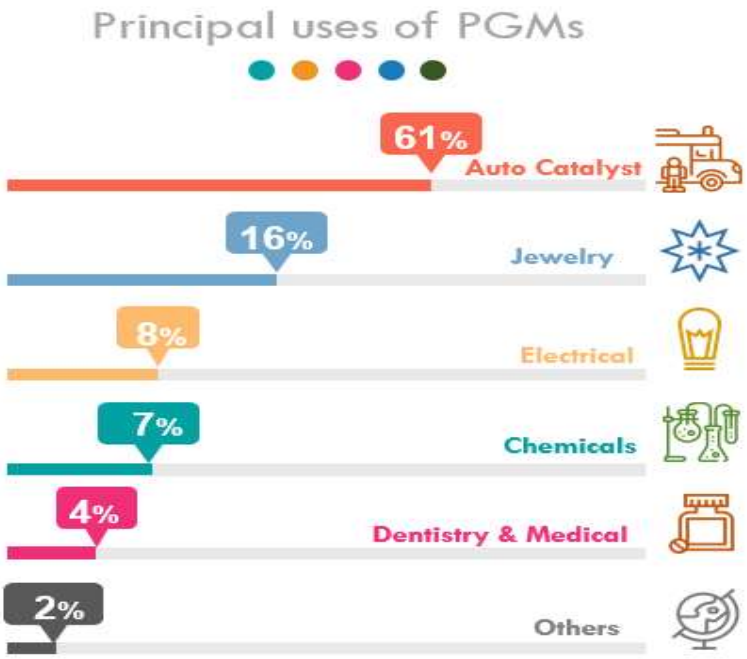

Figure 2.1 Percentage of PGMs production among their applications, own drawing.

The major use concentration involves Pt and Pd; nevertheless, Rh, Ir, and Ru are close behind them, with an increasing market each year. On the other hand, Os is not considered as an option for industrial applications.

This work will be focused on the catalytic properties of PGMs that make them indispensable to the car industry. This assessment will be concerned with the EU economic and regulatory region; therefore, a wider description of Europe's current PGMs demand and production scenario is presented in sequence.

2.2 PGMs and their relationship with the critical raw materials list of the EU

In 2008, the European Commission (EC) began the Raw Material Initiative (RMI), to tackle the challenges associated with the access to critical raw materials (CRM) with a main role in the EU manufacturing industry. These raw materials are essential to produce daily goods, to develop eco-friendly technologies and for the development of emerging industries. Securing a safe and stable supply of these materials became a vital challenge for the EC, especially because the dependence on import

operations and on the low local production (due to natural and geographical reasons) have reached an alarming point. This initiative is seen as a tool for trading, innovation, and industrial scale decisions, to promote recycling of these materials and to improve the circular economy point of view within this business (European Commission, 2017).

The RMI, through the Criticality Methodology, evaluates every three years the candidate materials for the Critical Raw Material List (CRML). In its latest version of 2017, the RMI evaluated a total of 78 materials, resulting in 26 materials listed in the CRML including PGMs (European Commission, 2017). These materials and their producers around the globe are given in Figure 2.2.

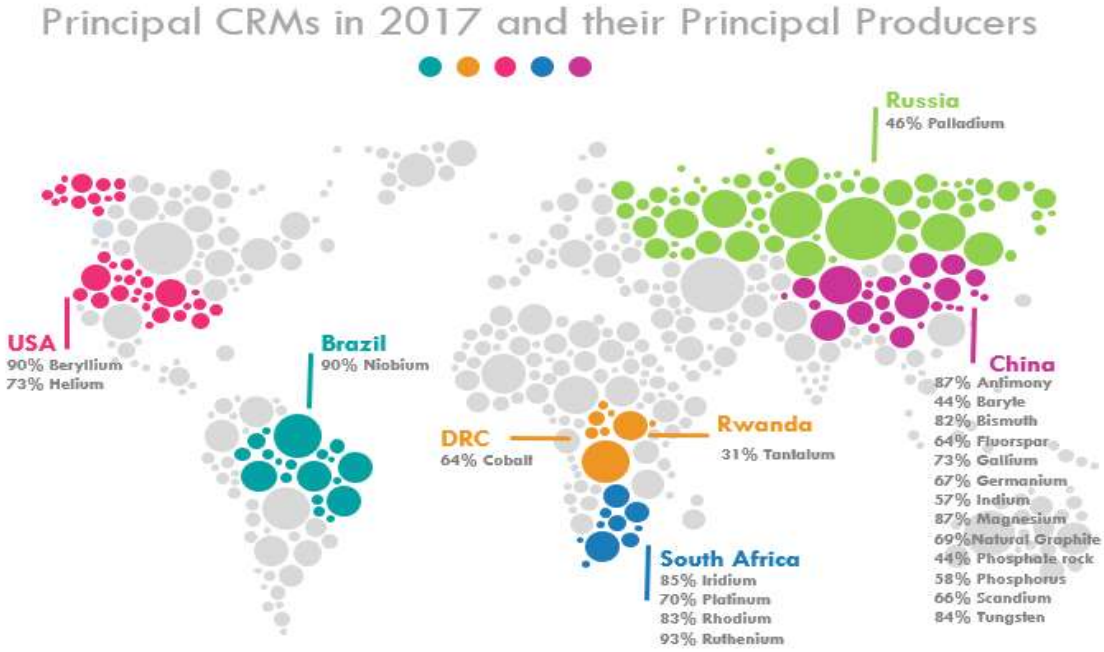

Figure 2.2 CRMs listed in 2017 and their main producer countries, own drawing.

According to the CRM list, PGMs are extracted mainly in Russia and South Africa (Table 2.2) (European Commission, 2017), where they are usually mixed with nickel (Ni) and copper (Cu) ores within the same mineral phases. A total estimation of about 66,000 tons of PGMs in the earth crust, together with their current global demand of

about 590 tons/year (Peng et al., 2017) generates a critical scenario for these materials.

Table 2.2 Main producers of PGMs		
Material	**Main global supplier**	**Share (%)**
Ru	South Africa	93
Rh	South Africa	83
Pd	Russia	46
Ir	South Africa	85
Pt	South Africa	70

With China playing a major role in the production of all kind of electronic devices, and with the natural reserves confined in a few countries, a vulnerability, risk in supply and price volatility in the market of PGMs is created. This generates a supply disruption in the EU, that is boosted with the poor local-production, leading to a rise in prices and a shortage of several products. To prevent the above-mentioned shortage, the EC decided to implement a methodology (GROW - Internal Market, 2017; European Commission, 2017) to assess the dependence on a CRM and to evaluate the possible strategies to guarantee its stable supply or to find suitable replacements. This methodology is described in the diagram in Figure 2.3.

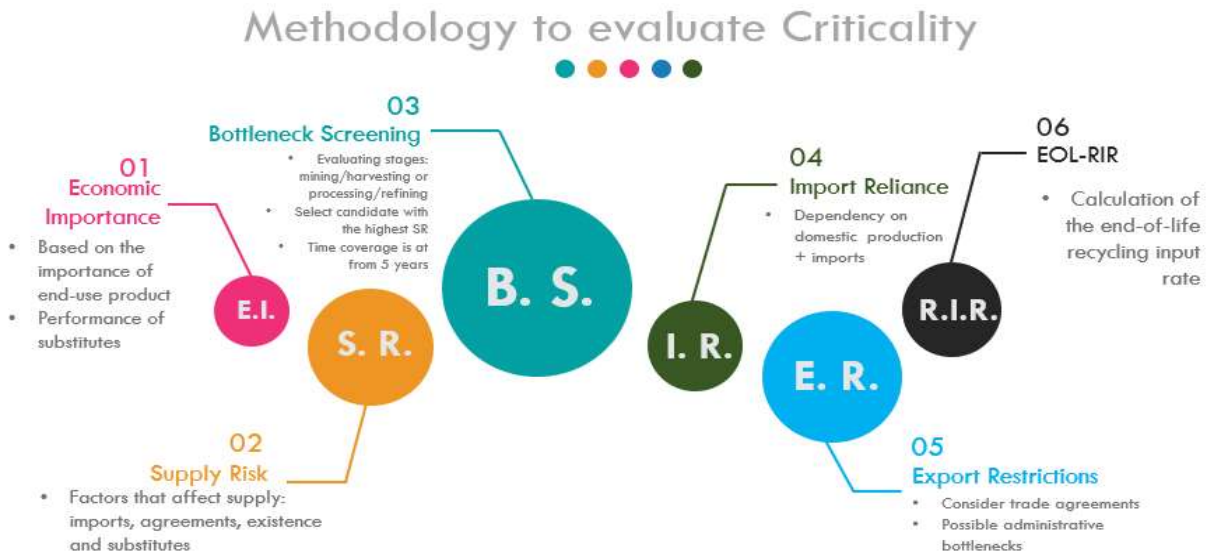

Figure 2.3 General methodology to assess the criticality of a material, own drawing.

The results of the application of the said methodology over PGMs, comprising the SR, EI, IR, and EOL-RIR for each metal and for the PGMs as a group (GROW - Internal Market, 2017), are reported in Table 2.3.

Table 2.3 Criticality results for PGMs				
Material	**Supply risk**	**Economic importance**	**Import Reliance (%)**	**EOL-RIR (5)**
Ru	3.4	3.5	100	11
Rh	2.5	6.6	100	24
Pd	1.7	5.6	100	10
Ir	2.8	4.3	100	14
Pt	2.1	4.9	98	11
PGMs	**2.5**	**5.0**	**99.6**	**14**
Notes: - Global supply data and processing stage were considered. - The threshold established is S.R.>1.0 & E.I.> 2.8				

Table 2.4 (GROW - Internal Market, 2017) presents the evaluation of the main producers of PGMs and points out the need of increasing the Recycling Input Rate as a way to decrease the Import Reliance Rate to mitigate the supply risk for the EU.

Table 2.4. Criticality results in terms of producers					
Economic Importance				**Supply Risk**	
Main global producers	**Main Importers to the EU**	**Sources of EU supply**	**Import Reliance Rate[6]**	**Substitution Indexes EI/SR[7]**	**Recycling Input Rate[8]**
Average 2010-2014					
- South Africa (83%) (Ir, Pt, Rh, Ru) - Russia (46%) (Pd)	Switzerland (34%) South Africa (31%) USA (21%) Russia (8%)	Switzerland (34%) South Africa (31%) USA (21%) Russia (8%)	99.6%	0.93/0.98	14%

Given the scarcity of the PGMs ores, the extensive industrial applicability and the high risk for supply of these metals, the need to recover PGMs from spent materials

[6] Imports Reliance Rate considers global supply, calculated as EU net imports/(EU imports + EU production).
[7] Measures how difficult it would be to replace the said material; values from 0-1, with 1=least sustainable.
[8] Recycling ratio from old scrap and the EU demand of the given material.

becomes urgent. These recovery processes should guarantee a high recovery rate, good quality of the final product, and economic and environmental feasibilities.

2.3 Processes to recover PGMs from secondary sources

The production of ACCs represents the estimated consumption of 34% of Pt, 55% of Pd and 95% of Rh; therefore, spent ACCs are the major secondary source of PGMs and their recycling becomes crucial. Studies have shown that recycling 2mg of spent ACCs can prevent the treatment of approximately 150 kg of ores because the spent devices have a high PGMs content with an average of ~4g of PGMs per kilogram of material (Fornalczyk and Saternus, 2009).

The recovery from secondary sources can be achieved principally by two routes: pyrometallurgical and hydrometallurgical processes (Steinlechner & Antrekowitsch, 2015), as shown in Figure 2.4. These processes have been already applied in industries like Umicore, Belgium; Hereaus, Germany; BASF, USA; Johnson Matthey, UK, and Nippon/Mitsubishi, Japan.

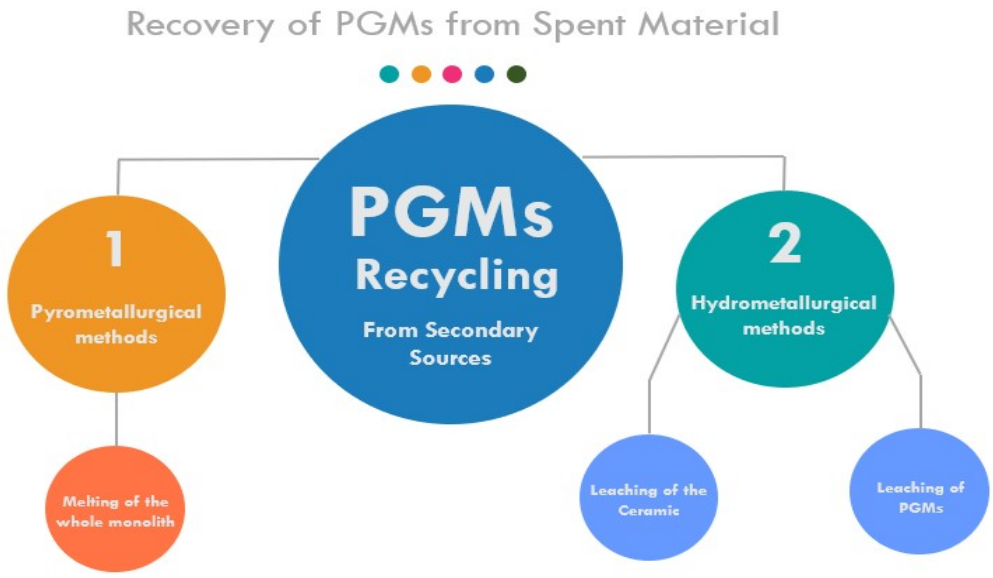

Figure 2.4 Possibilities in the recovery of PGMs from secondary sources, own drawing.

2.3.1 Pyrometallurgical processes in secondary sources' recovery

Pyrometallurgical processes are employed for the concentration and further refining of PGMs through crushing, batching, granulation, separation, and smelting operations (Fornalczyk and Saternus, 2009; Panda et al., 2018; Park et al., 2014). A smelting operation consists on the melting of the monolith and it is the most common route of action in pyrometallurgy (Steinlechner & Antrekowitsch, 2015). This process begins with the mixture of spent ACCs with fluxes, collectors and reductants to obtain a PGMs-collector alloy which will be purified later. The collector plays a key role and is selected according to the solubility and melting point shared with the sample, for example, Cu, Ni, Pb, and Fe are the most common collectors (Panda et al., 2018; Peng et al., 2017), as appreciated in the diagram of Figure 2.5.

Figure 2.5 Main pyrometallurgical processes, own drawing.

The main disadvantage of pyrometallurgy is the high energy consumption. This is often assessed by recycling the ACCs in parallel with the Ni, Cu and Co ores to take advantage of the PGMs already present in them (Steinlechner & Antrekowitsch, 2015). Nevertheless, the use of the previous method compromises the richness of the sample in terms of PGMs concentration and makes the separation steps more complicated; thus, it affects the efficiency of the process and its industrial applicability.

New techniques were investigated to ensure industrial applicability for the recovery of PGMs. In these new techniques, guaranteeing the scalability and reducing the energy consumption were the objectives. Hence, hydrometallurgical techniques were established, taking advantage of the solubility properties of PGMs in certain media.

2.3.2 Hydrometallurgical processes in secondary sources' recovery

The hydrometallurgical processes to recover PGMs from spent materials are split into two main routes (Havlik, 2008):

1. Leaching of the ceramic monolith, using NaOH or H_2SO_4 under pressure and concentrating the PGMs as remaining solids.
2. Leaching of the PGMs, by solubilizing them in a suitable acidic or alkaline media (such as H_2SO_4, HCl, HNO_3, NaCN, iodide solutions or a combination of them) in the presence of oxidizing agents like O_2, I_2, Br_2, Cl_2, and H_2O_2.

The solubilization in acidic media is the most used approach, with HCl as the most common complexing agent (to form metal chlorocomplexes) among other acids like HBr (Duche & Dhadke, 2001), nitric or sulfuric acid and *aqua regia* (a mixture of HCl and HNO_3 in proportion 3:1, respectively) (Panda et al., 2018; Steinlechner & Antrekowitsch, 2015). The hydrometallurgical processing also requires previous mechanical/physical steps for dismantling, canister removal and grinding of monoliths.

2.3.2.1 Leaching step in the hydrometallurgical recovery of PGMs

Leaching processes are selected depending on the composition of the spent catalyst, associated materials and contaminants (Park et al., 2014). Some of them might involve a pre-thermal treatment using an atmosphere of H_2, O_2, N_2 or air, depending on the undesired organic residues and on the impurities to be removed (Jha et al., 2013).

Leaching a metal consists in the formation of a soluble metal ion form. In the case of PGMs, this involves mainly the formation of a metal-complex with lower redox potential, thus facilitating its oxidation. PGMs are well known for forming stable

chlorocomplexes, such as $[PtCl_6]^{2-}$, $[PdCl_4]^{2-}$ and $[RhCl_6]^{3-}$ in concentrated aqueous chloride solutions (Nogueira et al., 2014; Papaiconomou et al., 2015), whose formation can be explained through Eq. 10 to Eq. 12, valid when using H_2O_2 as oxidizing agent (Steinlechner & Antrekowitsch, 2015).

$$Pt_{(s)} + 6H^+ + 2HO_2^- + 6Cl^- \rightarrow [PtCl_6]^{2-} + 4H_2O \qquad (Eq.10)$$

$$Pd_{(s)} + 3H^+ + HO_2^- + 4Cl^- \rightarrow [PdCl_4]^{2-} + 2H_2O \qquad (Eq.11)$$

$$Rh_{(s)} + 4.5H^+ + 1.5HO_2^- + 6Cl^- \rightarrow [RhCl_6]^{3-} + 3H_2O \qquad (Eq.12)$$

When *aqua regia* is used in the leaching, the formation of the chlorocomplexes can be explained throughout Eq. 13 (as example for Pt) (Jha et al., 2013).

$$3Pt + 18HCl + 4HNO_3 \leftrightarrow 3[PtCl_6]^{2-} + 6H^+ + 4NO + 8H_2O \quad (Eq.13)$$

The use of *aqua regia* has been widely explored by researchers. Table 2.5 (Jha et al., 2013) summarizes the most outstanding studies of the leaching approaches.

Table 2.5 Outstanding researches using *aqua regia* (or similar compositions) as leaching agents

Material	Leaching agent	Results	Author (s)
Spent reforming catalyst	*Aqua regia* solution	Pt-leaching reaction was controlled by surface chemical reactions, the E_a found was 72.1 kJ/mol	Baghalha et al. (2009)
Spent auto catalyst	HCl and HNO_3	Pt and Pd leached at 95 ºC	Bonucci and Parker (1984)
Pt/Rh bimetallic reforming catalyst	*Aqua regia* solution	Sample refluxed at an liquid/solid ratio of 5 and 2.5h time, >95% of Pt and Pd recovered	Jararifar et al (2005)
Pt and Pd honeycomb Al_2O_3	*Aqua regia* solution	Recoveries of 95% of Pt and 92.7% of Pd	Muraki and Mitsui (1986)
Spent automobile catalyst	HCl and HNO_3 equal concentration	Recoveries of 90% Pt and 70% Pd in a 5h reaction time	Tyson and Bautista (1987)

The use of *aqua regia* alone is not advised for industrial scale due to the formation of toxic gases like nitrosyl chloride (NOCl) and chlorine gas. To avoid this problem,

other strong oxidizing agents have been tested, trying to find a similar effect without the previous environmental impacts. H_2O_2 has been used in laboratory scale as a replacement of the oxygen used in industrial scale; it has provided some good results in the presence of a mineral acid. This process can be explained through the redox reactions displayed in Eq. 14 and Eq. 15, resulting in Eq. 16 (as example for Pt) (Jha et al., 2013).

$$2H_2O_2 + 4H^+ + 4e^- \leftrightarrow 4H_2O \qquad (Eq.14)$$

$$Pt + 6HCl \leftrightarrow [PtCl_6]^{2-} + 6H^+ + 4e^- \qquad (Eq.15)$$

$$2H_2O_2 + Pt + 6HCl \leftrightarrow [PtCl_6]^{2-} + 2H^+ + 4H_2O \qquad (Eq.16)$$

In the same way, the leaching of Pt can be explained through the redox reactions displayed in Eq. 17 and Eq. 18, resulting in Eq. 19.

$$2O_2 + 4H^+ + 4e^- \leftrightarrow 2H_2O_2 \qquad (Eq.17)$$

$$Pt + 6HCl \leftrightarrow [PtCl_6]^{2-} + 6H^+ + 4e^- \qquad (Eq.18)$$

$$Pt + 2O_2 + 6HCl \leftrightarrow [PtCl_6]^{2-} + 2H^+ + 2H_2O_2 \qquad (Eq.19)$$

The use of HCl and H_2O_2 as lixiviants attains a 95% recovery of Pt with a relationship of 10 HCl:1 H_2O_2. The extraction can be improved by increasing the liquid/solid ratio (L/S) when the temperature is around 60 ºC (Fornalczyk and Saternus, 2009; Havlik, 2008).

The use of HCl media also produces the side reaction of Eq. 20 (Steinlechner & Antrekowitsch, 2015).

$$Al_2O_{3(s)} + 6H^+ \rightarrow 2Al^{3+} + 3H_2O \qquad (Eq.20)$$

Thus, leaching dissolves Al from the coating of the monolith; in this case, the amount of Al in the leaching solution can be used to determine the selectivity of the developed methodology towards PGMs.

After leaching, a solvent extraction (SX) step**,** also known as liquid-liquid extraction (LLE), is generally used to refine and concentrate the metals from the leach liquor by using a proper solvent that shows affinity with the solute.

2.3.2.2 Solvent extraction step in the hydrometallurgical recovery of PGMs

The most efficient, cost-effective and eco-friendly separation method of PGMs from concentrated pregnant solutions coming from the leaching step is the LLE (Costa et al., 2016; Nguyen et al., 2016; Paiva, 2017; Regel-rosocka et al., 2015). This method commonly involves two main stages: the extraction, where the selected metals are transferred to the organic solution, and the stripping, where the extracted metals are transferred to a new aqueous phase for subsequent recovery. The loaded organic phase is regenerated and recycled to further extraction cycles.

The extraction will take place when the aqueous phase (in this case the pregnant solution coming from the leaching step) gets in contact with the organic phase**,** and the metal species of interest are recovered into it through several mechanisms, depending on the nature of the solvent. These mechanisms can be ion-pair, complexation or solvation (Paiva, 2017). After extraction, the stripping phase will take place; here the loaded solvent is equilibrated with a stripping aqueous medium, and the metals will be transferred to a new aqueous solution, from which their recovery and transformation into the metallic state (or other form with commercial interest) are easier. This whole process is depicted in a simplified way in Figure 2.6.

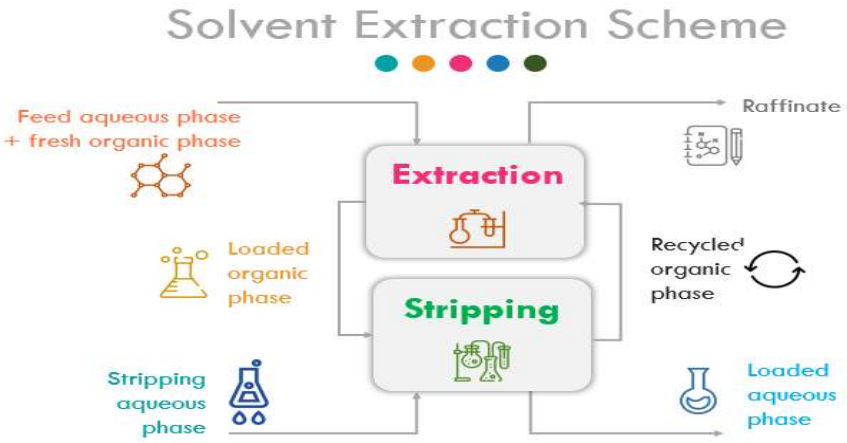

Figure 2.6 General scheme of a solvent extraction process, own drawing.

The main indicators considered during a SX process to evaluate its efficiency start with the distribution ratio (*D*), that expresses the *total concentration of the analyzed*

substance in the organic phase towards its concentration in the aqueous phase, both measured at the equilibrium. *D* can be calculated through Eq. 21 (Boudesocque et. al., 2019; Cieszyñska et. al., 2007; Nguyen et al., 2016; Paiva, 2017; Svecova et. al., 2016),

$$D = \frac{[M]_{org}}{[M]_{aq}} \qquad (Eq. 21)$$

where $[M]_{org}$ and $[M]_{aq}$ represent the concentration of the metal in the organic and aqueous phases, respectively; with *D* now we are able to obtain the extraction efficiency percentage**,** to evaluate the convenience of the process through Eq. 22 (Boudesocque et al., 2019; Cieszyñska et al., 2007; Nguyen et al., 2016; Svecova et al., 2016).

$$\%E = \frac{D}{D + \frac{V_{aq}}{V_{org}}}(100) \qquad (Eq. 22)$$

V_{aq} and V_{org} represent the volumes of the aqueous and organic phases, respectively, and *D* is the distribution ratio previously calculated. The values of Eqs. 21 and 22 are expected to be the highest possible, meaning to extract as much PGMs as possible. Selectivity of the SX system, also known as the separation factor (SF or β), is the prevalence of the metal A over the metal B, and that will make easier the further refining steps to produce a higher purity final product A; β can be calculated as in Eq. 23 (Paiva, 2017; Svecova et al., 2016).

$$SF = \beta = \frac{D_A}{D_B} \qquad (Eq. 23)$$

After the system has successfully extracted the metals into the organic phase, we will obtain a loaded organic phase, and we can perform the stripping to transfer the metals to a new aqueous phase, and prepare them to be reduced into their metallic form (or into any other form of interest). This will enable the organic phase to be reused in further extraction cycles. This is done through a stripping agent, whose

choice depends on the metal. The efficiency of this step can be measured as shown in Eq. 24 (Nguyen et al., 2016).

$$\%S = \frac{[M]_{st}\, V_{st}}{[M]_{\,st}\, V_{st} + [M]_{lorg} V_{lorg}}\ (100) \qquad (Eq.24)$$

V_{st} and $[M]_{st}$ stand for the volume and metal concentrations in the stripped liquor, and V_{lorg} and $[M]_{lorg}$ are the corresponding values in the loaded organic phase. After this stage, the stripped organic phase can be reused.

Figure 2.7 (Wei et al., 2016) represents a general diagram of a SX experiment. In this example, a HCl media solution containing Au(III), Pd(II) and Pt(IV) is submitted to a SX separation with Aliquat-336 reagent in the organic phase.

SX has proven to be a favorable method for the recovery of PGMs due to its selectivity towards the metal through the proper extractant. The extractant can be chosen from a vast and varied selection, from task-designed extractants to commercial reagents adapted for such purpose, depending on the metal and on the aqueous solution. In the case of the present work, some traditional extractants, together with one ionic liquid (IL), all commercially available, were revised and picked up as extractants in the SX step, taking advantage of their properties to benefit the process.

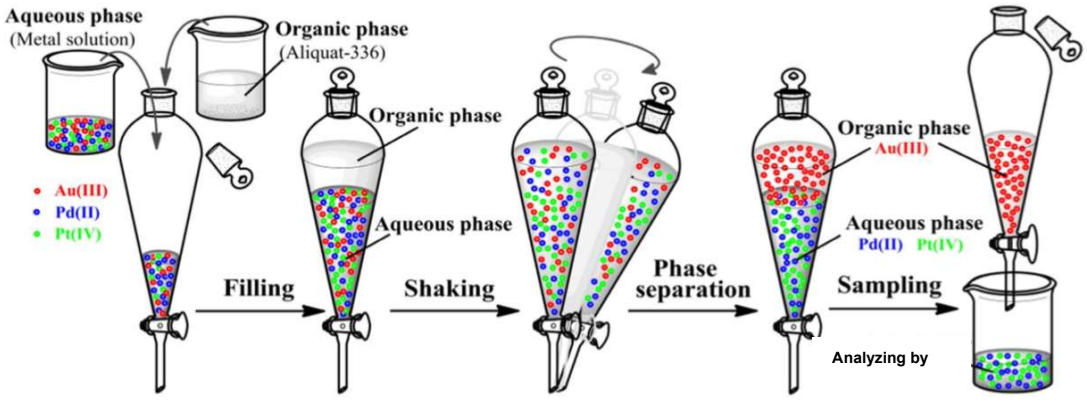

Figure 2.7 General illustration of a SX experiment. Adapted from "Selective recovery of Au(III), Pt(IV), and Pd(II) from aqueous solutions by liquid – liquid extraction using ionic liquid Aliquat-336" by Wei et. al. 2016.

2.3.2.2.1 Ionic liquids as extractants in SX

ILs are salts in the liquid state at room temperature, or at temperatures until 100 ºC, that have been acquiring popularity in the effort to replace conventional organic solvents. From ethyl ammonium nitrate as the first molten salt synthesized in 1914 by Paul Walden to the over 50,000 publications registered in 2000, their applications have changed from media for polymer synthesis to various fields such as reaction catalysts, electrolyte of energy storage devices, biosensors, separation/extraction agents, lubricants, etc (Anastas, 2010).

The interest in ILs has been growing because they are considered as more environmentally friendly solvents or green solvents, mainly because they exhibit a low vapor pressure, they are not flammable, exhibit moderate viscosity and a tunable solubility, present relatively large conductivity and high chemical/thermal and electrochemical stabilities (Boudesocque et al., 2019; Park et al., 2014). They are not more than a family of molten salts containing organic cations and organic/inorganic anions, but with the difference that while most ionic salts are solid at room temperature, they exhibit a melting point below 100 ºC that is explained due to the great difference in size of the cation and anion, resulting in a low lattice energy and receiving the name of room temperature ionic liquids (RTILs). Figure 2.8 (Park et al., 2014) shows the difference between the atom arrangements in a molten salt, in an ionic liquid and in an aqueous solution.

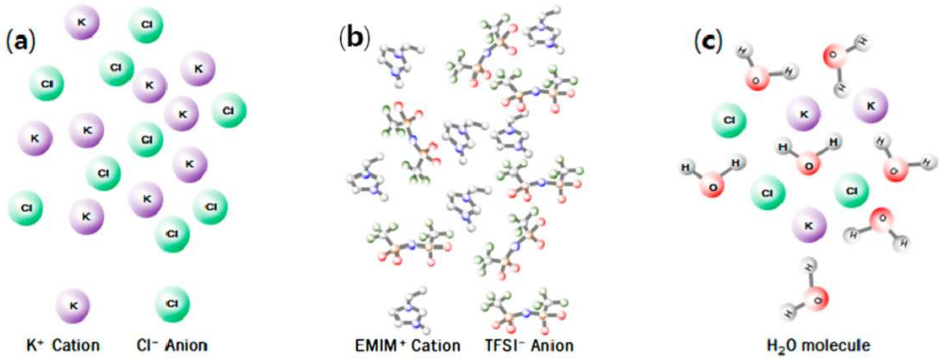

Figure 2.8. Atom arrangement for a molten salt (a), an ionic liquid (b) and an aqueous solution (c). Adapted from "Application of ionic liquids in hydrometallurgy" by Park et. al. 2014.

All the physicochemical characteristics of ILs are determined by the constituent ions and their combinations. For example, ILs for energy storage devices, such as lithium batteries, should be aprotic, with low volatility, non-flammable and with a high ionic conductivity, whereas ILs for fuel cells are required to be protic. Although there are various ways to synthesize an IL, the method shown in Figure 2.9 (Park et al., 2014) can be used for a vast majority of ILs. In this case, the example of [Dmim]BF_4, an imidazolium-based ionic liquid, is presented.

In this method, the process starts with the quaternization of the nitrogen atom of the amine, solvent removal, the anion exchange with a metal salt, the solvent/salt removal and the final refining; a wide range of ILs will be obtained by varying the alkyl-X and the anion species.

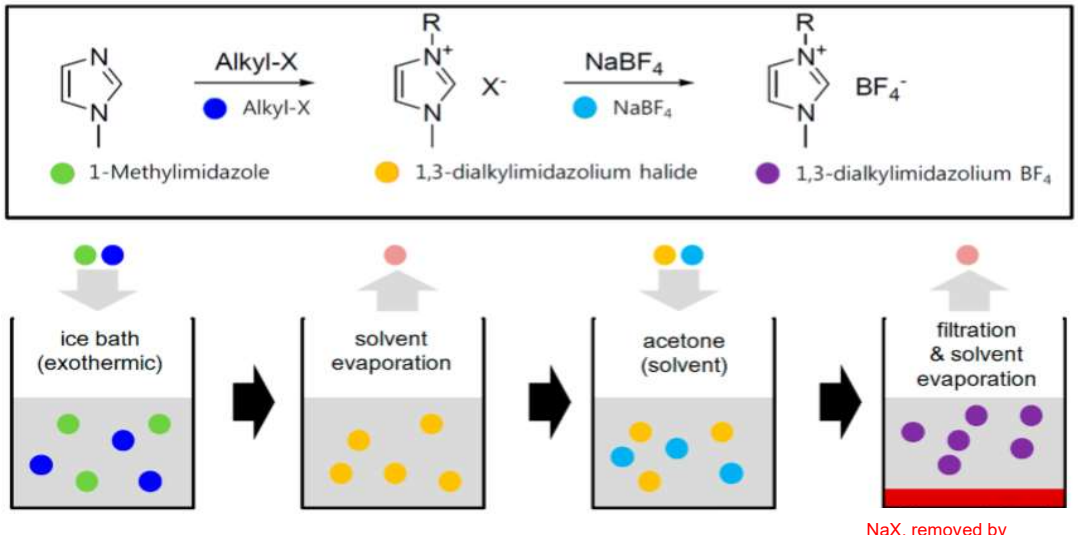

Figure 2.9. Common synthesis route for ILs. Adapted from "Application of ionic liquids in hydrometallurgy" by Park et al. 2014.

The understanding of the selection of anions and cations will lead to the development of task-specific ILs, with good results in hydrometallurgy or other applications. In the last decades, the potential of hydrophobic RTILs in SX processes for the extraction of ions such as Cu(II), Pt(IV) and Pd(II) has been studied, showing advantages towards their recyclability, together with the possibility of eliminating the organic diluents by a prior saturation with water for lowering the viscosity (Boudesocque et al., 2019).

Nevertheless, most of the commercially established ILs still require the use of organic diluents due to their high viscosity, impacting negatively on the mass transfer and the extraction kinetics. Accordingly, their applicability in a continuous process is challenging (Saguru et al., 2018), unless a diluent such as toluene or xylene is added to the reaction mixture (Cieszyñska et al., 2007; Nguyen et al., 2016). Some examples of these studies are the separation of Pt(IV), Pd(II), Rh(III) from HCl-leaching solution using both, commercially available and task-synthetized ILs, e.g., the use of $[C_4mim]PF_6$ with diisopentyl sulfide in nonane showed selective extraction of Pd(II) and Pt(IV) by leaving Rh(III) in the organic phase (Zhang et al, 2013). More examples of studies with satisfactory recovery of PGMs by commercially available ILs from chloride media are listed in Table 2.6, proving their suitability for this task.

Table 2.6 Outstanding research using ILs in the SX of PGMs

Targeted metals	Organic Phase	Aqueous Phase	% Extraction (%E)	Reference
Pd(II)	• Cyphos® 101 • Toluene as diluent	• 0.005M Pd(II) in [HCl]= 0.1–3M • 0.005M Pd(II) in [HCl]= 0.1-3 M + [NaCl]= 0.05–0.5M	• %E= 86%-97% at [HCl]= 0.1–3M, respectively • %E= 57% at [HCl]= 0.1-3M + [NaCl]= 0.05–0.5M	(Cieszyñska et al., 2007)
• Pt(IV) • Pd(II), • Rh(III)	• Cyphos® 101 • Xylene as diluent	• 100 mg/L Pt(IV), • 55 mg/L Pd(II), • 25 mg/L Rh(III) • [HCl]= 0.1-4M	[Cyphos® 101] = 0.2 and 2.0 g/L: - %E= 21.9% & 99.9% of Pd(II), respectively • %E= 8.5% & 98.1% of Pt(IV), respectively • Rh(III) was not extracted	(Nguyen et al., 2016)
• Pd(II), • Rh(III)	• Cyphos® 101 • Cyphos® 102 • Cyphos® 105 • Xylene as diluent	• 250 mg/L Pd(II), • 50 mg/L Rh(III) • [HCl]= 8M	•Cyphos®105 worked well at [HCl]=6-8M for Pd(II) •Cyphos®101 and Cyphos®102 separate quantitatively Pd(II) from Rh(III) •Rh(III) remained in the aqueous phase	(Svecova et al, 2016)

2.3.2.2.2 Main commercial extractants used for the SX of PGMs

2.3.2.2.2.1 Cyphos® 101

The phosphonium based ILs contain the cation of the generic form $[PR_3R']^+$ and combined with different anions. They form a family of molten salts that are liquid at room temperature. Most of them have melting points below 100ºC; within their main advantages we can list (Sigma Aldrich, 2003):

- Thermally more stable than the corresponding ammonium and imidazolium homologues, preventing the decomposition and allowing their use in a multiple step process;
- Phosphonium cations lack acidic protons; thus, they are stable in basic conditions;
- Less dense than water, benefiting the work-up steps of the product.

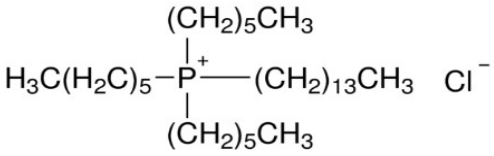

Figure 2.10 Cyphos® 101 chemical structure, own drawing.

Cyphos® 101 (Figure 2.10) is a phosphonium-based ionic liquid commercially available that has been tested in the SX recovery of PGMs using model solutions; the classification, labelling and packaging information (CLP), as well as its physicochemical properties, are depicted in Table 2.7 (Sigma Aldrich, 2003).

Table 2.7 General information of Cyphos® 101

Aspect	Specification
Chemical name	Trihexyl(tetradecyl)phosphonium chloride
CAS number	258864-54-9
Molecular formula	$C_{38}H_{68}ClP$
Molecular weight	519.31 g/mol
Density at 25 ºC	0.8819 g/cm^3
Viscosity at 25 ºC	1824 cP

In terms of PGMs extraction, Cyphos® 101 acts as anion exchanger thanks to its $[Cl]^-$ anion, that can be easily exchanged with the chlorocomplexes of the PGMs

species such as $[PdCl_4]^{2-}$ or $[PtCl_6]^{2-}$ (Firmansyah et al., 2018; Nguyen et al., 2016). The use of undiluted Cyphos® 101 has been specifically studied for the quantitative recovery of Rh(III) (Svecova et al., 2016); nevertheless, using it undiluted is not recommended due to its high viscosity, which will demand a high product consumption and will impact the economy of the process; therefore, in most of the studies a diluent such as toluene or xylene has been added.

A co-extraction of Pt(IV) and Pd(II) is expected when using this extractant, the extraction being explained through an anion-exchange mechanism. This is exemplified in Eq. 25 (Nguyen et al., 2016),

$$[A]^{n-} + \overline{n[P_{66614}]^{+}[Cl]^{-}} \leftrightarrow \overline{([P_{66614}]^{+})_n[A]^{n-}} + n[Cl]^{-} \qquad (Eq.25)$$

where the overbars represent the species in the organic phase, and $[A]^{n-}$ represents the metallic species to be extracted. Following the scheme of Eq. 25, and considering $[PtCl_6]^{2-}$ and $[PdCl_4]^{2-}$ as the predominant species in a HCl media, then the extraction of Pt(IV) and Pd(II) by Cyphos® 101 can be explained by Eq. 26 and Eq. 27 (Nguyen et al., 2016), respectively.

$$[\mathrm{PtCl_6}]^{2-} + \overline{2[P_{66614}]^{+}[Cl]^{-}} \leftrightarrow \overline{([P_{66614}]^{+})_2[\mathrm{PtCl_6}]^{2-}} + 2[Cl]^{-} \qquad (Eq.26)$$

$$[\mathrm{PdCl_4}]^{2-} + \overline{2[P_{66614}]^{+}[Cl]^{-}} \leftrightarrow \overline{([P_{66614}]^{+})_2[\mathrm{PdCl_4}]^{2-}} + 2[Cl]^{-} \qquad (Eq.27)$$

It is important to mention that Rh(III) is not likely to be extracted by Cyphos® 101 when this is diluted in organic diluents (Cieszyñska et al., 2007). This is because Rh(III) forms octahedral complexes with anions such as halides and with oxygen-containing ligands, namely $[RhCl_6]^{3-}$, $[RhCl_4(H_2O)]^{-}$, and $[RhCl_5(H_2O)]^{2-}$ which tend to be difficult to extract due to steric effects (Nguyen et al., 2016).

This difficulty has also been linked to the HCl concentration in the aqueous phase, since a decrease in the extraction efficiency is observed at higher HCl concentrations. For example, for HCl concentrations above 3M, the Rh(III) species change from $[RhCl_5]^{2-}$ to $[RhCl_6]^{3-}$ (Firmansyah et al., 2018), thus, affecting the efficiency due to the change in the chlorocomplex size. It is known that $[RhCl_5]^{2-}$ is smaller than $[RhCl_6]^{3-}$, therefore, its charge density is higher than in $[RhCl_6]^{3-}$, hence

making the extraction of $[RhCl_6]^{3-}$ harder because the ion extraction is directly proportional to the metal ion charge density.

Considering the above principle for the three chlorocomplexes of PGMs, the Pt one has proven to be the most stable and most likely to be extracted, this is because the diameter of the $[PtCl_6]^{2-}$ is larger than the rest, which is translated into a lower absolute value of the Gibbs energy of solvation and an easier extraction (Papaiconomou et al., 2015).

2.3.2.2.2.2 Cyanex® 921

The commercial family of compounds known as Cyanex® includes organophosphorus reagents that can exhibit different structural and chemical properties. In the market there are several Cyanex® extractants, such as Cyanex® 921, Cyanex® 272, Cyanex® 301, Cyanex® 923, Cyanex® 302, Cyanex® 905, Cyanex® 471X, etc. acting in two principal ways (Cytec, 2013):

- Acidic extractants, and
- Solvating extractants.

The acidic extractants, Cyanex® 272 and 301 were developed for the separation of Co from Ni, and the separation of rare earth metals from other elements; the solvating extractants Cyanex® 921 and 923 have a broader spectrum of applications, like the recovery of solutes and inorganic mineral acids from waste effluents and/or metal extraction processes.

Cyanex® 921 (Figure 2.11) is the commercial name for TOPO that contains trialkyl phosphine oxides as the active ingredient (Iyer & Pawar, 2002), and has been trading successfully for the recovery of metals like U and others. It is the most stable member of the family of organophosphorus solvating agents, and it exhibits a higher solubility in aromatic diluents than its homologues, together with the characteristics shown in Table 2.8 (Sigma Aldrich, 2010).

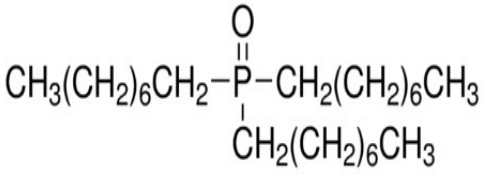

Figure 2.11 Cyanex® 921 chemical structure, own drawing.

Table 2.8 General information about Cyanex® 921	
Aspect	**Specification**
Chemical name	Trioctylphosphine oxide (TOPO)
CAS number	78-50-2
Molecular formula	$[CH_3(CH_2)_7]_3PO$
Molecular weight	386.63 g/mol
Density at 25 ºC	No available data
Viscosity at 55 ºC	15 cP

In the case of PGMs extraction, the use of Cyanex® 921 was tested for the separation of Pd(II), Pt(IV) and Rh(III) under two conditions: with and without addition of tin chloride ($SnCl_2$) in the aqueous feed (Mhaske & Dhadke, 2001). It showed selectivity towards Pd(II), with a quantitative extraction at HCl concentrations between 4.5 to 7M and without $SnCl_2$, while the extraction of Pt(IV) and Rh(III) for the same range was negligible.

The idea of the addition of $SnCl_2$ was an attempt to increase the extraction of the PGM-chlorocomplexes by the reduction to Rh(I)- and Pt(II)-tin complexes, with the simultaneous oxidation of Sn(II) to Sn(IV), in order to increase the extraction percentage (%E) of the two metal ions. The optimized conditions can be appreciated in Table 2.9 (Mhaske & Dhadke, 2001):

Table 2.9 Optimized conditions for the extraction of PGMs with Cyanex® 921			
%E	**Cyanex® 921 conc. (mM)**	**Equilibrium time (min)**	**Aqueous phase**
>99.40 Pd(II)	7.5	5	6M HCl + 1 mM Pd(II)
>99.90 Pt(IV)	10	1	6M HCl + 10 mM $SnCl_2$ + 1mM Pt(IV)
>99.60 Rh(II)	75	1	6M HCl + 250 mM $SnCl_2$ + 1mM Rh(III)

This proves effective the use of Cyanex® 921 for the extraction of PGMs from chloride media. The use of other Cyanex®-alike extractants has also been tested for this purpose, for example:

- The use of 0.5M Cyanex® 923 resulted in a 100% extraction of Pd(II) in HCl-solutions between 0.5 to 9M when diluted with kerosene (Truong & Lee, 2018).
- Another study shows that 0.1M Cyanex® 923 diluted in toluene was able to extract 100% of Pt(IV) at HCl above 0.5M; and >50% of Pd(II) in solutions of HCl above 0.2M (Gupta & Singh, 2013).

Therefore, the application of solvating compounds such as Cyanex® 921 and Cyanex® 923 can be very useful in the SX of PGMs.

2.3.2.2.2.3 Cyanex® 471X

Cyanex® 471X (Figure 2.12) is a phosphine-based extractant developed for the hydrometallurgical recovery of Ag, Pt, and Pd. Contrasting with its phosphine oxide counterparts, Cyanex® 471X is a soft Lewis base, and following the HSAB-principle[9] it will interact readily with metal ions considered as soft acids, such as Pd(II), Pt(II), Ag(I), Cd(II), Hg(I), Hg(II) and Au(I) due to their low oxidation states and their easiness to be polarized (Ahmed et al., 2011; Cytec, 2013). Its general information is shown in Table 2.10 (Cytec, 2013).

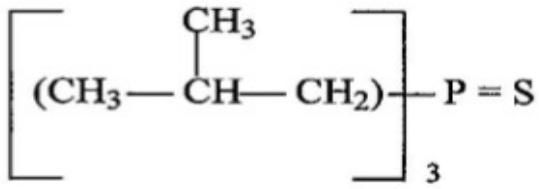

Figure 2.12 Cyanex® 471X chemical structure, own drawing.

Table 2.10 General information about Cyanex® 471X

Aspect	Specification
Chemical name	Triisobutyl phosphine sulfide
CAS number	-
Molecular formula	$[(CH_3)_2CHCH_2)]_3P=S$
Molecular weight	238.38 g/mol
Density at 25 ºC	No available data
Viscosity at 25 ºC	No available data

[9] Identifies the products of a Lewis acid-base reaction and their stability. In this case, Cyanex® 471X is a soft base, therefore, will form strong and stable bonds with a soft acid (Dictionary, 2018).

The characteristic of having an S-atom as a donor atom makes this compound appropriate for the extraction of noble metals but can make its stripping challenging. It has been used for the recovery of Pt(IV) and Pd(II) in different acidic media showing promising results, such as:

- A 0.1M Cyanex® 471X system dissolved in toluene was tested in a range of 0.1 to 8M HBr and the results were compared with results for HCl. In this study, Cyanex® 471X extracted over 99% of Pd(II) and over 98% of Pt(IV) from an aqueous phase of 6M HBr + 0.1M $SnCl_2$, and such results proved to be comparable with a HCl media (Duche & Dhadke, 2001).
- Another study showed a >90% recovery of Pd(II) using 0.01M Cyanex® 471X dissolved in kerosene for an aqueous feed of 0.5M HNO_3; in here, according to the experimental results a relationship between the *D* ratio and the [Cyanex® 471X] gave a straight line with a slope around one, this indicates that the 1 mol of Cyanex® 471X extracts one Pd(II) species according to Eq. 28 (Ahmed et al., 2011).

$$Pd(NO_3)_2 + \text{Cyanex® 471X} \leftrightarrow Pd(NO_3)_2 \cdot \text{Cyanex® 471X} \qquad (\text{Eq. } 28)$$

In both cases, the proposed mechanism of extraction is a solvation mechanism; with this mechanism, the %E increased with the increased stability of the bond between the donor atom of the reagent and the central metal ion. In studies for the extraction of Pd(II) from HBr media with Cyanex® 471X, the slope of the plot log *D* vs log [Cyanex® 471X] was one, which indicates that the stoichiometry of the reaction is 1:1, in agreement with other reports (Duche & Dhadke, 2001).

MATERIALS AND METHODS

3. MATERIALS AND METHODS

In the present work two different spent ACCs were received, described as follows:

- Spent ACC from a Seat Ibiza 1995, with 23 years of use, henceforth **I95**.
- Spent ACC from a Honda Civic 1998, with 20 years of use, henceforth **H98.**

Both I95 and H98 were received complete, this is, received in the metallic shell with entrance and exit tubes. These metallic components were removed with a metal saw in order to extract the honeycomb. Figures 3.1 and 3.2 show the metallic shell and the honeycombs for H98 and I95, respectively.

Figure 3.1 Metallic shell and H98-honeycomb, after removal.

Figure 3.2 Metallic shell and I95-honeycomb, after removal.

3.1 Preparation of the samples

Once the honeycombs were extracted, a grinding operation was performed with the objective of the homogenization of the material and the reduction of the particle size to improve the reaction rate (Havlik, 2008). In this grinding operation a K, MF 10

Basic IKA Werke cutting mill with a 2.0 mm discharged grid was used at a speed of 3000 rpm. After the milling, the resulting powder of the ACCs was collected and weighted, with the following total mass values:

- H98= 505.85 g total weight
- I95= 850.51 g total weight

3.1.1 Particle size characterization

The particle size characterization was assessed using a Retsch AS 2000 apparatus, with a sieve series from 43µm to 2.83mm of aperture, shacked mechanically at a 60-amplitude cycle for a total time of 60 min.

3.1.2 Grinding and separation

To guarantee the homogeneity of the material in further tests, both samples were divided into their quarter portions using a Jones riffle splitter, which consists in a steel sheet with 16 opposite chutes, which are inclined 45º, allowing the separation into two identical samples of a smaller size (Sommer, 1986). The resulting weights after this division are presented in Table 3.1.

Table 3.1 Weights of the portions after the splitter division

Sample	Total weight (g)	Half portions (g)		Quarter portions (g)	
H98	505.81	245.53	**260.28**	124.42	**135.10**
I95	850.51	417.56	**432.95**	209.73	**220.62**

The portions marked in bold font in Table 3.1 were submitted to a further division. This second division consisted in the use of a Spinning Riffle Sampling Microscale-LTD device to divide them into sixteen parts. The resulting homogenized samples were used in all the leaching experiments. The total mass used was:

- 16 samples of I95 of 16.75g.
- 16 samples of H98 of 16.90g.

3.2 Elemental composition

After the homogenization and preparation of the catalyst samples, a digestion employing *aqua regia* (mixture of 3 parts of HCl 37%, analytical reagent grade provided by Fisher Scientific UK and 1 part of HNO_3 65% PA-ISO provided by Panreac) was performed in order to know the initial elemental composition of H98 and I95. The digestion was performed in triplicate, using a mass of 0.5g of each catalyst, 30 mL of *aqua regia*, a temperature of 100 ºC, and a total time of 2h. After the reaction, a 1 mL aliquot was taken and gouged in a 50 mL volumetric flask, for each of the experiments (as shown in Figure 3.3). These solutions were analyzed by Inductively Coupled Plasma-Atomic Emission Spectrometry (ICP-AES)[10], Horiba Jobin-Yvon Ultima model.

Figure 3.3 Solutions after the digestion with aqua regia and prior to the ICP analysis.

3.3 Leaching step

3.3.1 Pre-treatment reaction with H_2SO_4

As discussed in the previous section, pre-treatment steps are often used to reduce the amount of Al in this type of procedures; therefore, a digestion with H_2SO_4 (98%, provided by Sigma Aldrich) was performed prior to the leaching step with HCl, with the intention of obtaining a more PGMs-concentrated liquor. The tests were carried

[10] Annex II provides a deeper description of this analytical method and the determination limits used.

out on a 2g sample of each catalyst with 1g of H_2SO_4 for 1h, at 200 ºC. The remaining solids were then submitted to a leaching step with water during 2h at 60ºC, using two different L/S ratios, one of 5 L/kg and another of 25 L/kg. Finally, after the water leaching, the solids were submitted to HCl-leaching using a concentrated solution of HCl 11.6M and 1% wt/v of H_2O_2, for 3h at 60 ºC, with a L/S ratio of 2 L/kg.

3.3.2 Direct HCl-leaching

Figure 3.4 Cylindrical glass reactor used in the HCl leaching experiments.

For the case of the HCl leaching experiments, the leaching samples were prepared by dissolution of appropriate volumes of HCl (37%, analytical reagent grade provided by Fisher Scientific UK) directly as received, without further purification.

These experiments were carried out in a 50mL closed cylindrical glass reactor, provided with a temperature control, to measure the temperature inside the reaction pulp, and controlled magnetic stirring set up at the appropriate stirring speed according to the experimental scheme. The device is shown in Figure 3.4. The reaction time was set when the solids were dropped into the reactor, which already contained the HCl solution at the desired temperature.

When the leaching experiments reached 20min, 1h and 3h, small volumes of the pulp were taken and centrifugated; from these volumes a 1mL aliquot of the clear solution was taken and gauged in a 20mL volumetric flask, to be sent to ICP-AES analysis. At the end of each experiment, the resulting suspensions were filtered, and the solids were washed with 70mL of demineralized water, dried and weighted.

3.3.3 Analysis of the residues

After the HCl-leaching process, the remaining solids were kept in an oven for 48h at 55 ºC to evaporate the remaining water from the washing procedure. When appropriate, a 0.5g sample of the solids was taken and submitted to a second digestion with 15 mL of *aqua regia* for 2h at 100 ºC; the resulting solution was gouged in a 20 mL volumetric flask and sent to ICP-AES analysis to determine the metal concentration in the residues, to allow a correction in the mass balances of the metal concentrations, and thus a rectification of the leaching yields whenever that confirmation was necessary. In fact, the procedure of analysing the final residues was applied to the tests where the results appeared to be out of the expected, due to the heterogeneity of the catalyst samples.

3.4 Solvent extraction step

Once all the experiments of the leaching step were completed, and the appropriate reaction conditions were established, leaching experiments with larger catalyst amounts and leaching volumes were carried out. At the end, the following metal concentrations (mg/L) for the two catalyst samples were obtained (Table 3.2):

Table 3.2 Initial metal concentrations in real solutions from the leaching step

Sample	T (°C)	L/S ratio (L/kg)	[HCl] (M)	Initial Vol (L)	Metal concentration in the sample (mg/L)				
					Pd	Pt	Rh	Al	Ce
H98	60	2	11.6	0.0338	1610	412	62.4	4579	6354
I95	60	2	11.6	0.0335	0	785	65.7	3562	6870
Combined concentrations					805	599	64	4071	6612

The above PGM concentrations became the targeted concentrations to be extracted during the SX step. Due to the reduced mass available to perform the leaching experiments and, consequently, the reduced volume of the real leaching solutions obtained to develop the SX scheme (and considering the different types of extractants suggested in the literature), it was decided the employment of model solutions using laboratory standards, to emulate the concentration of the real solutions, in order to test several extractants and conditions prior to their application in the tests with real solutions.

3.4.1 SX scheme with model solutions

In the preparation of the model solutions, it was decided to use one-third of the value of the combined real concentrations, to decrease the volume of standards needed. Also, according to the revised literature, the extractants chosen showed better results at lower HCl concentrations; therefore, the model solutions were prepared in order to have 6M and 3M HCl concentrations. Table 3.3 shows the theoretical concentrations of the model solutions.

Table 3.3 Theoretical initial concentration (mg/L) of model solutions

[HCl] (M)	Solution	Pd	Pt	Rh	Al	Ce	Fe
6	M1	265	200	20	1360	3300	100
3	M2	133	100	10	680	1650	50
6	M3	265	200	20	1360	3300	100

The stoichiometric calculations were performed accordingly, and adequate quantities of Pd (Pd standard solution 1000µg/mL in 10-20% HCl provided by Chem-Lab), Pt (Pt standard solution 1000 mg/L ± 4mg/L in 5% w/w HCl provided by Fluka), Rh (Rh standard for AAS 999 mg/L ± 9 mg/L in 5% w/w HCl provided by Fluka), $AlCl_3 \cdot 6H_2O$ (99% reagent plus provided by Sigma-Aldrich) and $FeCl_3$ (provided by BDH Laboratories) were mixed in order to acquire the desired metal concentrations for a volume of 100mL of model solution M1 and M3. Solution M2 was acquired by dilution of 50mL of M1 until reaching a volume of 100mL.

The preparation of the extractants followed the principle of maintaining a 45 times excess concentration in regard to the PGMs concentration; therefore, adequate quantities of tributylphosphate (TBP) (provided by Sigma-Aldrich) , Cyanex® 471X (provided by Cytec Canada Inc.), Cyanex® 923 (TOPO) (provided by Sigma-Aldrich) and Adogen® 464 (provided by Sigma-Aldrich) were dissolved separately in toluene to prepare 100mL of a 0.1M organic phase solution for all the cases.

Finally, for the SX experiments, equal volumes of each organic phase were put in contact with the model solutions (15mL, A/O= 1) during 1h, at a constant and fixed

agitation. The aqueous phases were filtered and collected for ICP-AES analysis. The metal concentrations in the organic phases were calculated by mass balance.

3.4.2 SX scheme for the real leaching solutions

For the SX experiments in the real leaching solutions, and after the determination of the suitability of the chosen extractants in the model solutions, the scheme presented in Figure 3.5 was applied for the SX of the H98 sample.

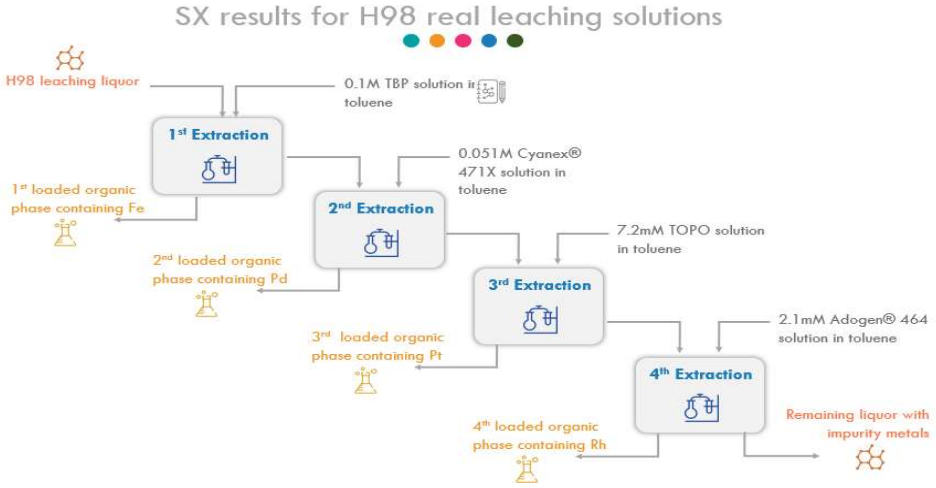

Figure 3.5 SX scheme for the real leaching solution from H98.

On the other hand, and due to the lack of Pd(II) in the I95 sample, the SX scheme used for the leaching of the I95 real solutions is disclosed in Figure 3.6.

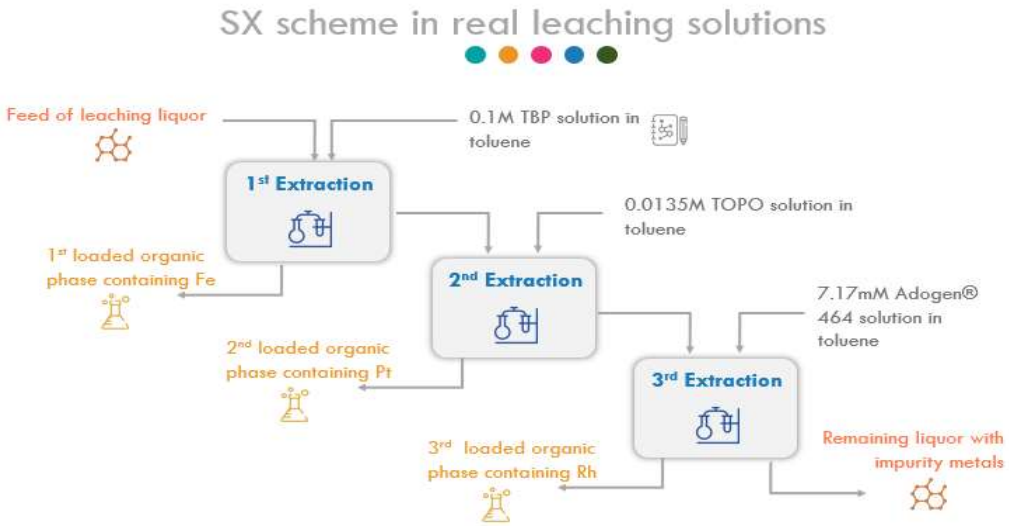

Figure 3.6 SX scheme for the real leaching solution from I95.

In both cases, the concentrations of the extractants were calculated considering a 45 times excess concentration in regards of the PGMs concentrations. Both leaching solutions were diluted once, with equal volumes of demineralized water, in order to reach a 6M HCl concentration. As previously, samples of the aqueous phases after each extraction were taken for metal analysis by ICP-AES.

It is important to mention that even though the SX scheme for the real leaching solutions considered in Figures 3.5 and 3.6 was considered a good approach, due to the low concentration of Rh(III) in the catalyst samples, and the economic viability, it was decided to not perform the fourth extraction test shown in Figure 3.5, neither the third extraction test shown in Figure 3.6.

Cyphos® 101 was tested separately; therefore, the extraction scheme for both catalyst samples was the same. In this SX scheme, the leaching liquors were diluted twice, until reaching a 3M HCl concentration; after that, a first extraction cycle using a 0.1M TBP solution in toluene, to remove the content of Fe was performed, followed by a second extraction cycle with a solution of 0.1M Cyphos® 101 (provided by Sigma-Aldrich) in toluene in order to extract Pd(II) and Pt(IV). In this case, due to the low content of Rh(III) it was decided not to perform any further extraction and leave the Rh(III) in the final aqueous phase. As before, samples of the aqueous phases after extraction were collected for ICP-AES analysis.

The stripping of the organic phases coming from model and real solutions was performed after the extraction step. For this purpose several stripping agents were searched in the literature (Paiva, 2017; Regel-rosocka et al., 2015) and the most suitable to our project were chosen as follows:

- A 1M HCl solution to strip Fe from TBP
- A 0.4M malonic acid solution (provided by Sigma-Aldrich) to strip Pt from TOPO
- A stabilised solution of 1M $Na_2S_2O_3$ to strip Pd from Cyanex® 471X.

The sodium thiosulfate solution was chosen from the safety data sheet provided by the manufacturer of Cyanex® 471X (Cytec, 2013). To prepare 1L of solution the

following steps were carried out: in 600mL of water at 50ºC 240g of $Na_2S_2O_3 \cdot 5H_2O$ (provided by Merck) were dissolved, with agitation for 10min; after that point, the addition of 15g of Na_2SO_3 (provided by M&B Laboratory), 48mL of CH_3COOH (28%) (provided by Sigma-Aldrich), 7.5g of crystals of H_3BO_3 (provided by Panreac Quimica SA) and 15g of $AlK(SO_4)_2 \cdot 12H_2O$ (provided by M&B Chemicals) was performed, one reagent after another, until all were incorporated. The solution was stirred for more 30min and then cooled down to room temperature.

For the stripping stage, the stripping of Pd(II) and Pt(IV) from Cyphos® 101 was performed sequentially. The first cycle was the use of a 1M HCl solution to strip Fe from the TBP organic phase, followed by a second cycle using a 0.1M KSCN solution (provided by Sigma-Aldrich) to strip Pt(IV), and finally, a third cycle employing 0.1M CH_4N_2S (provided by Sigma-Aldrich) in 5% v/v HCl solution to strip Pd(II) from the IL. The analytical procedure for the analysis of the aqueous phases was carried out similarly. The treatment of the results from the ICP-AES analysis were carried out as the ones from the leaching step, meaning, considering a 5% uncertainty affecting the measurements of the corresponding metrics of the SX.

RESULTS AND DISCUSSION

4. RESULTS AND DISCUSSION

4.1 Particle size characterization

The catalyst samples were processed and grinded according to the procedures previously described and were subsequently characterized. Tables 4.1 and 4.2 show the particle size distribution of H98 and I95, respectively.

Table 4.1 Particle size analysis for H98

No. Sieve	Aperture (mm)	H98 retained (g)	%	% accumulated
7	2.83	0	0.00	0.00
10	2.00	0	0.00	0.00
14	1.41	0.13	0.10	0.10
18	1.00	0.59	0.47	0.58
25	0.71	11.35	9.13	9.71
35	0.50	34.92	28.10	37.81
45	0.35	22.05	17.74	55.55
60	0.25	9.2	7.40	62.95
80	0.177	6.89	5.54	68.50
120	0.125	11.73	9.44	77.94
170	0.088	7.07	5.69	83.63
230	0.063	5.5	4.43	88.05
325	0.044	6.51	5.24	93.29
330	0.043	8.34	6.71	100.00
total		**124.28**	**100**	**100.00**

Table 4.2 Particle size analysis for I95

No. Sieve	Aperture (mm)	I95 retained (g)	%	% accumulated
7	2.83	0	0.00	0.00
10	2.00	0.02	0.02	0.02
14	1.41	0.04	0.04	0.06
18	1.00	0.29	0.28	0.34
25	0.71	9.99	9.75	10.10
35	0.50	29.03	28.35	38.44
45	0.35	19.57	19.11	57.55
60	0.25	9.2	8.98	66.54
80	0.177	6.8	6.64	73.18
120	0.125	5.59	5.46	78.63
170	0.088	4.34	4.24	82.87
230	0.063	5.79	5.65	88.53
325	0.044	6.12	5.98	94.50
330	0.043	5.63	5.50	100.00
total		**102.41**	**100**	**100.00**

Using the data from Tables 4.1 and 4.2, the appropriate metrics to describe the particle size distribution were obtained. The D-values D10, D50 and D90, corresponding to the characteristic sizes of the 10, 50 and 90% of the particle cumulative weight, respectively (Technology, 2018) are shown in Table 4.3 for both catalysts.

Table 4.3 D-values of the particles for H98 and I95

D-value	H98 size (mm)	I95 size (mm)
D10	0.708	0.710
D50	0.397	0.409
D90	0.056	0.058

According to Table 4.3, 50% of the particles weight (D50) of H98 have a size of 0.397mm or less; for I95, the 50% of the particles weight have a size of 0.409mm or less. In the same way, 90% of particles weight of H98 are 0.056mm or less, and the 90% of particles weight of I95 are 0.058mm or less. In Annex III, a photographic presentation of the sievings and the particles retained for I95 is shown.

4.2 Elemental composition

A visual evaluation of the solutions from the digestion with *aqua regia* prior to the ICP-AES analysis showed light-yellow colored solutions, which is within the range of colors expected due to the oxidation number of PGMs dissolved (Cotton, 1997). The reference concentrations for the ICP-AES test were 9M HCl and 4M HNO_3. With this test ten of the most common metals found on ACCs, according to the literature, were evaluated (Ahmed et al., 2011; Mhaske & Dhadke, 2001). An average initial concentration for all the metals, and the corresponding standard deviations, are shown in Table 4.4.

Table 4.4 Initial metal composition for both catalysts

Sample	wt%	Pt	Pd	Rh	Al	Ce	La	Mg	Zr	Ca	Fe
H98	average	0.1014	0.3403	0.0205	2.6218	0.8094	0.4358	0.7591	0.0005	0.5526	0.0693
	std dev	0.0118	0.0395	0.0021	0.7559	0.0870	0.0432	0.2284	0.0001	0.0654	0.0129
I95	average	0.1373	-	0.0110	0.8091	0.7810	0.0068	0.1480	0.0002	0.0761	0.0297
	std dev	0.0142	-	0.0010	0.1292	0.0527	0.0007	0.0308	0.0001	0.0038	0.0008

Note: The contents express the soluble forms attained by the *aqua regia* chemical attack.

Table 4.4 states a clear difference between the catalysts. I95 does not contain Pd and, for this reason, the leaching experiments were performed separately, in order to evaluate the behavior respecting the different metal compositions.

An X-ray fluorescence analysis, in a Thermo Fisher Scientific equipment, was performed for the determination of the wt% of Al and Ce, because these elements are not soluble enough in *aqua regia* media to take the results from ICP-AES as reliable. For the PGMs, further corrections were also considered during the execution of the experimental leaching work, since several final residues were analysed and, subsequently, some of the initial contents could be rectified (by mass-balance between leach liquors and residues compositions).

These calculations led to the data presented in Table 4.5, where the corrected values considered in all further calculations as the initial metal contents of each catalyst are shown. It is worth noting that, from this point on, only Pd(II), Pt(IV), Rh(III), Al(III) and Ce(III) will be considered in the calculations, since the former three elements are the targeted metals of this study and the last two elements are considered here as the main impurities involved in the process.

Table 4.5 The initial average content of metals (wt%)

wt%	Pd	Pt	Rh	Al[11]	Ce[12]
H98	0.347	0.102	0.020	18.1	3.23
I95	-	0.149	0.012	20.8	4.51

4.3 Leaching step

4.3.1 Pre-treatment step results

In the leaching of PGMs, the use of pre-treatment steps to increase the concentration of PGMs in the leached liquors, as well as the kinetics and economics of the process may be advisable. These steps usually consist in the reduction of the PGMs to the ground state, thus facilitating the leaching recovery, or in the oxidation of impurities (in this case, Al). Both approaches could enrich the concentration of the metals (Saguru et al., 2018).

In the case of the pre-treatment employed in this work, a digestion with H_2SO_4 was applied, followed by water leaching (varying L/S of 5 and 25 L/kg) to dissolve the metal sulfates formed. The residues obtained were then leached in a second step with a 11.6M HCl solution using a L/S= 2 L/kg. The results of this process for H98, considering the H_2SO_4 digestion, the water leaching and the subsequent HCl leaching at the two selected L/S ratios, as well as the global results for the whole process are displayed in Figures 4.1 and 4.2.

[11] Wt% of Al taken from the XRF analysis.
[12] Wt% of Ce taken from the XRF analysis.

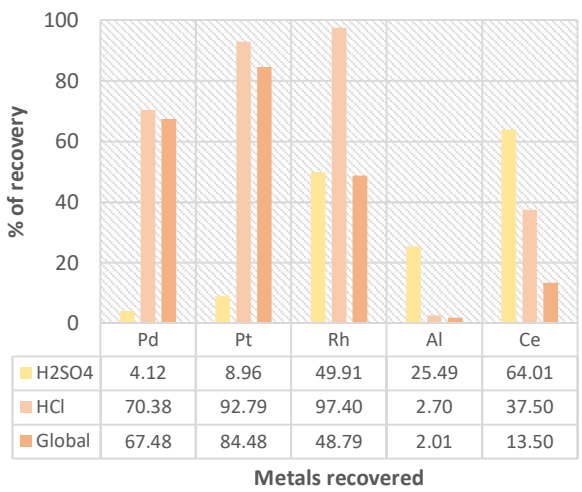

	Pd	Pt	Rh	Al	Ce
H2SO4	4.12	8.96	49.91	25.49	64.01
HCl	70.38	92.79	97.40	2.70	37.50
Global	67.48	84.48	48.79	2.01	13.50

Figure 4.1 Recoveries (%) for H98 for the H_2SO_4 digestion, the water and HCl leachings, with L/S= 5 L/kg.

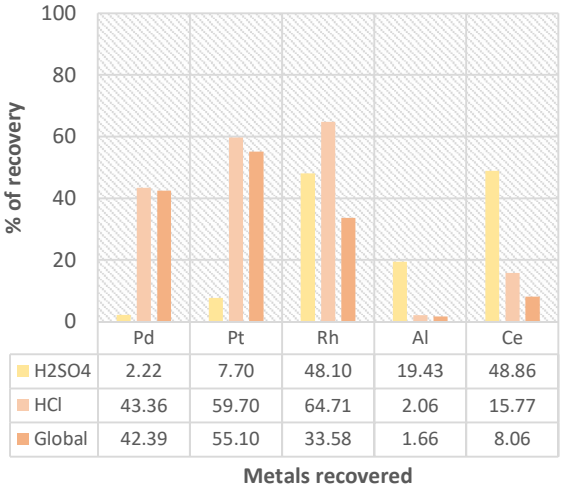

	Pd	Pt	Rh	Al	Ce
H2SO4	2.22	7.70	48.10	19.43	48.86
HCl	43.36	59.70	64.71	2.06	15.77
Global	42.39	55.10	33.58	1.66	8.06

Figure 4.2 Recoveries (%) for H98 for the H_2SO_4 digestion, the water and HCl leachings, with L/S= 25 L/kg.

From Figures 4.1 and 4.2, it can be observed that H_2SO_4 helps to remove a considerable amount of impurities at both L/S ratios, with an approximate 20-25% removal of Al, and between 48-64% removal of Ce from the initial amount of the sample; less than 10% of Pd(II) and Pt(IV) in both cases were removed; nevertheless, this step also showed that almost half of the content of Rh was removed regardless of the L/S ratio.

The followed-up HCl-leaching proved to be more suitable at the smaller L/S ratio, extracting ~93% and ~97% of Pt(IV) and Rh(III), respectively, and about 70% of Pd(II) for L/S= 5 L/kg; in the case of L/S= 25 L/kg, the extraction of the three PGMs lies in the range of 43-65%, and this is a factor to consider in the applicability of this step.

The global yields indicated in Figures 4.1 and 4.2 represent the metals recovery in the second step of HCl leaching in reference to the initial content, in opposition to the yields indicated in the "HCl" data, which represent the recovery of that single operation, taken from the residue produced in the previous step (H_2SO_4 digestion plus water leaching). As a global process for H98, the pre-treatment with H_2SO_4 for a L/S= 5 L/kg represents a recovery of 67, 84 and 48% of Pd(II), Pt(IV) and Rh(III), respectively; and for the L/S= 25 L/kg the recovery is even lower, with 42, 55 and

33% for Pd(II), Pt(IV) and Rh(III), respectively. These percentages are even worse considering the number of metals lost during the two previous steps; therefore, the use of a pre-treatment with H_2SO_4 is not advised for H98 and was not further investigated in this work.

In the same way, Figures 4.3 and 4.4 represent the recovery percentages of the pre-treatment with H_2SO_4, the followed-up leaching step with HCl and the global recoveries for I95, for L/S= 5 and 25 L/kg of the volume of water, respectively.

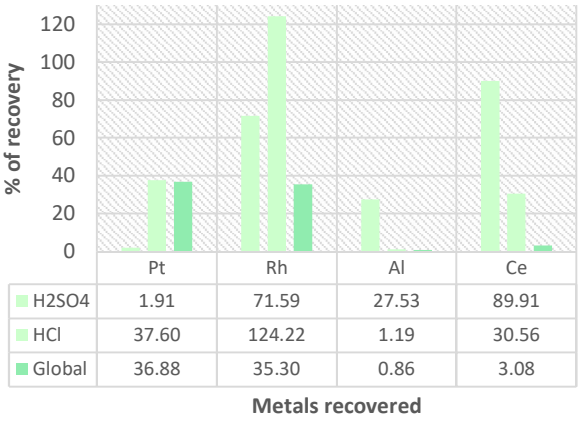

Figure 4.3 Recoveries (%) for I95 for the H_2SO_4 digestion, the water and HCl leachings, with L/S= 5 L/kg.

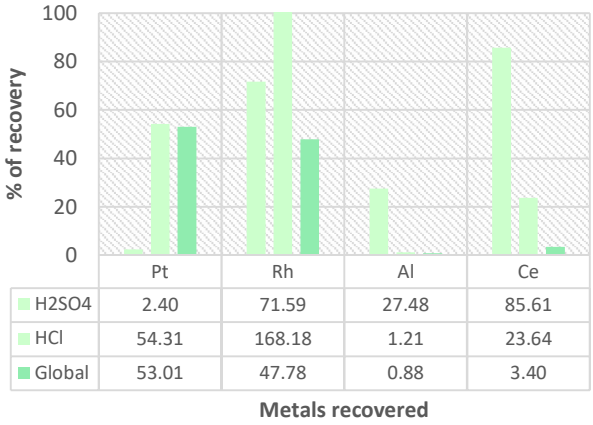

Figure 4.4 Recoveries (%) for I95 for the H_2SO_4 digestion, the water and HCl leachings, with L/S= 25 L/kg.

As depicted in Figure 4.3, for I95 at a L/S= 5 L/kg, the extraction of Rh(III) in the H_2SO_4 pre-treatment is above 70%, while the removal of Al(III) is only of about 27%, accompanied by 90% of Ce(III). In the following HCl-leaching, the totality of Rh(III) was extracted (values are even higher than 100% due to experimental errors) but only 37% of Pt(IV) was recovered, with a low contamination of Al(III), of about 1.2%. As for an L/S= 25 L/kg, showed in Figure 4.4, we can observe a similar behavior, with 71% of Rh(III) extracted in the pre-treatment with H_2SO_4, and with 54% of Pt(IV) leached in the HCl-leaching, together with the totality of Rh(III).

As a global process, the pre-treatment with H_2SO_4 for I95 is also not advised, since it only allowed the recovery of ~37% of Pt(IV) and 35% of Rh(III) of the initial amount,

for an L/S= 5 L/kg. Similarly, 53% of Pt(IV) and ~48% of Rh(III) of the total amount, in the case of L/S= 25 L/kg were again retrieved.

Therefore, as a general conclusion, the employment of a pre-treatment with H_2SO_4 is not recommended due to the low leaching percentages of the PGMs in the general process for both catalysts. Accordingly, this pre-treatment was not further investigated.

4.3.2 Direct HCl-leaching results

In the case of the direct HCl-leaching of the catalysts, the evaluation of the variables with the greater influence over the process was considered, such as temperature (T), leachant concentration ([HCl]), particle size (D_{50}), stirring (min^{-1}), and L/S ratio (L/kg) in order to find the optimized conditions for which the highest recovery of PGMs could be achieved. In all tests, the leaching solution also contained an oxidizer, 1% w/v H_2O_2, whose concentration was not changed during all the experimental work. In Table 4.6 the general template for the 11 leaching experiments carried out is shown. It is worth noting that time control was set at 1h and 3h for all the experiments. The HCl concentrations of 11.6 M correspond to the use of concentrated acid (37 wt% or 12M), the difference from 12 M being due to the slight dilution occurred with the addition of H_2O_2.

Table 4.6 Scheme of the complete set of leaching experiments

Test	Ref.	T (ºC)	L/S ratio (L/kg)	[HCl] (M)	D_{50} (mm)		Stirring (min^{-1})
					H98	I95	
1	L1	60	2	6.0	0.397	0.409	250
2	L2	60	2	8.0	0.397	0.409	250
3	L3	60	2	11.6	0.397	0.409	250
4	L4	60	2.5	8.0	0.397	0.409	250
5	L5	60	3	8.0	0.397	0.409	250
6	L6	20	2	11.6	0.397	0.409	250
7	L7	40	2	11.6	0.397	0.409	250
8	L8	60	2	11.6	0.397	0.409	0
9	L9	60	2	11.6	0.014	0.006	250
10	L10	40	2	8.0	0.397	0.409	250
11	L11	50	2	9.8	0.397	0.409	250

4.3.2.1 Influence of temperature

The evaluation of the influence of temperature was to seek for the lowest possible temperature to carry out the process, while attaining the highest leaching percentages. A low temperature will mean a lesser energy consumption and, therefore, the cost of the process will decrease when scaled-up to an industrial application.

Three different temperatures were evaluated: 20 ºC (room temperature), 40 ºC (average between the lower and upper limit) and 60 ºC (most common temperature in leaching processes) to assess leaching efficiency of the PGMs. On these experiments, the remaining factors (L/S ratio, time, D_{50}, stirring) were kept constant, and two different acid concentrations were considered (8.0 and 11.6M) for both catalysts (Figures 4.5 and 4.6, for H98 and I95, respectively).

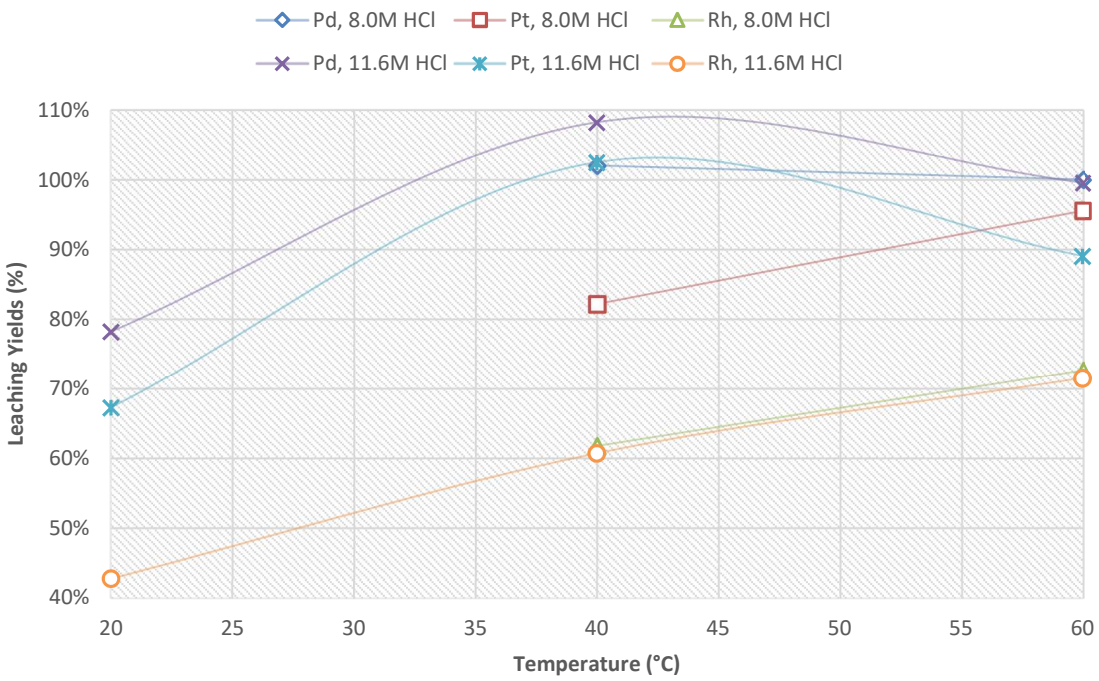

Figure 4.5 Influence of temperature in the leaching yields of Pd, Pt, and Rh of H98 for two HCl concentrations. Remaining factors are constant, t=3h, L/S= 2 L/kg.

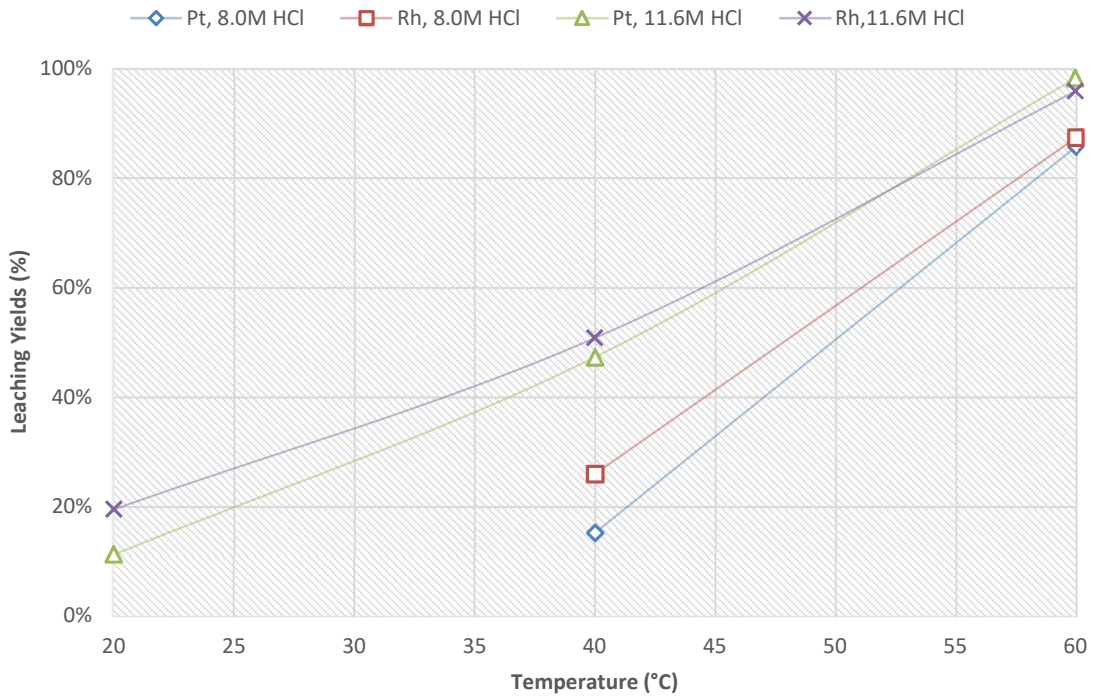

Figure 4.6 Influence of temperature in the leaching yields of Pt, and Rh of I95 for two HCl concentrations. Remaining factors are constant, t=3h, L/S= 2 L/kg.

According to Figures 4.5 and 4.6, the temperature is a determinant factor in the leaching process of PGMs. For this case, the reaction time was set at 3h to assess the difference in behaviors for both catalysts. As a first conclusion, it is stated that the yields of the PGMs increased with the increase of temperature for both leachant concentrations, the highest values being achieved at 60 ºC. The findings confirm the fact that this is the most used temperature in leaching processes among the literature (Jha et al., 2013). The second conclusion obtained is the reactivity of the metals towards the leaching conditions, that can be expressed as Pd(II)>Pt(IV)>Rh(III), with Rh(III) having the lowest yields for the two acidic concentrations studied.

With the conditions employed, the recoveries of Pd(II) and Pt(IV) at 60ºC and 11.6M HCl concentration, for H98 are 100% and 90%, respectively, whereas for I95 the recovery of Pt(IV) is 98% at the same temperature and acidity. Rh(III) yields for H98 at 60ºC are 73% and 72%, for 8M and 11.6M, respectively, while for I95 they are

87% and 96% for the same conditions, indicating that more drastic conditions should be employed for H98 in order to achieve satisfactory recoveries for Rh(III) from this ACC.

4.3.2.2 Influence of acid concentration

The influence of the leachant concentration (in this case, the HCl concentration) was evaluated after the determination of the ideal temperature by two sets of experiments at two different temperatures (40 and 60 ºC), and with three different acid concentrations of 6.0, 8.0 and 11.6M, alternatively considered. Figure 4.7 shows the leaching yields for H98 under these conditions.

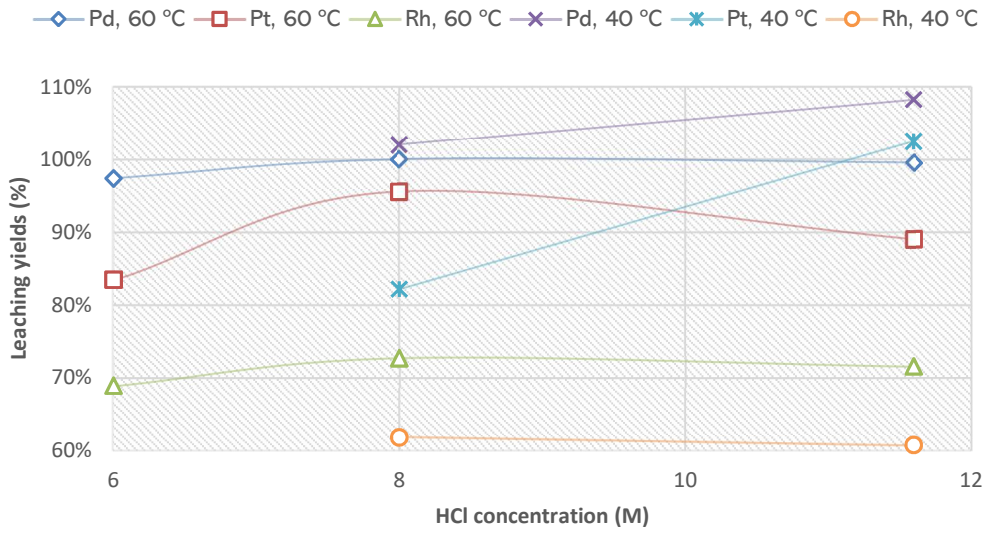

Figure 4.7 Influence of HCl concentration in the leaching yields of PGMs on H98 for two temperatures. Remaining factors are constant, t=3h, L/S= 2 L/kg.

As depicted in Figure 4.7, the highest yields are obtained above 8.0M acid concentration, being practically stabilized after this concentration. The leaching yield of Rh(III) is the lowest among the three metals at both temperatures and for the three acid concentrations proposed; this reassures the hypothesis that Rh might require stronger conditions to provide satisfactory yields. Regarding the yields of Pd(II) and Pt(IV), they showed no relevant difference between 8.0 and 11.6M HCl concentrations at 60ºC, being both concentrations open for consideration as the most favorable acid concentration of the process. Nevertheless, for the same metals,

the yields at 40 ºC showed to be higher than those at 60 ºC; therefore, a deeper analysis was performed regarding the metal concentrations in the final solutions, in order to decide which condition represented the best option. The above-mentioned analysis is presented in Figure 4.8 for 8.0 and 11.6M HCl.

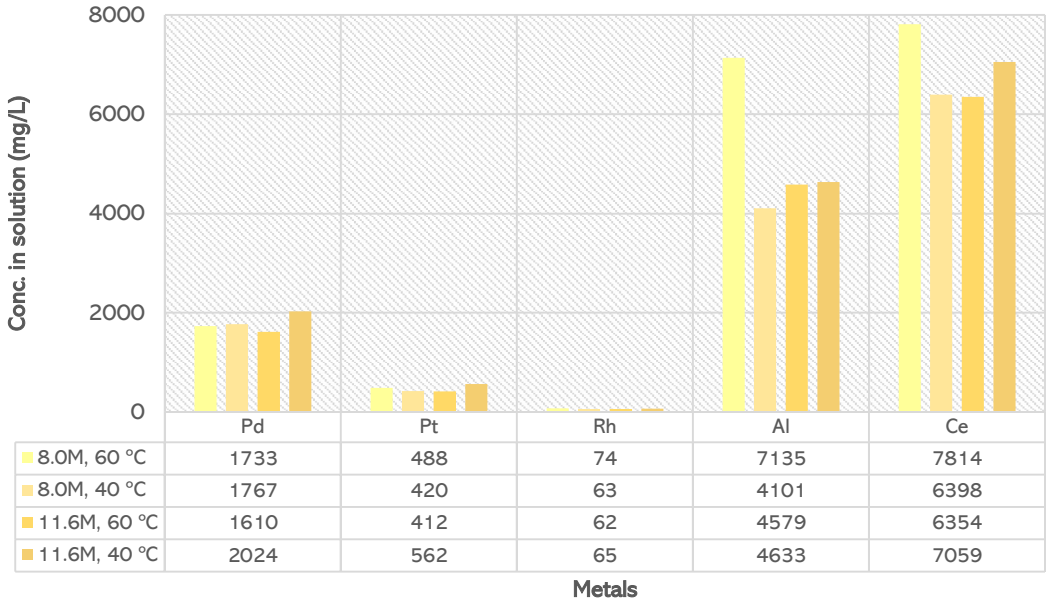

	Pd	Pt	Rh	Al	Ce
8.0M, 60 °C	1733	488	74	7135	7814
8.0M, 40 °C	1767	420	63	4101	6398
11.6M, 60 °C	1610	412	62	4579	6354
11.6M, 40 °C	2024	562	65	4633	7059

Figure 4.8 Metal concentrations in the leach solutions of H98 at 8.0 and 11.6M HCl concentrations, at two different temperatures. Remaining factors are constant, t=3h.

We can observe the differences between the metal concentrations among the leaching conditions; it can be appreciated that the content of PGMs is very similar among the tests, ranging from 1600 to 2000 mg/L for Pd(II), 410 to 562 mg/L for Pt(IV) and 62-74 mg/L of Rh(III). However, this analysis should also be focused on the concentration of those metals considered impurities, such as Al and, in this case, Ce, since it is not one of the targeted metals. Accordingly, analyzing the content of Al in the final solutions, we can firstly discard 8.0M HCl and 60 ºC condition for coextracting up to 60% more Al, in average, compared with the rest of the conditions. Based on the previous information and in terms of acid concentration, the most favorable concentrations for leaching H98 are 8M HCl at 40ºC and 11.6M HCl at 60ºC, for providing a higher PGM-concentrated final solution and, at the same time, coextracting the smallest amounts of Al and Ce.

According to Figure 4.9, the leaching yields for both metals in I95 increased with the increase of the HCl concentration, starting to be considerable (above 80%) from 8.0M HCl and showing satisfactory yields (96 and 98% for Pt(IV) and Rh(III), respectively) at a concentration of 11.6M HCl and a temperature of 60 ºC, making the combination of factors 60 ºC and 11.6M HCl the appropriate conditions for I95. When the yields were measured at 40 ºC, an increase of %E when increasing HCl concentration was also observed; nevertheless, the highest yields attained at this temperature were 47% for Pt(IV) and 51% for Rh(III) with 11.6M HCl, and at 8.0M HCl the yields only attained 15% and 26% for Pt(IV) and Rh(III), showing the disadvantage of the application of 8.0M HCl and 40 ºC for I95.

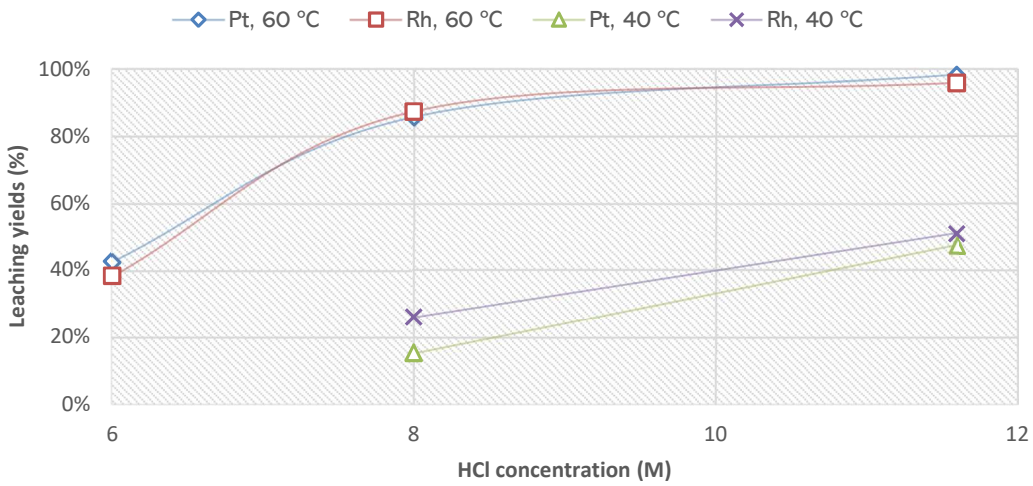

Figure 4.9 Influence of HCl concentration in the leaching yields of PGMs on I95 for two temperatures. Remaining factors are constant, t=3h, L/S=2 L/kg.

With the aim of a further mixture of the catalysts for the SX step, the HCl concentration defined as appropriate was 11.6M, in accordance with the hypothesis that a bigger amount of chloride ions enhance the dissolution of PGMs in the solution, producing satisfactory leaching yields at this stage. Consequently, the best compromise seems to involve a 11.6M HCl concentration and a temperature of 60ºC.

4.3.2.3 Influence of the L/S ratio

The evaluation of the L/S ratio was made in order to obtain an appropriate relationship between the solid sample (kg) and the amount of liquid (L) needed to attain the highest yields possible. This parameter is considered important in the economic evaluation of the leaching process if an industrial scalability is pursued. It is important to emphasize that this work has always aimed at the use of low L/S ratios to, simultaneously, generate concentrated PGM liquors and minimize the co-extraction of impurities present in higher contents in the catalysts. Therefore, three different L/S ratios near the unity were evaluated: 2, 2.5 and 3 L/kg (lower values seemed impracticable regarding handling and mixing), and the results are shown in Figures 4.10 and 4.11 for H98 and I95, respectively.

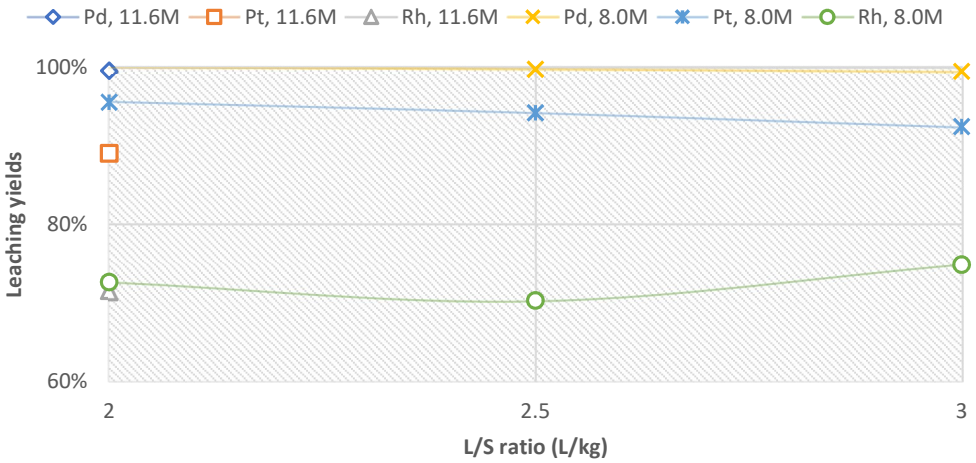

Figure 4.10 Influence of L/S ratio in the leaching yields of PGMs on H98 for 8.0M HCl and single evaluation of L/S= 2 L/kg at 11.6M HCl. Remaining factors are constant, t=3h, T= 60 ºC.

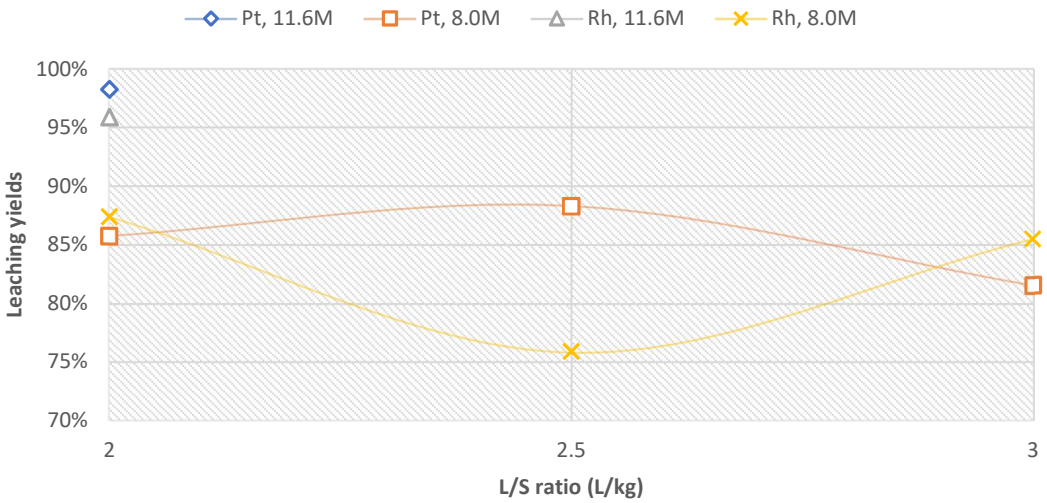

Figure 4.11 Influence of L/S ratio in the leaching yields of PGMs on I95 for 8.0M HCl and single evaluation of L/S= 2 L/kg at 11.6M HCl. Remaining factors are constant, t=3h, T= 60 °C.

As depicted in Figure 4.10, for a HCl concentration of 8.0M the leaching yields showed a small variation (2% only) among the three different L/S ratios evaluated, with the highest yields at 2 L/kg ratio (100, 96 and 73% for Pd(II), Pt(IV) and Rh(III), respectively), and the lowest yields were observed for a L/S ratio of 3 L/kg; these values contribute to the economic factor of the process, because they require a lower amount of leachant and lesser inventory than bigger L/S ratios. On the other hand, a single evaluation of a L/S ratio of L/kg at a concentration of 11.6M HCl was performed, this to evaluate the behavior in a more concentrated media, and it proved to be the most efficient; consequently, the yields in this test were 100, 89 and 72% for Pd(II), Pt(IV) and Rh(III), respectively, proving to be satisfactory for H98.

For I95, Figure 4.11 shows that the yields obtained at 8.0M HCl were lower than for the other catalyst, being L/S= 2 L/kg again the ratio with the highest yields, with 86% for Pt(IV) and 87% for Rh(III); the lowest recovery of Pt(IV) was observed at L/S= 3 L/kg, with only 82%, and the lowest recovery of Rh(III) was obtained at a ratio of 2.5 L/kg. For this catalyst, an evaluation with concentrated HCl was also performed, and greater yields were obtained, with 98% and 96% recoveries of Pt(IV) and Rh(III), respectively.

In order to choose the appropriate L/S ratio for both catalysts, and due to the similarities between the yield percentages at 8.0M and 11.6M HCl, the decision was made in terms of the concentration of metals (mg/L) present in the leached solution. Hence, as previously, an analysis of the % yields with the higher concentrations of PGMs and lower concentrations of Al in the solution was carried out, and can be seen in Figure 4.12 for H98.

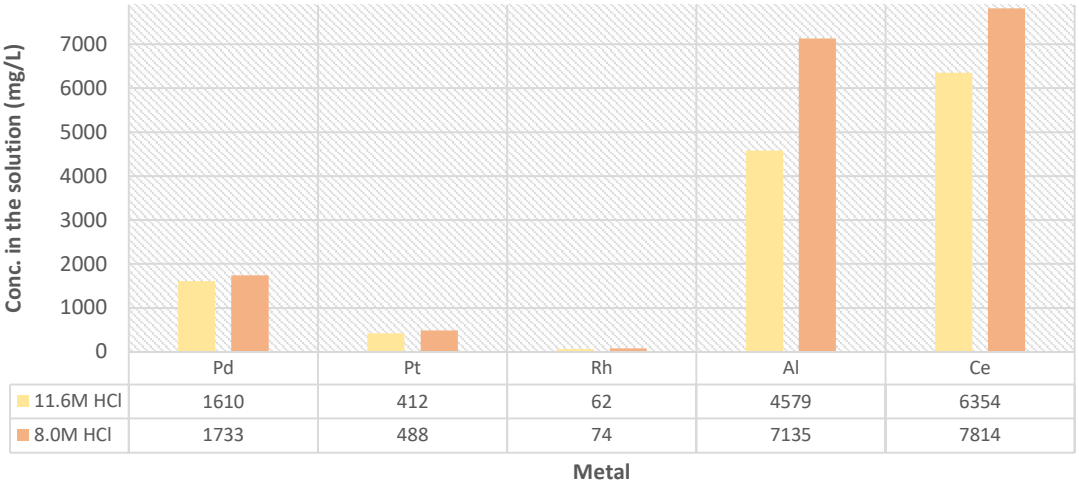

Figure 4.12 Metal concentrations in the leached solutions of H98 at L/S= 2 L/kg at two different HCl concentrations. Remaining factors are constant, t=3h, T= 60 ºC.

According to Figures 4.10 and 4.12, the L/S should be 2 L/kg at a HCl concentration of 11.6M for H98; even though the percentages of Pt(IV) and Rh(III) are a bit lower than those for 8.0M HCl, the concentration of these metals is bigger in this solution and, moreover, the concentration of Al at 11.6M HCl is 4579 mg/L against 7135 mg/L, observed in the leaching at 8.0M HCl. Therefore, in terms of metal recovery and selectivity of the process, the leaching at 11.6M HCl and L/S= 2 L/kg proved to be satisfactory for this sample.

Figure 4.13 confirms the fact that, for I95, the best L/S ratio is 2 L/kg at 11.6M HCl concentration; at these conditions, the leaching yields and the concentration of PGMs in the solution are considerably higher than for 8.0M HCl. This condition is

reaffirmed with the 3561 mg/L of Al contained in the solution at 11.6M HCl against 4970 mg/L of Al coextracted at 8.0M HCl concentration.

Hence, after the evaluation of the corresponding parameters and surrounding variables, the adoption of an L/S= 2 L/kg was accomplished for both catalysts.

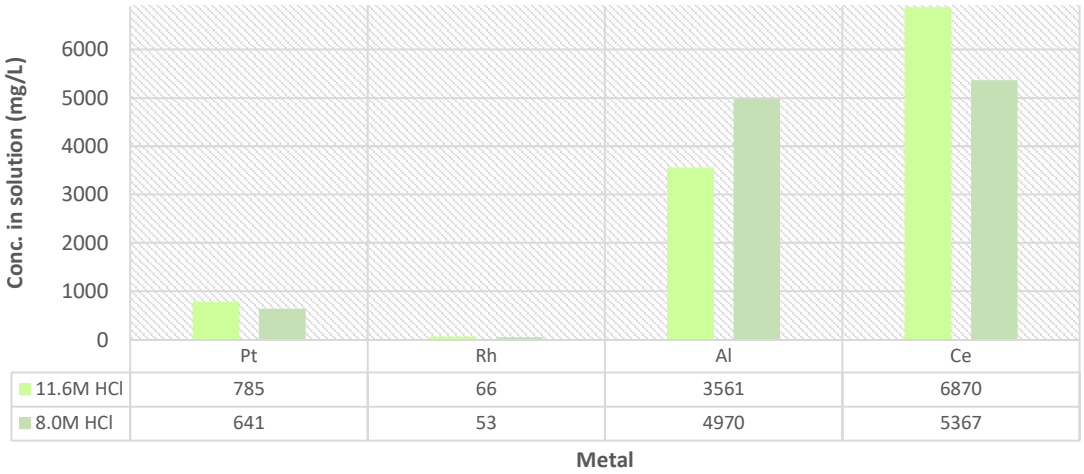

Figure 4.13 Metal concentrations in the leached solutions of I95 at L/S= 2 L/kg at two different HCl concentrations. Remaining factors are constant, t=3h, T= 60 ºC.

4.3.2.4 Influence of time

The reaction time is considered one of the most important variables in any process. In the previous sections, the results were obtained using the fixed time of 3h, but the idea of evaluation of shorter times was materialized, in an attempt to establish a shorter residence time and, in this way, contribute with a lower energy consumption (due to heating and stirring) and lower equipment size, and thus increase the economic viability of the process. The following results (Figure 4.14) are based in three different reaction times (20min, 1h, and 3h) for three different HCl concentrations, all evaluated at 60 ºC.

In Figure 4.14, the leaching yields for Pd(II), Pt(IV) and Rh(III) as a function of time, for three different HCl concentrations are presented for H98. The highest yields are attained always at 3h reaction time, and the lowest yields correspond to the reaction time of 0.3h (20min), regardless the acid concentration of the media. The Pd(II) dissolution shows to be faster than for the other metals: it is above 70% after 20min

for 6.0M HCl, and above 75% for more concentrated HCl solutions. At 3h reaction time, the recovery is 100% for 8.0M and 11.6M, and 97% for 6.0M.

For Pt(IV), half of the initial amount is leached after 20min even for the lower HCl concentration, and continued increasing with the rise of reaction time, reaching 96% extraction for 8.0M HCl and 89% for 11.6M HCl after 3h. Rh(III) extraction proved to be slower regardless of time and HCl concentration, which agrees with the previous results, Rh(III) being the most difficult metal to dissolve in the leaching process.

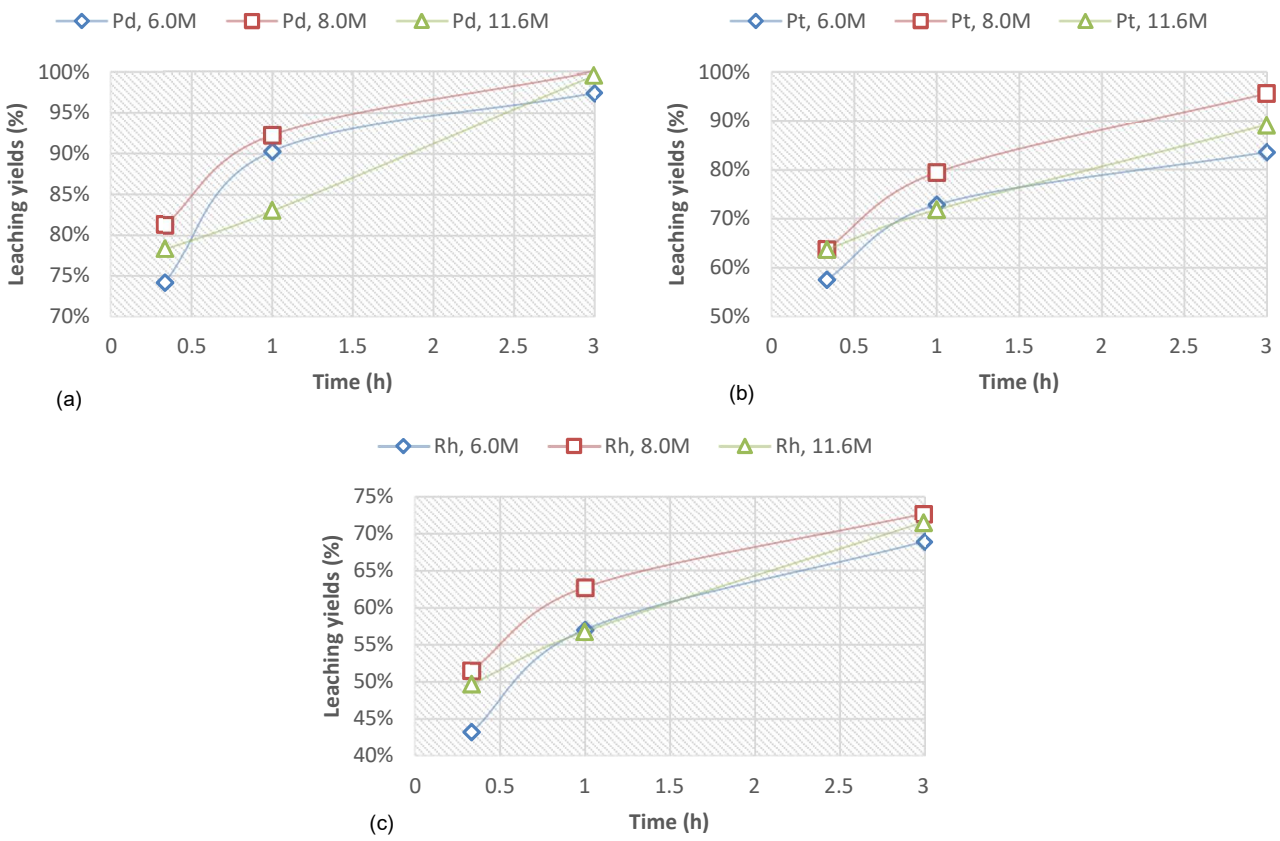

Figure 4.14 Leaching yields (%) of PGMs in H98 as a function of time at 6.0, 8.0 and 11.6M HCl: (a) Pd(II), (b) Pt(IV) and (c) Rh(III). Remaining factors are constant, L/S= 2 L/kg, T= 60 ºC.

The previous results discard 6.0M HCl as a possible leaching condition. Nevertheless, they showed similar percentages for 8.0 and 11.6M HCl. In order to select the best reaction condition, an analysis of the metal concentrations in the final

solutions for both acid concentrations after 3h was needed. This analysis has been already disclosed in Figure 4.12, for the H98 sample.

From Figure 4.12 we can appreciate that, even though the concentration of PGMs is between 10 and 20% bigger at 8.0M HCl, this condition seems to be not suitable when Al coextraction is considered. When comparing the 7135 mg/L of Al coextracted at 8.0M HCl towards the 4579 mg/L of Al present in the leached solution at 11.6M HCl, we can clearly see that the second acid concentration provides a less contaminated solution and a higher selectivity towards PGMs. The above reasoning points out to the use of 11.6M HCl for a 3h reaction time for the H98 sample.

The evaluation of reaction time for I95 was performed in a similar way, and the results are shown in Figure 4.15.

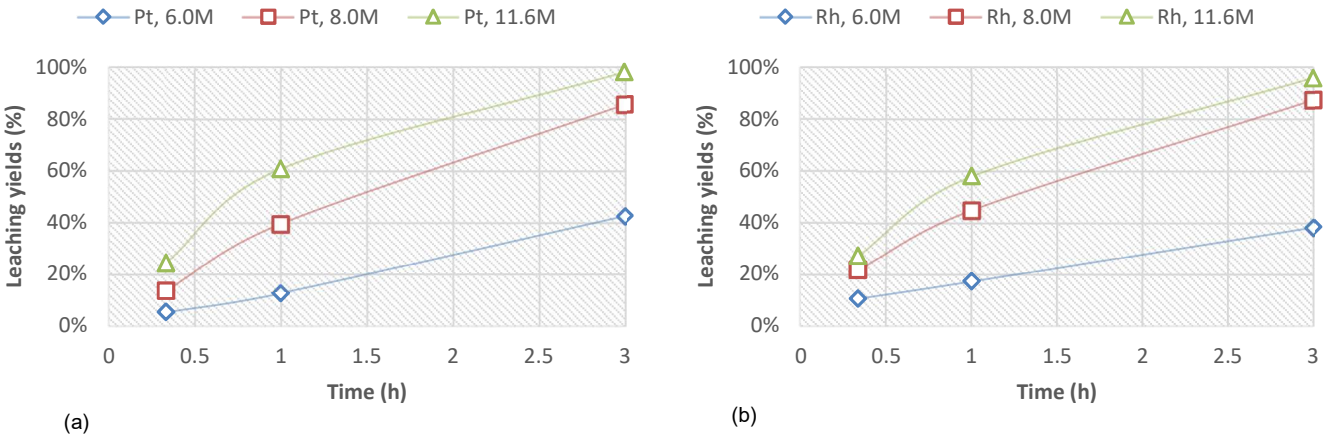

Figure 4.15 Leaching yields (%) of PGMs in I95, as a function of time at 6.0, 8.0 and 11.6M HCl: (a) Pt(IV) and (b) Rh(III). Remaining factors are constant, L/S=2 L/kg, T= 60 ºC.

The leaching yields for Pt(IV) and Rh(III) of I95 are clearly lower for the initial reaction times, proving that PGMs in this catalyst sample react at lower rates than in the other sample. Again the use of 6.0M HCl medium can be discarded, because it provided the lowest leaching yields, only 43% of Pt(IV) and 38% of Rh(III); on the other hand, the maximum yields attained for I95 were 98% and 96% for Pt(IV) and Rh(III), respectively at 11.6M HCl at the end of the test (3h).

It is important to mention that the Rh content of I95 seems to be more reactive than that of H98 (higher final recovery yields for I95, although slower reaction rates). This

different behavior might be attributed to the lifetime conditions of the catalyst, which are unknown. Identifying the species of PGMs present in each catalyst, i.e. by X-ray diffraction would probably be unsuccessful due to their low contents.

4.3.2.5 Influence of stirring

Evaluating the influence of stirring of the leaching step is part of the economic and energy consumption analysis, as stirring is one of the fixed energy consumption requirements in multiple industrial processes; therefore, if it can be eliminated, it will represent less energy and a bigger economic viability of the process.

In the case of the leaching of PGMs from H98 and I95, two stirring conditions were evaluated. In the first one, the stirring was set in automatic mode in the reactor controls, having a value of 250 min^{-1}. For the second condition, the stirring was deactivated to evaluate if the kinetics of the reaction would be the same, namely, to check if temperature and fine particle size were enough to achieve satisfactory leaching yields.

In these experiments, the remaining factors (previously evaluated) were kept constant, and the results obtained are depicted in Figure 4.16 for H98, based on the concentrations of metals in the leached solutions.

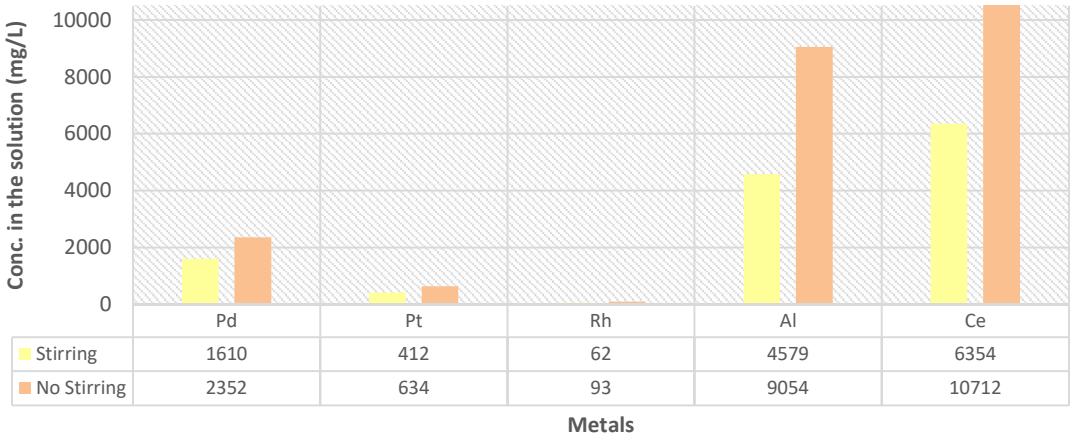

Figure 4.16 Metal concentrations in the leached solutions of H98 for stirred and not stirred leaching experiments. Remaining factors are constant, t=3h, T= 60 ºC.

We can observe that the PGMs in the non-stirred leaching process are 1.5 times more concentrated in the leach solution than in the stirred process; furthermore,

when analyzing the concentration of Al, we can verify that in the non-stirred process around 9000 mg/L of Al were coextracted, whereas in the stirred process only ~4580 mg/L of Al are present. This fact represents an increase of 97% in the coextracted amount of Al and, therefore, this is an important setback in the possibility of a leaching process without any stirring force; the selectivity of the process towards PGMs is necessarily diminished by the increased concentration of Al.

For the analysis of the non-stirred condition for I95 an equal procedure was carried out, and the concentrations of metals in the final solutions are shown in Figure 4.17.

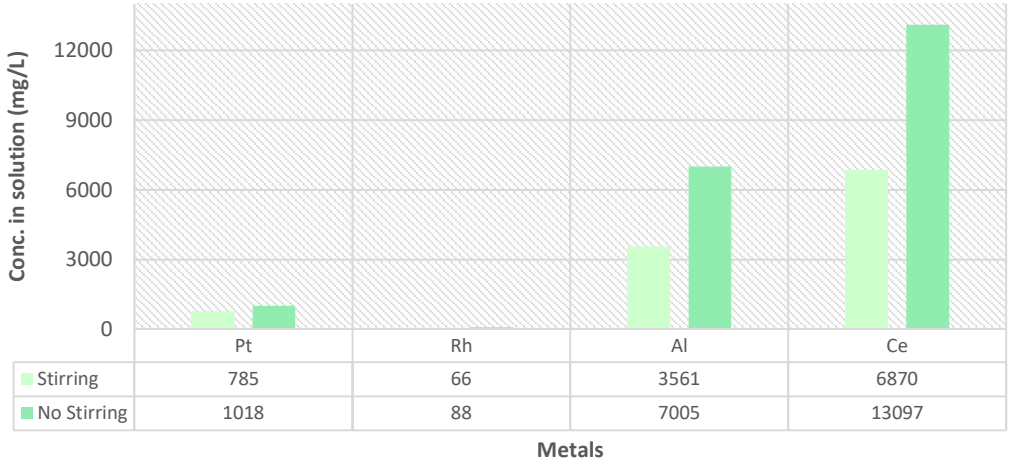

Figure 4.17 Metal concentrations in the leached solutions of I95 for stirred and not stirred leaching experiments. Remaining factors are constant, t=3h, T= 60 ºC.

We can again observe that the concentration of PGMs is about 30% higher in the non-stirred process, but when looking at the corresponding concentration of Al and compare it with the counterpart in the stirred process we can see that the absence of stirring leads to the coextraction of 96% more Al into the final solution, creating a more contaminated liquor, and therefore decreasing the selectivity of the process towards PMGs.

The strong increase in the metal concentrations observed in the leachates under the non-stirring conditions was surprising, and we believe that other non-controlled factors can be responsible for it. The absence of stirring also hinders the convection and the heat dispersion inside the reactor, and therefore probably the temperature

inside was substantially higher than the measured values (namely in the bottom of the vessel, in contact with the heating plate). This can lead to higher dissolutions than expected, namely, in the case of the metal oxides (Al and Ce).

Consequently, after the evaluation of the non-stirred condition for both catalysts, it was found that it is not convenient for the process in terms of PGMs selectivity, as higher amounts of Al are coextracted than in the stirred processes; even though stirring will represent a source of energy consumption, it is a requirement that cannot be suppressed.

4.3.2.6 Influence of particle size

The hypothesis that a finer particle size of the solid samples would provide better leaching yields was also evaluated. This evaluation was done by varying the average particle size. To obtain finer particles, the samples were milled again in a high-energy disk mill for 30 seconds; the resulting powder was size-characterized in a CILAS-1064 equipment by laser diffraction granulometry. Table 4.7 shows the D-values of the finer particles.

Table 4.7 D-values of the particles for H98 and I95 measured by laser diffraction granulometry

D-value	H98 size (mm)	I95 size (mm)
D10	0.0014	0.0010
D50	0.0139	0.0065
D90	0.0463	0.0344

According to the values displayed in Tables 4.3 and 4.7, a reduction of 28 times in the average particle size (D_{50}) for H98 particles, and a 62 times reduction for I95 particles, for the same D-value, were observed. The leaching yields for the finer particles, and the regular particles handled along the previous experiments, are shown in Figure 4.18 for H98.

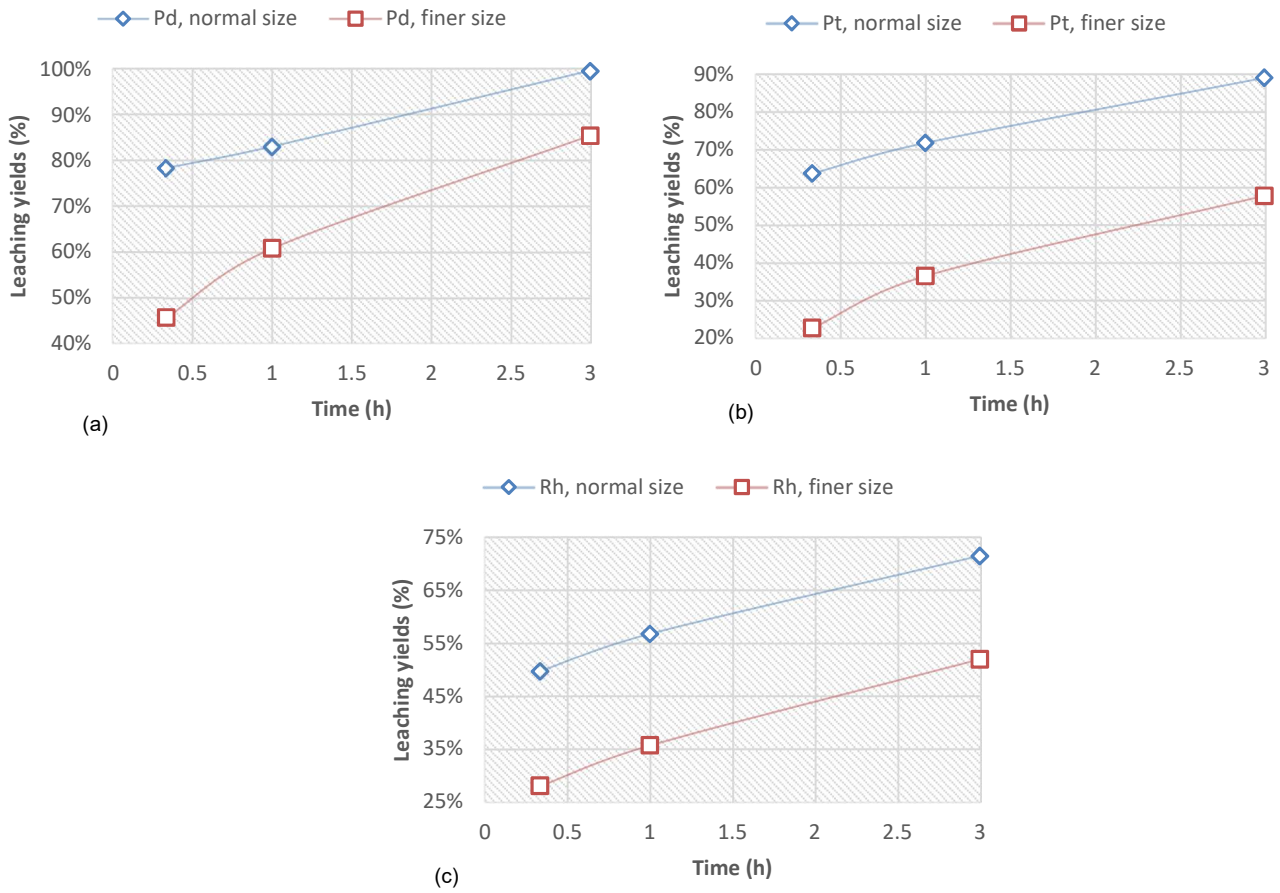

Figure 4.18 Leaching yields (%) of PGMs in H98 at two different particle sizes: (a) Pd(II), (b) Pt(IV) and (c) Rh(III). Remaining factors are constant, L/S= 2 L/kg, T= 60 ºC, [HCl]=11.6M.

This analysis shows a clear difference between the yields obtained with the particle size achieved after the first milling operation, and the smaller particle size acquired after the second milling procedure. As previously demonstrated, the yields increased with the growth of the reaction time, nevertheless, the values with finer particle diameters are not satisfactory in comparison with bigger diameters. The maximum yields attained with a second milling operation are 85%, 58% and 52% for Pd(II), Pt(IV) and Rh(III), respectively, against 100%, 89% and 72% leaching yields at the same reaction conditions but with a bigger particle size. Therefore, decreasing the diameter of the particles is not recommended for H98. This conclusion does not affect the process because a second milling operation would represent a bigger cost

and a higher energy consumption, and if it is not justified by higher yields, then the idea should be discarded.

In the case of I95, the yields obtained for smaller and bigger particle sizes showed to be very similar, as it can be appreciated in Figure 4.19.

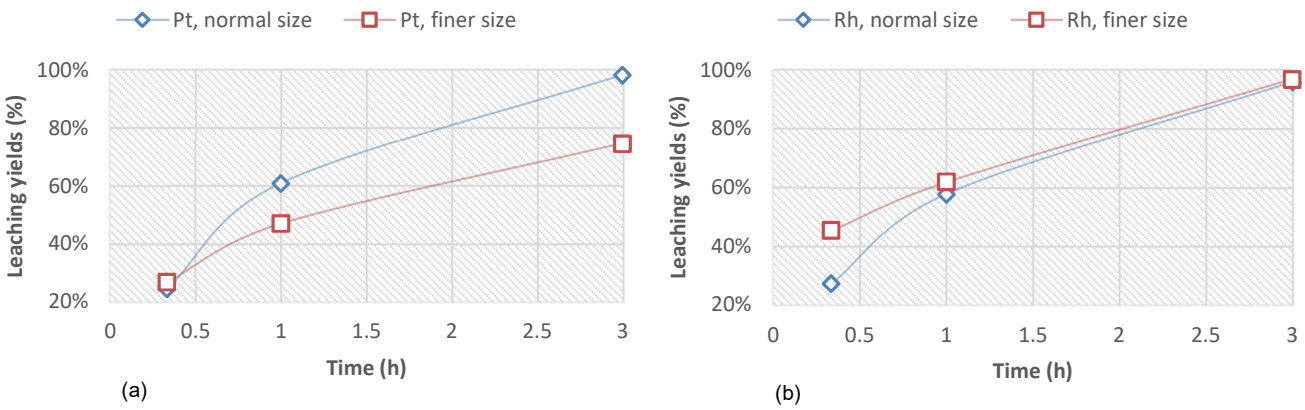

Figure 4.19 Leaching yields (%) of PGMs in I95 for two particle sizes: (a) Pt(IV) and (b) Rh(III). Remaining factors are constant, [HCl]= 11.6M, L/S=2 L/kg, T= 60 ºC.

From Figure 4.19(a), we can appreciate a clear difference in the leaching yields for Pt(IV), with 98% leached from particles with regular diameters towards only 75% extracted from particles with smaller diameters. Nevertheless, the behavior for Rh(III) did not show a great difference regarding the change of diameters in the particles, with 96% leached from regular diameters towards a 97% leached from the particles with a smaller diameter. From the above, even though the first analysis favours regular diameters, the analysis of the metal concentrations in the liquors was made to support the decision. This analysis is depicted in Figure 4.20.

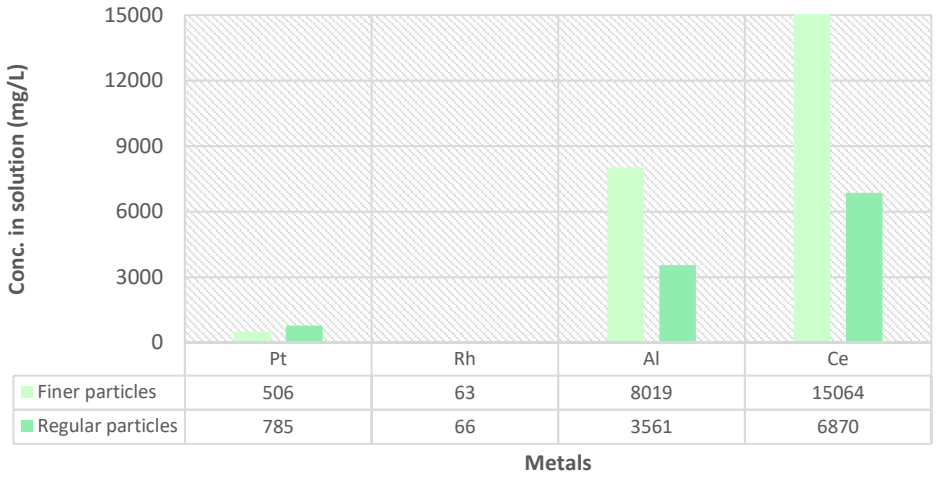

Figure 4.20 Metal concentrations in the leached solutions of I95 for finer and regular particle size experiments. Remaining factors are constant, t=3h, T= 60 ºC, [HCl]= 11.6M.

In opposition to the behavior found for PGMs, Figure 4.20 shows in a clearer way that the metal concentration of Al co-extracted increased 225% for the smaller particles, and therefore, the resulting solution is more contaminated. The same principle is applied for the concentration of Ce: using finer particles represents 219% more Ce co-extracted in the final solution than with regular particle diameters. As mentioned before, the ideal leaching media has to keep the coextraction of Al and Ce at the minimum possible which, in this case, is not achieved.

In conclusion, for both catalysts is believed that the PGMs particles are distributed unequally among the surface of the monolith, and by causing a finer particle the obstruction effect between particles increases. Therefore, the employment of finer particles was not pursued any further, since is not suitale for any of the samples. This conclusion is reinforced by the fact that different types of mills were used in the preparation of the samples at different particle sizes. The type of mechanical forces involved, being different, can also contribute to the different leaching behaviors found.

4.3.3 Factorial Design Methodology

The leaching scheme was performed by evaluating the relevant factors of a leaching process on their own and the interactions among them. For such purpose, a factorial design methodology (FDM)[13] was used, as it has been suggested in the literature (Nogueira et al., 2014). For the application of the FDM, a 2^3 program considering three independent factors at two contribution levels (low and high) was employed, and it is expressed as:

1. Temperature (T): 40º and 60 ºC, codded factor x_1: -1 and +1.
2. Leachant concentration ([HCl]): 8.0M and 11.6M, codded factor x_2: -1 and +1.
3. Reaction time (t): 1h and 3h, codded factor x_3: -1 and +1.

Table 4.8 Leaching yields according to the FDM scheme

	# Test	Ref.	T (°C)	HCl (M) 1 v/v% H_2O_2	t (h)	H98-leaching yields (%)			I95-leaching yields (%)	
						Pd(II)	Pt(IV)	Rh(III)	Pt(IV)	Rh(III)
Variation of the factors	1	L10.1	40	8.0	1	89	68	50	6	15
	2	L10.2	40	8.0	3	102	82	62	15	26
	3	L7.1	40	11.6	1	96	79	45	21	26
	4	L7.2	40	11.6	3	108	102	61	47	51
	5	L2.2	60	8.0	1	92	79	63	40	45
	6	L2.3	60	8.0	3	100	96	73	86	87
	7	L3.2	60	11.6	1	83	72	57	61	58
	8	L3.3	60	11.6	3	100	89	72	98	96
Central Points	9	L11	50	9.8	2	111	99	73	56	64
	10	L12	50	9.8	2	106	89	70	52	61
	11	L13	50	9.8	2	105	91	65	45	59
	12	L14	50	9.8	2	103	84	64	43	53

Table 4.8 presents the leaching yields (the objective function or response or dependent variable) for the PGMs present in both catalysts, for the experiments within the factorial plan. The first eight experiments correspond to the appropriate combination between factors and levels, and experiments nine to twelve correspond to the central points of the program, used to calculate the associated error. During

[13] Annex IV provides more information regarding a FDM.

the twelve experiments, the other factors were kept constant, with the values previously optimized for both catalysts (L/S= 2 L/kg, stirring= 250 min $^{-1}$, and particle size of $D50_{H98}$= 0.397mm and $D50_{I95}$= 0.409mm).

In the following tables, the Analysis of Variance (ANOVA) for each metal is displayed individually. This analysis was performed considering a Confidence Level (CL) of 95% or a p-value of 0.05 or below, in order to consider a factor and/or an interaction of factors as significant for the process.

Table 4.9 ANOVA for leaching yields (%) of Pd(II) in H98

	Variable	Effect	Sum of Squares	DoF	Mean Square	F	p	CL
main factors	T	-5.203	54.1	1	54.1	5.28	**0.105**	**89.5**
	[HCl]	0.753	1.1	1	1.1	0.11	**0.761**	**23.9**
	t	12.308	303.0	1	303.0	29.53	**0.012**	**98.8**
interactions	T & [HCl]	-5.643	63.7	1	63.7	6.21	**0.088**	**91.2**
	T & t	-0.146	0.0	1	0.0	0.00	**0.953**	**4.7**
	[HCl] & t	2.133	9.1	1	9.1	0.89	**0.416**	**58.4**
	T, [HCl] & t	2.297	10.6	1	10.6	1.03	**0.385**	**61.5**
residuals			299.5	4	74.9			
Total			741.2	11	516.5			

According to Table 4.9, for the leaching of Pd(II) in H98, the increasing of temperature has a negative effect on the yield, noted for the negative sign, meaning, the increase of temperature represents a decrease of 5.2 percentual units in the leaching yields. On the other hand, the only significant effect in this process is time, represented by a positive value of 12.308; this is confirmed with the p-value of 0.012, which is lower than the proposed value of 0.05; therefore, the significance of time falls within a CL of 98.8%. The polynomial representation of the process, expressing leaching yield "y" as a function of the significant factors (only x_3 in this case), determined from the regression analysis using the minimum squares method, is described in Eq. 28:

$$y = 99.6 + 6.154x_3 \qquad (Eq. 28)$$

The ANOVA analysis for Pt(IV) in H98 catalyst is described in Table 4.10.

Table 4.10 ANOVA for leaching yields (%) of Pt(IV) in H98								
	Variable	**Effect**	**Sum of Squares**	**DoF**	**Mean Square**	**F**	**p**	**CL**
main factors	T	0.977	1.9	1	1.9	0.04	**0.847**	**15.32**
	[HCl]	4.450	39.6	1	39.6	0.92	**0.408**	**59.15**
	t	17.785	632.6	1	632.6	14.68	**0.031**	**96.87**
interactions	T & [HCl]	-11.492	264.1	1	264.1	6.13	**0.090**	**91.04**
	T & t	-1.017	2.1	1	2.1	0.05	**0.841**	**15.94**
	[HCl] & t	2.458	12.1	1	12.1	0.28	**0.633**	**36.69**
	T, [HCl] & t	-1.935	7.5	1	7.5	0.17	**0.705**	**29.51**
residuals			**270.88**	4	67.72			
Total			1230.7	11	1027.6			

For the case of Pt(IV) in H98, Table 4.10 shows the ANOVA analysis. The three factors have positive effects on the process; nevertheless, only the effect of time should be considered significant due to its bigger value, 17.78 units. This is confirmed by the p-value of 0.031 or a confidence level of 96.87%. This effect can be translated as the leaching yields will increase in 17.7 percentual units, in average, with the increasing of time from the low to the high levels. The behavior of the process will be dictated by the polynomial expression in Eq. 29:

$$y = 85.8 + 8.892x_3 \qquad (Eq. 29)$$

Regarding the leaching yields of Rh(III) in H98, the behavior can be described through the ANOVA analysis shown in Table 4.11.

Table 4.11 ANOVA for leaching yields (%) of Rh(III) in H98								
	Variable	**Effect**	**Sum of Squares**	**DoF**	**Mean Square**	**F**	**p**	**CL**
main factors	T	11.47	263.0	1	263.0	13.93	**0.033**	**96.65**
	[HCl]	-3.34	22.3	1	22.3	1.18	**0.357**	**64.30**
	t	12.9	335.5	1	335.5	17.77	**0.024**	**97.56**
interactions	T & [HCl]	-0.201	0.1	1	0.1	0.00	**0.951**	**4.81**
	T & t	-0.604	0.7	1	0.7	0.04	**0.856**	**14.32**
	[HCl] & t	2.245	10.1	1	10.1	0.53	**0.517**	**48.21**
	T, [HCl] & t	0.153	0.0	1	0.0	0.00	**0.963**	**3.66**
Residuals			**211.4**	4	52.84		62.7	
Total			843.1	11.0	684.6			

Table 4.11 shows that for the leaching of this metal, temperature and time are significant factors, because they have positive and notorious effect values, 11.47 and 12.9, respectively. This means that the increase of temperature and time will have a great impact, 11.47 and 12.9 units, respectively, in the leaching yields. In both cases, the p-values are lower than 0.05, conferring a 96.65% and 97.56% confidence level for temperature and time, respectively. On the other hand, the leaching of Rh(III) from H98 shows a negative effect for the HCl concentration, implying that the increase of acid concentration impacts negatively in the leaching yields, in a 3.34 units order, but this effect is not statistically significant. The mathematical expression for the behavior of Rh(III) can be expressed by Eq. 30.

$$y = 62.7 + 5.73x_1 + 6.47x_3 \qquad (Eq.30)$$

As explained before, the I95 catalyst shows no content of Pd(II) and, therefore, the ANOVA analysis was performed exclusively for Pt(IV) and Rh(III). The analysis of the leaching behavior of Pt(IV) is shown in Table 4.12.

Table 4.12 ANOVA for leaching yields (%) of Pt(IV) in I95

	Variable	Effect	Sum of Squares	DoF	Mean Square	F	p	CL
main factors	T	48.8	4760.1	1	4760.1	147.3	**0.001**	**99.88**
	[HCl]	20.1	807.8	1	807.8	25.0	**0.015**	**98.46**
	t	29.9	1789.8	1	1789.8	55.4	**0.005**	**99.50**
interactions	T & [HCl]	-3.2	20.5	1	20.5	0.6	**0.484**	**51.64**
	T & t	11.9	284.9	1	284.9	8.8	**0.059**	**94.09**
	[HCl] & t	2.2	9.6	1	9.6	0.3	**0.624**	**37.64**
	T, [HCl] & t	-6.5	85.6	1	85.6	2.7	**0.202**	**79.80**
residuals			**111.1**	4	27.8			
Total			7869.5	11	7786.2			

According to Table 4.12, the leaching of Pt(IV) from I95 is significantly influenced by the three factors evaluated. They showed important positive effects, meaning that the leaching yields of Pt(IV) are higher at the combination of the high temperature, the high acid concentration and the longer reaction time. The above is verified by the three p-values below 0.05, and falling within a confidence level of 99.88%,

98.46% and 99.50% for temperature, acid concentration and time, respectively. The polynomial expression for the leaching yield of Pt(IV) in I95 is described by Eq. 31.

$$y = 47.7 + 24.39x_1 + 10.04x_2 + 14.96x_3 \qquad (Eq. 31)$$

Finally, the ANOVA analysis for Rh(III) in I95 is presented in Table 4.13.

Table 4.13 ANOVA for leaching yields (%) of Rh(III) in I95

	Variable	Effect	Sum of Squares	DoF	Mean Square	F	p	CL
main factors	T	42.0	3535.1	1	3535.1	182.6	**0.001**	**99.91**
	[HCl]	14.5	423.2	1	423.2	21.9	**0.018**	**98.15**
	t	29.1	1688.5	1	1688.5	87.2	**0.003**	**99.74**
interactions	T & [HCl]	-3.8	28.3	1	28.3	1.5	**0.313**	**68.67**
	T & t	11.2	250.3	1	250.3	12.9	**0.037**	**96.31**
	[HCl] & t	2.1	9.0	1	9.0	0.5	**0.545**	**45.48**
	T, [HCl] & t	-4.4	38.1	1	38.1	2.0	**0.255**	**74.48**
residuals			**249.6**	4	62.4			
Total			6222.0	11	6034.8			

For Rh(III) in I95, the three factors are significant, having positive and important effects over the process, but also the interaction between temperature and time resulted to be significant. The significance of the interactions means that the effect of temperature over the leaching yields is higher at the higher level of time, therefore, any modification of one of these factors will greatly affect the final yield. The mathematical representation of this process is expressed by Eq. 32.

$$y = 53.3 + 21.02x_1 + 7.27x_2 + 14.52x_3 + 5.59x_1x_3 \qquad (Eq. 32)$$

After the realization of the ANOVA analysis, and after obtaining the polynomial expressions for the leaching yields of each metal on both samples, the comparison between the leaching yields obtained theoretically and experimentally was performed.

4.3.4 Experimental results vs predictions from the ANOVA analysis

An additional advantage of the ANOVA analysis, and the polynomial expression development, resides in the ability to develop a mathematical model to predict the behavior of the leaching yields of the metals. Considering the evaluated factors and their interactions, this analysis is valid within the range of values assigned, and considers a linear response. In this section, a comparison between the theoretical and experimental leaching yields is presented.

For Pd(II) in H98, Figure 4.21 shows the yields obtained by using Eq. 28 and the yields obtained experimentally, for the same values of the contribution levels. In this case, the leaching of Pd(II) depends, statistically speaking, on the temperature of the process; these values consider the low contribution level as -1 (40ºC) and the high contribution level as +1 (60ºC).

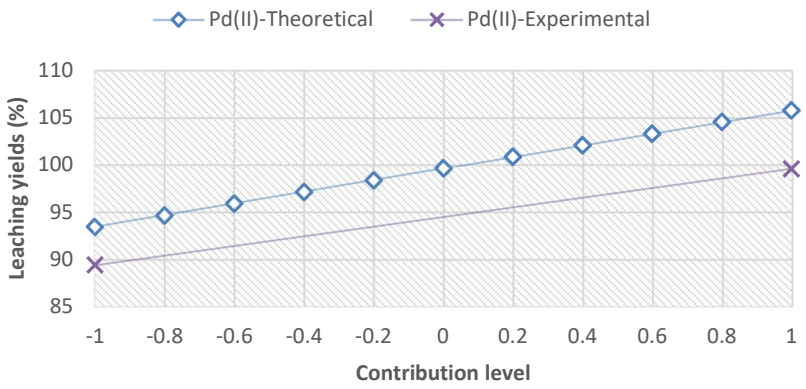

Figure 4.21 Comparison of the leaching yields (%) of Pd(II) in H98 obtained theoretically and experimentally.

From this comparison, we can observe that the leaching yields from the ANOVA analysis are 5% higher than the real leaching values, showing a satisfactory prediction of the behavior of Pd(II) in this catalyst sample.

In the case of Pt(IV) in H98, the Eq. 29 indicates that the leaching yields for this metal also depend on the temperature of the process. Figure 4.22 represents the comparison between the theoretical and experimental leaching yields, obtained within the range of 40 and 60ºC.

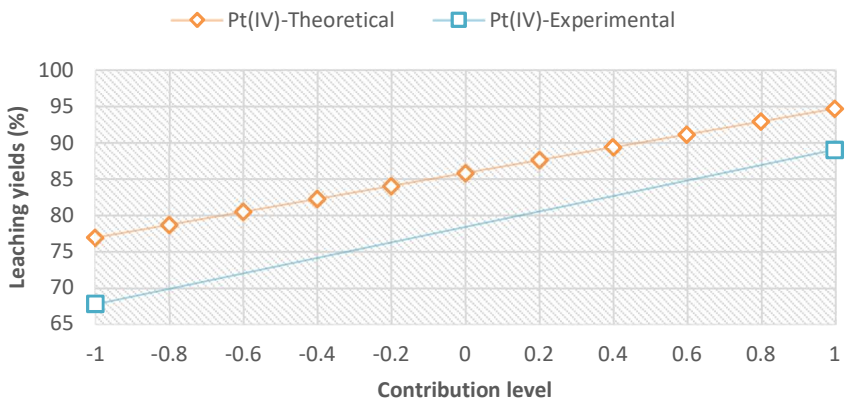

Figure 4.22 Comparison of the leaching yields (%) of Pt(IV) in H98 obtained theoretically and experimentally.

In here, the leaching yields predicted with the ANOVA differ from the real values in an average of 7.5% from the low to the high contribution level. This can be appreciated with the predicted value of 95% yields at 60ºC against the 89% obtained experimentally.

Finally, regarding the behavior of Rh(III), the use of Eq. 30 and the leaching yields obtained experimentally, give us Figure 4.23, with the graphical comparison between these two leaching data approaches.

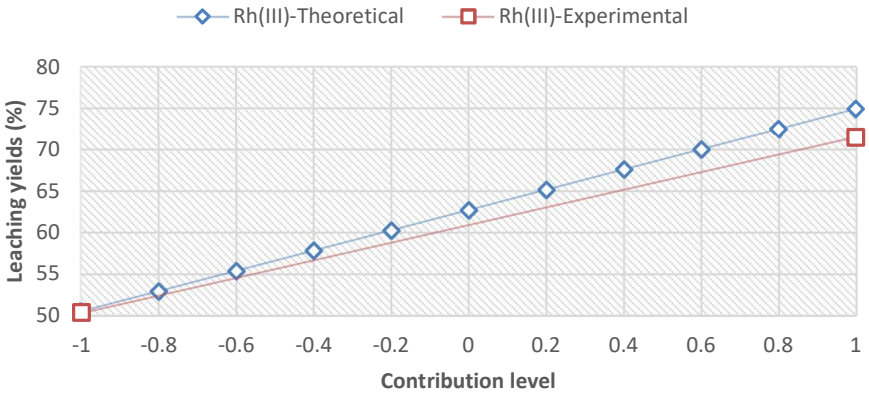

Figure 4.23 Comparison of the leaching yields (%) of Rh(III) in H98 obtained theoretically and experimentally.

In this case, we can observe that at the low contribution level, the values obtained are practically the same, 50% leaching as an experimental result and 51% as a predicted value; on the other hand, at the high contribution level, the value of the

predicted leaching is 3% higher (75%) than the value obtained in the experiment (72%). Therefore, it can be stated that the ANOVA analysis, and the subsequent polynomial expressions obtained, are in good accordance with the experimental results acquired for the leaching of the PGMs from H98.

In the case of I95, the use of Eq. 31 and the leaching yields obtained experimentally give us Figure 4.24, with the graphical comparison of the influence of temperature by these two methods.

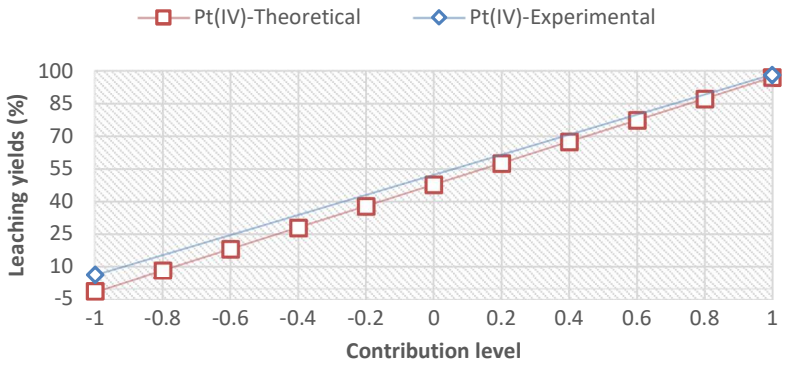

Figure 4.24 Comparison of the leaching yields (%) of Pt(IV) in I95 obtained theoretically and experimentally.

In this case, the theoretical model is predicting the leaching yield only with 1% of difference, 97% predicted towards the 98% of Pt(IV) leached in the experimental procedure. In the low contribution level, the model predicts a negative leaching, meaning no leaching observed under these conditions, which can be supported with the 6% leaching yield obtained experimentally, proving to be a very low yield.

Finally, the comparison of the experimental results and Eq. 32 give us Figure 4.25, which compares the two models for the leaching of Rh(III) in I95.

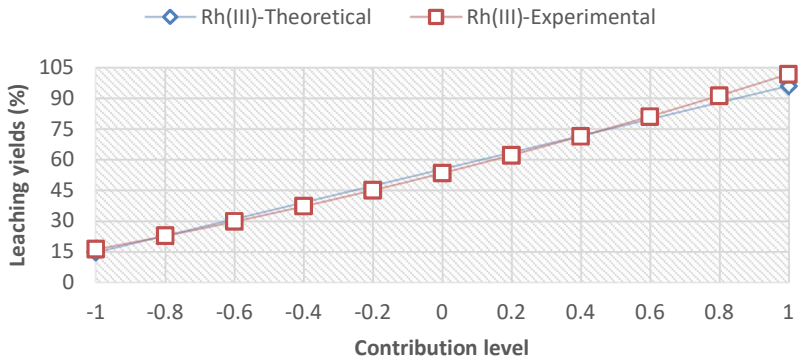

Figure 4.25 Comparison of the leaching yields (%) of Rh(III)) in I95 obtained theoretically and experimentally.

For this developed model, the yields obtained are also in accordance with those obtained by the experimental procedure; at the high contribution level, the model predicts a 102% leaching yields which matches with the 96% obtained experimentally. On the other hand, at the low contribution level, the theoretical model only differs from the experimental yield by 1%, predicting 16% leaching towards the 15% yield obtained.

4.4 Solvent extraction step

4.4.1 SX-experiments with the model solutions

The exact initial metal concentrations of the model solutions were corroborated by an ICP-AES analysis. Table 4.14 shows the initial metal concentrations, together with the exact HCl concentration for each of them.

Table 4.14 Initial metal concentrations (mg/L) for the model solutions

[HCl] (M)	Solution	Pd	Pt	Rh	Al	Ce	Fe
5.96	M1	277.5	197.2	19.7	1368	2196	61.3
2.98	M2	129.9	87.4	8.9	607	951	27.9
5.96	M3	297.9	209.7	18.8	1423	2432	83.5

As described in the previous chapter, an A/O ratio of 1 was used in the contact of the organic and aqueous phases, and the SX experiments were performed in the order shown below. For each extractant, the metal concentrations of the aqueous

phases at the two HCl concentrations, the *D* values and the extraction efficiency in terms of percentage are presented.

4.4.1.1 With TOPO

The SX experiments were carried out under the above-mentioned conditions with a 0.1M solution of TOPO in toluene. Table 4.15 shows the results of this set of extractions and the *D* values for the model solutions at 6M HCl.

Table 4.15 SX in model solution at 6M HCl using 0.1M TOPO							
Extraction	**Solution**	**Metal concentrations (mg/L)**					
		Pd	**Pt**	**Rh**	**Al**	**Ce**	**Fe**
A1	M1	277.5	197.2	19.7	1368	2196	61.3
	Aqueous	210.2	30.9	19.9	1176	1750	1.0
	Organic	67.3	166.2	-	192	446	60.3
	Distribution ratio values						
	D	0.32	5.4	-	0.16	0.25	60.4

In the same way, Table 4.16 shows the results of the SX with TOPO using the model solution at 3M HCl concentration. Therefore, Figure 4.26 shows the comparison of these two conditions in terms of extraction efficiency (%).

Table 4.16 SX in model solution at 3M HCl using 0.1M TOPO							
Extraction	**Solution**	**Metal concentrations (mg/L)**					
		Pd	**Pt**	**Rh**	**Al**	**Ce**	**Fe**
A4	M2	129.9	87.4	8.9	607	951	27.9
	Aqueous	94.7	15.5	9.7	690	1083	0.5
	Organic	35.2	71.9	-0.8	-83	-132	27.4
	Distribution ratio values						
	D	0.37	4.6	-	-	-	55.9

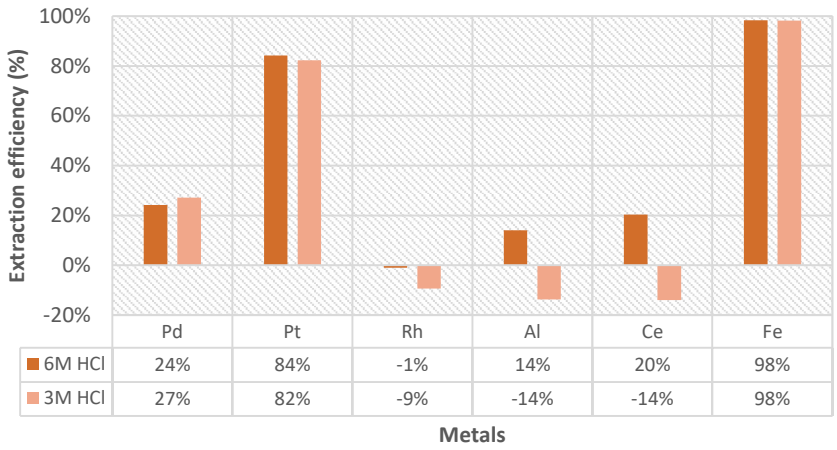

Figure 4.26 Metal extraction efficiencies (%) by the 0.1M TOPO solution.

As appreciated from the tables, the highest values of *D* correspond to Fe and Pt, which is in accordance with Figure 4.26, with the highest percentages of extraction for these two metals. Both HCl concentrations showed similar results; therefore, the first conclusion is that TOPO shows a higher affinity towards Pt and Fe, regardless the acid concentration.

For the stripping of the loaded TOPO, according to the disclosed in the literature, a solution of 0.4M of malonic acid was chosen as stripping agent (Gupta & Singh, 2013). Figure 4.27 displays the results of the stripping experiments for the two TOPO loaded organic phases from the two different HCl concentrations.

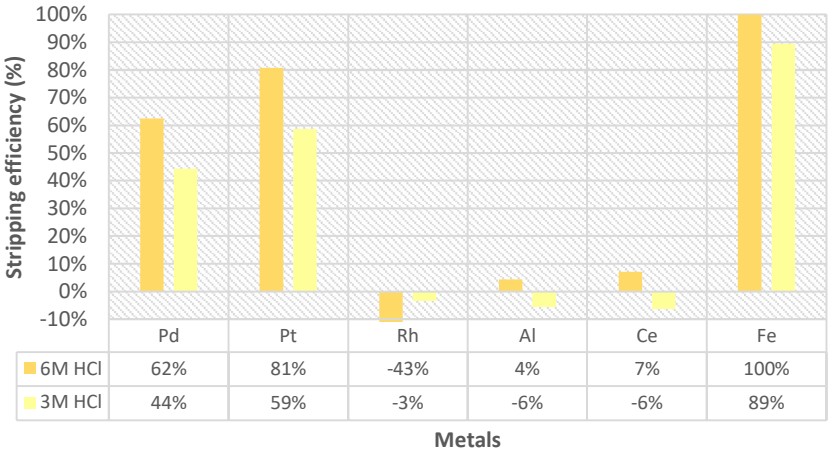

Figure 4.27 Metal stripping efficiencies (%) from the TOPO loaded organic phases by a 0.4M solution of malonic acid.

We can see that the solution of malonic acid stripped 81% of Pt(IV) and 100% of Fe from the loaded organic phase coming from the test at 6M HCl; therefore, it was decided to employ this reagent as stripping agent for TOPO.

4.4.1.2 With TBP

The same experimental conditions were followed when testing TBP as a possible extractant for removing Fe(III), leaving the PGMs in the aqueous phase; the SX tests were performed again at 3M and 6M HCl concentrations. Table 4.17 shows the results for the 6M HCl solution.

Table 4.17 SX in model solution at 6M HCl using 0.1M TBP

Extraction	Solution	Metal concentrations (mg/L)					
		Pd	Pt	Rh	Al	Ce	Fe
A2	M1	277.5	197.2	19.7	1368	2195	61.3
	Aqueous	288.6	207.3	19.6	1433	2315	3.7
	Organic	-11.1	-10.1	0.1	-65	-119	57.7
	Distribution ratio values						
	D	-	-	0.005	-	-	15.8

Table 4.18 presents the results of the SX with the model solution at 3M HCl concentration. In the same way, Figure 4.28 shows the graphical comparison between the results of these two extraction experiments.

Table 4.18 SX in model solution at 3M HCl using 0.1M TBP

Extraction	Solution	Metal concentrations (mg/L)					
		Pd	Pt	Rh	Al	Ce	Fe
A5	M2	129.9	87.4	8.9	607	951	27.9
	Aqueous	133.9	93.7	9.7	656	1046	23.2
	Organic	-4.02	-5.8	-0.8	-49	-95	4.7
	Distribution ratio values						
	D	-	-	-	-	-	0.20

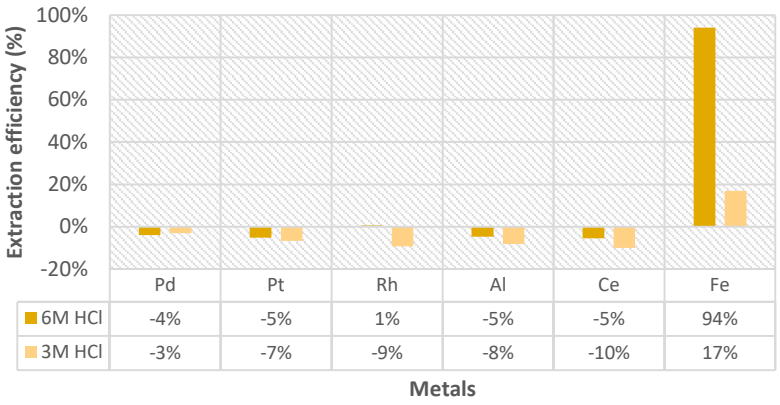

Figure 4.28 Metal extraction efficiencies (%) by a 0.1M TBP solution.

From the figure above and tables 4.17 and 4.18, we appreciate how TBP had only a positive and significant *D* value at 6M HCl concentration for Fe, acquiring the extraction of 94% of the total content; therefore, it was concluded that TBP is a selective extractant for Fe at the mentioned acid concentration, offering a possibility of a pre-SX with this reagent in order to ensure a more effective PGMs extraction in the further steps.

After this conclusion, the use of an acidic solution of 1M HCl was employed as stripping agent for the loaded organic phase to remove the extracted content of Fe and prepare the TBP solution to be reused in further SX cycles. Figure 4.29 displays the results in terms of stripping % for both TBP loaded organic phases.

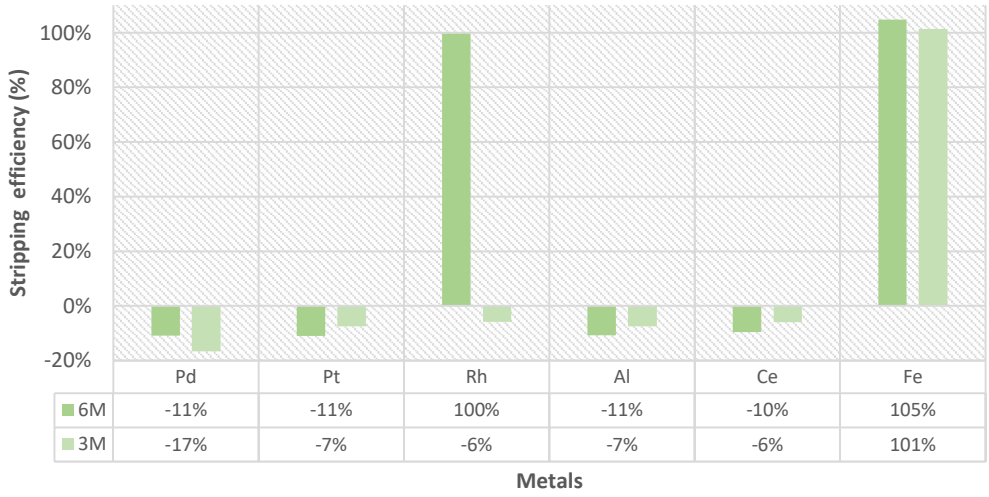

Figure 4.29 Metal stripping efficiencies (%) from the TBP loaded organic phases by a 1M HCl solution.

In this case, we observe the stripping of the totality of Fe at both HCl concentrations. The stripping of 100% of Rh(III) at 6M HCl was also acquired, but this number can be meaningless due to the very low amount of Rh extracted in the extraction stage; the 100% value observed is only 0.11 mg/L, therefore, it can be neglected. As a conclusion, 1M HCl solution was agreed to be a good stripping agent for Fe(III) when TBP is used as extractant.

4.4.1.3 With Cyanex® 471X

Cyanex® 471X was the first of this family of extractants tested in the model solutions. Tables 4.19 and 4.20 show the SX results obtained with the model solutions at 6M and 3M HCl, respectively. Figure 4.30 presents the comparison of the extraction efficiencies for these two trials.

Table 4.19 SX in model solution at 6M HCl using 0.1M Cyanex® 471X

Extraction	Solution	Metal concentrations (mg/L)					
		Pd	Pt	Rh	Al	Ce	Fe
A3	M1	277.5	197.2	19.7	1368	2196	61.3
	Aqueous	1.1	203.7	19.4	1451	2308	2.1
	Organic	276.5	-6.6	0.28	-83	-112	59.2
	Distribution ratio values						
	D	259.6	-	0.014	-	-	28.8

Table 4.20 SX in model solution at 3M HCl using 0.1M Cyanex 471X

Extraction	Solution	Metal concentrations (mg/L)					
		Pd	Pt	Rh	Al	Ce	Fe
A6	M2	129.9	87.4	8.9	607	951	27.9
	Aqueous	4.20	90.8	9.3	646	1015	23.7
	Organic	125.7	-3.4	-0.4	-39	-64	4.2
	Distribution ratio values						
	D	30	-	-	-	-	0.18

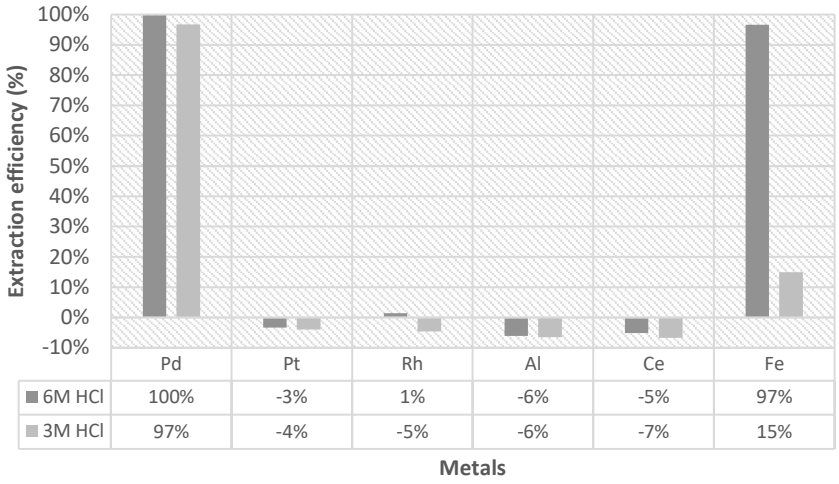

Figure 4.30 Metal extraction efficiencies (%) by a 0.1M Cyanex® 471X solution.

As observed in the previous tables, the highest positive *D* values, and therefore significant, correspond to the extraction of Pd at both HCl concentrations, and there is another significant value for the extraction of Fe at 6M HCl; therefore, Cyanex® 471X was found to be a selective extractant towards Pd and Fe at 6M HCl. In terms of the following stripping stage, a stabilized solution of 1M $Na_2S_2O_3$ was used as stripping agent, this selection being based on the safety data sheet provided by the manufacturer of Cyanex® 471X. Figure 4.31 shows the results of the metals stripping with this solution of sodium thiosulfate.

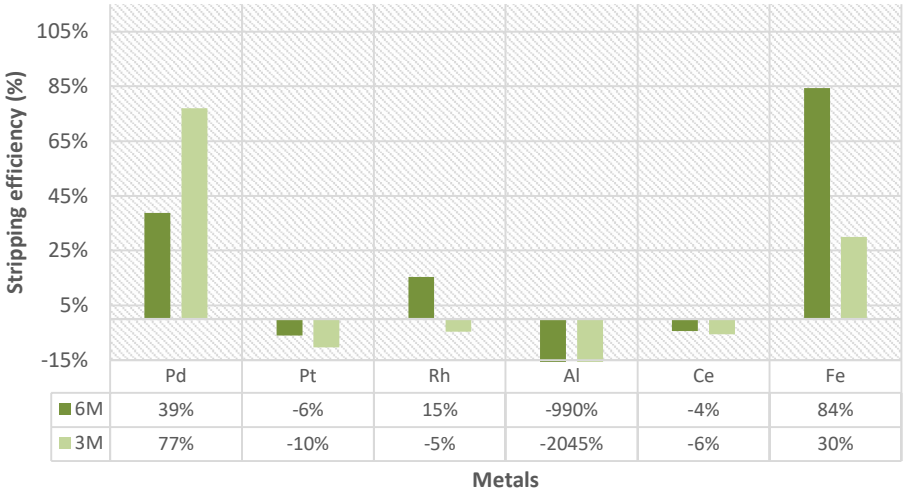

Figure 4.31 Metal stripping efficiencies (%) from Cyanex® 471X loaded organic phases by a stabilized solution of 1M $Na_2S_2O_3$.

In the previous figure, a 39% stripping of Pd(II) was observed at 6M HCl and a 77% stripping at 3M HCl. These results are reported at room temperature, due to the seeking of environmental friendliness of the process; nevertheless, further research within the information provided by the manufacturer disclosed the possibility of increasing the Pd(II) stripping efficiency when the stripping is performed at 50ºC. This new temperature was decided to be tested only during the experiments with the real leaching solutions. In general, the sodium thiosulfate solution was chosen to be the stripping agent for Pd(II) when Cyanex® 471X is employed as extractant.

4.4.1.4 With Adogen® 464

In terms of ILs, the literature search showed the employment of quaternary ammonium salts as an attempt to solve the problem of the simultaneous separation of the PGMs from the multi-metal leaching solutions. In this way, ILs such as Aliquat® 336, a hydrophobic quaternary ammonium salt (with a general structure of $[R_3NCH_3]^+[Cl]^-$ and available in the market), have gained attention for showing good results in terms of metal extractions. Aliquat® 336 has been tested for different metals, such as Au(III). Pt(IV) and Pd(II) (Wei et al., 2016), showing extractions above 60% for Pt(IV) and Pd(II) and 100% for Au(III).

The use of this IL was not possible due to availability and time constraints; nevertheless, another reagent was available, Adogen® 464, which is also a quaternary ammonium salt, and sharing similar properties with Aliquat® 336, including its affinity with the PGMs previously reported. In this way, Adogen® 464 was decided to be tested instead of Aliquat® 336, and the same extraction conditions were followed with a 0.1M solution of Adogen® 464. Tables 4.21 and 4.22 present the results for the model solutions at 6M and 3M HCl concentration.

Table 4.21 SX in model solution at 6M HCl using 0.1M Adogen® 464

Extraction	Solution	Metal concentrations (mg/L)					
		Pd	Pt	Rh	Al	Ce	Fe
A7	M3	297.9	209.7	18.8	1423	2432	83.5
	Aqueous	1.09	0.3	9.6	726	1144	0.6
	Organic	296.8	209.4	9.2	697	1288	82.9
	Distribution ratio values						
	D	271.5	709.3	0.96	0.96	1.1	149.3

Table 4.22 SX in model solution at 3M HCl using 0.1M Adogen® 464							
Extraction	Solution	Metal concentrations (mg/L)					
		Pd	Pt	Rh	Al	Ce	Fe
A8	M2	129.9	87.4	8.90	607	951	27.9
	Aqueous	26.0	0.83	24.3	1972	3396	0.22
	Organic	103.9	86.6	-15.4	-1365	-2445	27.7
	Distribution ratio values						
	D	4.0	104.5	-	-	-	123.5

Figure 4.32 shows the metal extraction efficiencies comparison between the two different acid concentrations when Adogen® 464 was used.

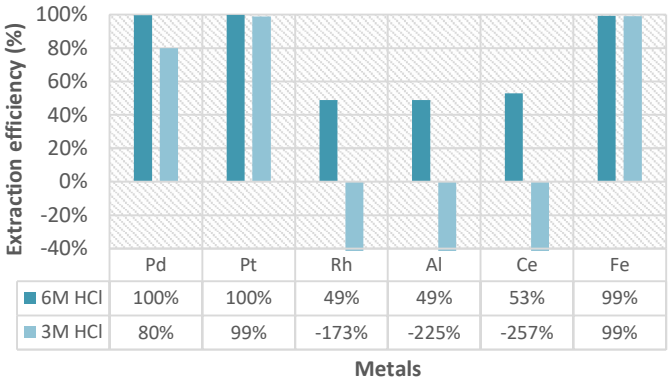

Figure 4.32 Metal extraction efficiencies (%) by a 0.1M Adogen® 464 solution.

From the figure, we can appreciate that Adogen® 464 extracted the totality of Pd(II) and Pt(IV) at both HCl concentrations. Regarding the extraction behavior of the rest of the metals, the extractant proved to be able to extract 49% of Rh(III) at 6M HCl but it also co-extracted practically half of the content of Al and Ce. For both cases, Adogen® 464 extracted the totality of Fe; therefore, a preliminary conclusion was the possibility to employ Adogen® 464 for the extraction of PGMs, specially because it showed the greatest affinity for Rh(III) than the extractants previously tested.

In terms of Rh(III), due to the low content of this metal in the samples, it was decided to not perform any experiment regarding the stripping of it from the loaded organic phases, because it is not economically viable neither feasible in terms of amount of stripping agent used against the quantity of Rh that would be recovered.

4.4.1.5 With Cyphos® 101

Another IL was also tested for the SX experiments. Cyphos® 101 was tried with the model solutions, in order to evaluate its suitability for PGMs extraction. In this case, a 0.1M solution of Cyphos® 101 in toluene was again employed, and Tables 4.23 and 4.24 show the SX results when using this IL with the model solutions at 6M and 3M HCl concentrations, respectively.

Table 4.23 SX in model solution at 6M HCl using 0.1M Cyphos® 101

Extraction	Solution	Metal concentrations (mg/L)					
		Pd	Pt	Rh	Al	Ce	Fe
A9	M3	297.9	209.7	18.8	1423	2432	83.5
	Aqueous	8.3	0.6	19.2	1356	2339	0.1
	Organic	289.6	209.1	-0.4	66	93	83.4
	Distribution ratio values						
	D	34.9	338	-	0.05	0.04	1012

Table 4.24 SX in model solution at 3M HCl using 0.1M Cyphos® 101

Extraction	Solution	Metal concentrations (mg/L)					
		Pd	Pt	Rh	Al	Ce	Fe
A10	M2	129.9	87.4	8.9	607	951	27.9
	Aqueous	0.8	0.3	9.6	686	1102	0.1
	Organic	129.1	87.1	-0.7	-78	-150	27.8
	Distribution ratio values						
	D	169.8	256.5	-	-	-	226.7

Figure 4.33 shows the metal extraction efficiencies (%) using this IL in the model solutions, at both acid concentrations.

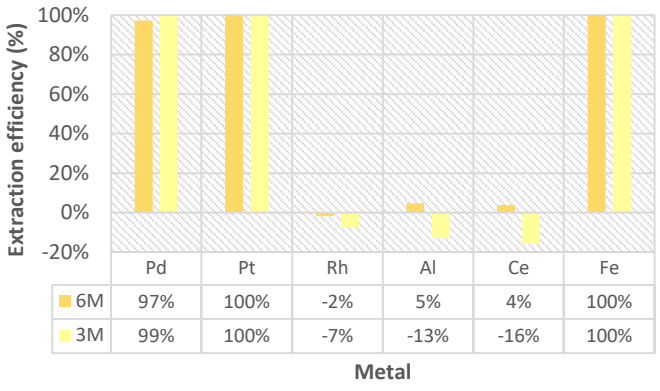

Figure 4.33 Metal extraction efficiencies (%) by a 0.1M Cyphos® 101 solution.

From the figure, we concluded that Cyphos® 101 was able to extract the totality of Pd(II) and Pt(IV) at both HCl concentrations, and that showed selectivity towards the rest of the metals, except Fe(III); therefore, it could be employed alone to extract Pd and Pt from the leaching solutions. On the other hand, Cyphos® 101 also co-extracted 100% of Fe for both acidic conditions, thus, a pre-removal of Fe is necessary in order to not compromise the extraction of the PGMs.

The stripping of Pd(II) and Pt(IV) from the loaded organic phases of Cyphos® 101 was performed sequentially in two stages; in the first, a 0.1M KSCN solution to strip the content of Pt(IV) was used, followed by a second stripping with 0.1M CH_4N_2S in 5% v/v HCl solution to strip Pd(II) (Nguyen et al., 2016) . The results of this stripping scheme were not satisfactory for the model solutions, because only a 3% stripping recovery of Pt(IV) was achieved with the 0.1M KSCN solution, and a 2% stripping recovery of Pd(II) acquired with the thiourea solution.

The above results are not satisfactory, they represent a poor stripping of the PGMs from Cyphos® 101, but a lack of time prevented the further investigation of other stripping agents for this IL. A possible explanation of this behavior is that in the literature, the stripping has been carried out with model solutions containing only Pd or either only Pt, thus, the co-existence of these two metals in our model solution may have caused the poor performance of the stripping agents.

Finally, after the individual evaluation of the chosen extractants with the model solutions at 6M and 3M HCl concentrations, the applicable considerations were taken in order to establish a SX scheme that could be tested in the real leaching solutions.

4.4.2 SX scheme with the real leaching solutions

4.4.2.1 With traditional extractants

The SX experiments for the real leaching solutions were performed according to the schemes disclosed in section 3.4.2. For the case of the traditional extractants, the liquors were diluted once, reaching approximately a 5.8M HCl concentration. This small difference between 5.8M and the 6M expected is due to the addition of small

volumes of H_2O_2 at the beginning of the leaching step. A small loss of acidity is also expected during the leaching reactions. It is worth to note that, after the reconsideration of the obtained results from the model solution experiments, the extraction carried out with Cyanex® 471X was performed at 50ºC in the real leaching solutions. Finally, it was decided to not perform the SX cycle employing Adogen® 464 to extract Rh(III), due to its low concentration in both catalyst samples.

Table 4.25 shows the SX results for H98. The table displays the metal concentrations in the aqueous and organic phases after each extraction, and the values of *D*. In this case, the initial concentrations found prior to the first SX cycle were: Pd=405.8 mg/L, Pt=127.1 mg/L, Rh=0.20 mg/L, Al=1663 mg/L, Ce=2212 mg/L, Fe=71.5 mg/L, La=524 mg/L and Nd=424 mg/L; therefore, the metal concentrations of the organic phases in each cycle were obtained by mass balance between the initial and final concentrations in the aqueous phases.

Table 4.25 SX results for H98 with traditional extractants				
SX cycle	**Metal**	**Aqueous phase**	**Organic phase**	***D***
		Concentrations (mg/L)		
First SX cycle with 0.1M TBP	Pd	389.7	16.1	0.04
	Pt	124.4	2.7	0.02
	Rh	0.2	0.01	0.07
	Al	2066	-403	-
	Ce	2897	-686	-
	Fe	68	3.5	0.05
	La	484	40	0.08
	Nd	370	53.9	0.14
Second SX cycle with 0.05M Cyanex® 471X	Pd	324.8	65	0.2
	Pt	122.7	1.7	0.01
	Rh	0.18	-	0.003
	Al	2924	-858	-
	Ce	3844	-947	-
	Fe	57	11	0.19
	La	470	14	0.03
	Nd	317	52	0.16
Third SX cycle with 7.12mM TOPO	Pd	270.1	54.7	0.20
	Pt	63.4	59.3	0.94
	Rh	0.2	0.02	0.11
	Al	800	2124	2.65
	Ce	1022	2823	2.77
	Fe	0.1	57	**783**
	La	389	82	0.21
	Nd	273	45	0.16

Figure 4.34 complements the previous table, in here the extraction efficiencies (%) of the extractants towards the targeted metals are displayed.

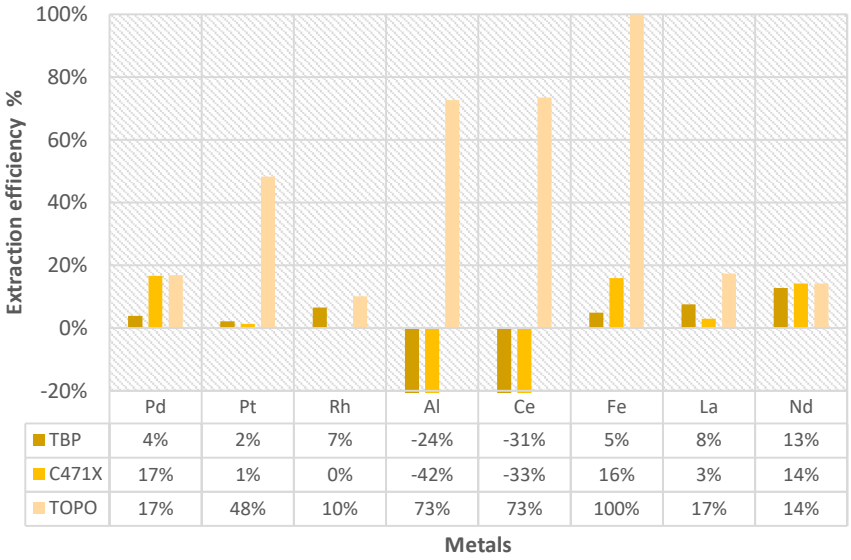

Figure 4.34 Metal extraction efficiencies (%) for the SX step for H98, using traditional extractants.

We can appreciate that the SX scheme for H98 using traditional extractants did not work as expected. In the first cycle, TBP was supposed to remove the Fe content prior to the extraction of PGMs; nevertheless, it only removed 5% Fe and 13% Nd, leaving the rest of the iron in the aqueous solution for the second cycle. In the second cycle, Cyanex® 471X was used to extract Pd(II); nevertheless, it only acquired a 17% extraction of this metal, and a coextraction of 16% Fe; for the rest of the metals, their extractions with Cyanex® 471X can be neglected in this cycle, for being below 15%. Finally, TOPO was intended to extract Pt(IV); in this case, the results showed an extraction of only 48% Pt(IV). These results did not match with the expected 84% of Pt(IV) extracted from the model solution at a similar HCl concentration; TOPO also co-extracted 17% of Pd(II), this percentage was also lower than the one observed in the model solution. For the case of Rh(III), a co-extraction of 10% was observed, this extraction was not found for the model solution; nevertheless, it is still not enough to be considered satisfactory. As for the previous SX cycles, TOPO co-extracted the Fe in the sample, but for this specific cycle, it extracted the 100% of the remaining content of Fe.

The stripping for the H98 loaded organic solution was in accordance with the developed schemes with the model solutions. Table 4.26 presents the stripping efficiencies (%) acquired with the use of the above-mentioned stripping agents in the H98 sample.

Table 4.26 Stripping efficiencies (%) for H98										
Stripping cycle	Stripping agent	Organic phase	Metal recovery (%)							
			Pd	Pt	Rh	Al	Ce	Fe	La	Nd
1	HCl	TBP	4	7	66	0	0	75	2	2
2	$Na_2S_2O_3$	C471X	26	6	100	0	0	54	8	2
3	Malonic acid	TOPO	35	82	100	0	0	100	2	3

As a preliminary observation from the table, although the stripping percentages of Rh obtained in every cycle are high, they represent the 66% and 100% stripped from the 7% and 10% extracted during the extraction; therefore, these high percentages can be neglected due to the very low concentration of the metal in the stripped solution.

As for the first stripping cycle, 75% of Fe was removed from the TBP organic phase by the 1M HCl solution together with small quantities of the other metals. Due to the low extraction efficiencies observed in the previous step, this stripping agent is taken as satisfactory and would allow the organic phase to be reused in further experiments. In the second cycle, the solution of sodium thiosulfate was expected to strip at least 40% of Pd(II) (as observed in the model solutions); nevertheless, only a 26% of Pd(II) stripping was observed, together with a 54% stripping of Fe available in that solution. Finally, in the third cycle, malonic acid was used to strip the content of Pt(IV), achieving 82% stripping from the organic phase, together with a 35% stripping of Pd(II) and the 100% stripping of Fe available on this phase. Generally, the stripping scheme for H98 provided good results in terms of the targeted metals in each cycle, but the presence of Fe in all the organic phases was the determining factor for efficiencies lower than the ones observed with the model solutions.

For the case of I95, the SX scheme applied is the one displayed in Figure 3.6. Table 4.27 presents the results acquired in this set of experiments, showing the metal concentrations of the aqueous and organic phases after each cycle, as well as the *D* values. For I95, the initial metal concentrations in about 6M HCl were Pt=182.8 mg/L, Rh=18.2 mg/L, Al=955 mg/L, Ce=2039 mg/L, and Fe=34 mg/L; in this case,

La and Nd were not considered due to the preliminary results of the XRF analysis, showing that for this sample the content of these metals was less than 0.01%.

Table 4.27 SX results for I95 with traditional extractants				
		Concentrations (mg/L)		*D*
		Aqueous phase	Organic phase	
First SX cycle with 0.1M TBP	Pt	189.3	-6.5	-
	Rh	19.7	-1.4	-
	Al	995	-39.5	-
	Ce	2140	-101.1	-
	Fe	33	1.3	0.04
Second SX cycle with 0.0135M TOPO	Pt	168.6	20.7	0.12
	Rh	18.5	1.1	0.06
	Al	909	86	0.1
	Ce	1956	185	0.1
	Fe	0.1	33	**504**

Figure 4.35 shows the metals extraction efficiencies (%) for this SX scheme.

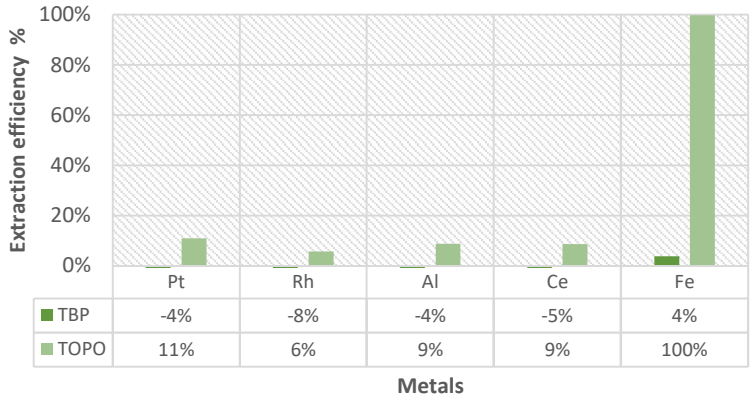

Figure 4.35 Metal extraction efficiencies (%) for I95, using traditional extractants.

The SX scheme chosen for I95 also did not provide the results expected from its development with the model solutions. The employment of TBP, intended to remove around 94% of Fe at 6M HCl concentration, only acquired a 4% removal of this metal, thus, compromising the selectivity of the second cycle. For the second SX cycle, the use of TOPO was addressed to extract the Pt(IV) contained in the solution; nevertheless, only 11% extraction was observed, with a poor co-extraction of Rh(III),

of only 6%. In this cycle, TOPO co-extracted the totality of the Fe in the sample, thus proving to be non-effective for this catalyst sample. These conclusions are supported by the values of the distribution ratios, with the only positive and significant value for Fe (*D*=504) during the use of TOPO, and the rest of them being less than 1.

The stripping stage for I95 involved the same stripping agents already disclosed. The results of this step are shown in Table 4.28.

Table 4.28 Stripping efficiencies (%) for I95

Stripping cycle	Stripping agent	Organic phase	Metal recovery (%)				
			Pt	Rh	Al	Ce	Fe
1	HCl	TBP	0	1	0	0	100
2	Malonic acid	TOPO	73	2	1	2	95

The stripping scheme for I95 proved to be more effective. The first cycle managed to selectively extract 100% of Fe in the organic phase, allowing the TBP to be reused later. For the second cycle, the malonic acid solution stripped 73% of the Pt(IV) in the organic phase, proving to be satisfactory enough; also, this reagent stripped 95% of the Fe contained in this second organic phase, allowing the TOPO solution to be reused in further cycles.

As a general observation, after the application of the SX schemes in the real leaching solutions we can state that the behaviors of the model and real solutions vary greatly. This can be attributed to the complexity of the real solutions, to the amount of different metals involved, and their concentrations. A further and deeper analysis of the initial metal concentrations of the catalyst samples would be required, in order to guarantee a better understanding of the possible behaviors during the SX step. In our case, the initial screening was performed based on previous knowledge of the metal concentrations and choosing only the metals that would provide the highest concentrations in the samples.

4.4.2.2 With ionic liquid Cyphos® 101

The IL Cyphos® 101 selected for the SX step was tested separately. In this case, the leaching solutions were diluted twice, reaching a HCl concentration of 2.98M. The concentration of the IL for both cases was 0.1M.

Table 4.29 shows the SX results acquired for H98 with the use of Cyphos® 101, and Figure 4.36 displays the extraction efficiencies (%) of this SX scheme. In this set of experiments, the initial metal concentrations for the sample were: Pd=270.3 mg/L, Pt=74.9 mg/L, Rh=0.11 mg/L, Al=820 mg/L, Ce=986 mg/L, Fe=42.2 mg/L, La=273mg/L, and Nd=198 mg/L.

Table 4.29 SX results for H98 with Cyphos® 101

		Concentrations (mg/L)		*D*
		Aqueous phase	Organic phase	
First SX cycle with 0.1M TBP	Pd	245.6	24.8	0.10
	Pt	71.6	3.3	0.05
	Rh	0.1	0.01	0.05
	Al	719	101	0.14
	Ce	849	137	0.16
	Fe	40	2	0.05
	La	231	42.1	0.19
	Nd	160	37.6	0.23
Second SX cycle with 0.1M Cyphos® 101	Pd	0.7	245	351
	Pt	0.2	71.4	419
	Rh	0.07	0.03	0.41
	Al	569	150	0.27
	Ce	629	219	0.35
	Fe	0.5	39.8	81
	La	7.2	223.6	31
	Nd	17	144	9

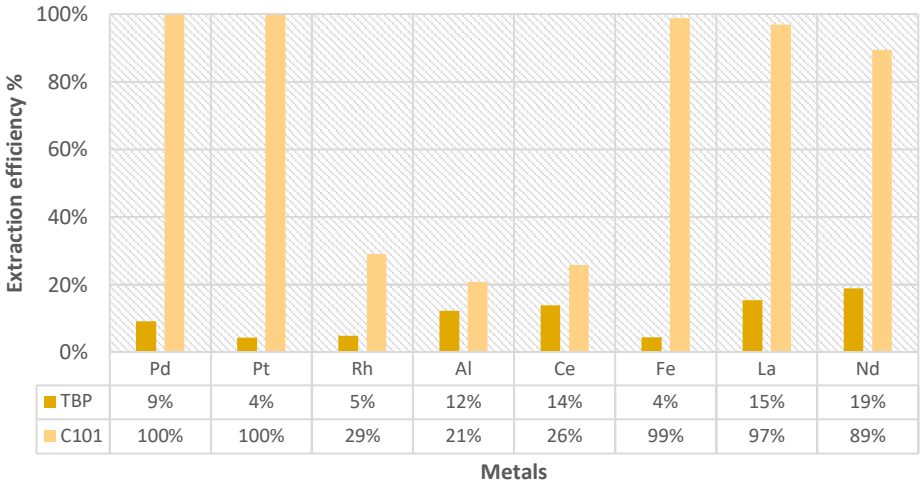

Figure 4.36 Metal extraction efficiencies (%) for H98, using Cyphos® 101.

In this SX scheme, we can appreciate again that TBP failed in its duty to remove the content of Fe, with only a removal of 4% of the total, compromising the selectivity of the IL towards Pd(II) and Pt(IV). For the second cycle, Cyphos® 101 extracted 100% of Pd(II) and Pt(IV) as was expected from the test with model solutions. A different behavior in the extraction of Rh(III) was observed; with the real leaching solutions, Cyphos® 101 managed to extract 29% of Rh(III) against the no-extraction observed with the model solutions. In terms of the remaining metals, the IL showed a high co-extraction of Fe, La and Nd (99%, 97% and 89%, respectively), and a 21% and 26% extraction of Al and Ce, respectively. These results impacted greatly in the whole model, the selectivity was severely affected because it was not possible to extract only the PGMs and the resulting liquor was contaminated with metal impurities.

After the SX experiments, the stripping tests were carried out, and Table 4.30 shows the stripping efficiencies (%) for this step.

Table 4.30 Stripping efficiencies (%) for H98 from Cyphos® 101

Stripping cycle	Stripping agent	Organic phase	Metal recovery (%)							
			Pd	Pt	Rh	Al	Ce	Fe	La	Nd
1	HCl	TBP	2	4	21	1	2	12	1	1
2	KSCN	Cyphos® 101, to strip Pt	0	0	79	3	2	17	1	1
3	thiourea	Cyphos® 101, to strip Pd	19	5	100	0	0	11	0	0

According to these results, the stripping of metals from the IL resulted more difficult than expected. In the first cycle, the 1M HCl solution only managed to strip 12% of Fe from the organic phase, which is a very low percentage. For the second and third cycles, both stripping agents failed in the stripping of the PGMs, with 0% Pt(IV) and 19% Pd(II) stripped, respectively. Again, even though the % for the stripping of Rh(III) seems high, it should be considered that this is the totality of Rh stripped from the 29% extracted during the extraction; therefore, the metal concentration is very low and cannot be considered as satisfactory.

For the SX of I95 using Cyphos® 101, Table 4.31 and Figure 4.37 display the results after the sequential contact of the phases. In this sample, the initial metal concentrations were Pt=100.6 mg/L, Rh=10.21 mg/L, Al=449 mg/L, Ce=921 mg/L, and Fe=17.3 mg/L.

Table 4.31 SX results for I95 with Cyphos® 101

		Concentrations (mg/L)		*D*
		Aqueous phase	Organic phase	
First SX cycle with 0.1M TBP	Pt	91.9	8.7	0.09
	Rh	9.9	0.3	0.03
	Al	457	-8.3	-
	Ce	936	-15	-
	Fe	15	1.5	0.1
Second SX cycle with 0.1M Cyphos 101	Pt	0.08	91.9	1091
	Rh	4.7	5.3	1.14
	Al	489	-32	-
	Ce	966	-30	-
	Fe	1.8	14	7.8

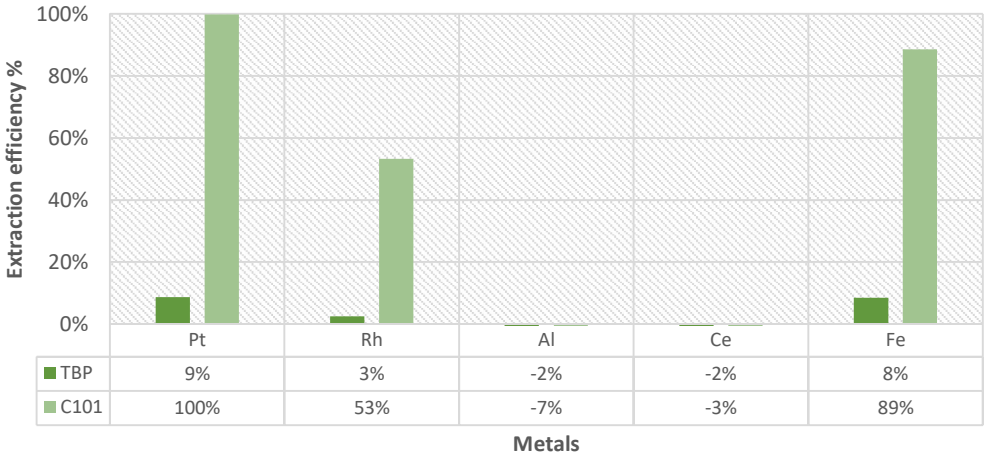

Figure 4.37 Metal extraction efficiencies (%) for I95, using Cyphos® 101.

For the case of I95, again TBP was not effective to remove Fe during the first extraction cycle, with only a 8% removal of Fe(III), this result is worse than the 17% Fe removed from the model solution. This compromised the second cycle again. Such inconvenience is reflected in the extraction of 89% of Fe with Cyphos® 101; this high percentage of co-extraction can be the cause of the poorly performance towards Rh(III), with only a 53% extraction. On the other hand, the Pt(IV) agrees with the results obtained from the tests with model solutions, and it reached a 100% extraction of Pt(IV). For this sample, the co-extraction of Al and Ce during the two cycles can be neglected. The stripping step for this sample is displayed in Table 4.32

Table 4.32 Stripping efficiencies (%) for I95 using Cyphos® 101

Stripping cycle	Stripping agents	Organic phase	Metal recovery (%)				
			Pt	Rh	Al	Ce	Fe
1	HCl	TBP	3	0	0	0	56
2	KSCN	Cyphos® 101, to strip Pt	0	0	0	0	0

The stripping step of this sample also proved to be ineffective. The first cycle only achieved a 56% stripping of Fe from the TBP organic phase, this means that only 4% of the total Fe contained at the beginning was able to be removed from the sample. The second cycle, with the KSCN solution, it showed no interaction with the Cyphos® 101 organic phase, giving zero stripping for all the metals involved; therefore, this organic phase cannot be reused in further extractions because it

contains a high amount of Fe (89% coming from the extraction step), together with a concentration of Pt(IV) that was not able to be removed under the tested conditions.

CONCLUSIONS

5. CONCLUSIONS

The recovery of PGMs from spent automobile catalysts is a complex process. The hydrometallurgical approach offers certain advantages compared with the traditional pyrometallurgical technologies, for example, a considerable reduction of the energy consumption and the elimination of the generation of green-house effect gases; nevertheless, since the hydrometallurgical approach is still at an early development stage it presents several challenges regarding the adaptability and repeatability of the methodologies when working with samples of different metal compositions.

In the case of this work, the methodology implied two stages, a leaching stage and a solvent extraction stage. The leaching methodology developed here proved to be effective for the two different samples treated. After the performance of the planned experiments, the reached conclusions were similar for both catalysts, independently of their metal composition. For H98, time proved to be the determining factor at the moment to acquire satisfactory leaching yields. On the other hand, for I95, the three factors studied, temperature, time and HCl concentration, resulted determinant for satisfactory leaching yields. It is also worth to mention that the leaching kinetics for the two catalyst samples is clearly different, meaning that the reaction rate for I95 is slower than the one for H98. Nevertheless, once the equilibrium has been reached, the leaching yields attained for I95 were higher than the leaching yields for H98. This different behavior, even though the catalysts have similar matrixes and metal compositions, revealed that the transformations occurred during their lifetime can affect significantly their recycling behavior. Generally, it can be stated that the leaching step of this work provided satisfactory results, with 100% Pd(II), 89% Pt(IV) and 72% Rh(III) leached from H98, and 98% Pt(IV) and 96% Rh(III) leached from I95.

During the second stage of the methodology, the solvent extraction step, we acquired very different results when working with model solutions and with the real leaching solutions. The preparation of the model solutions was done following the metal concentrations found in the previous step, but it did only consider the targeted

metals and Al, Ce and Fe as main contaminants; this hypothesis was supported by the XRF results, which showed those metals with higher concentrations than others in the sample. It is possible that this relatively low complexity of the model solutions misleads the results, because the extractants were not interacting with any other metal neither impurity, therefore, they were highly effective and selective towards the PGMs. On the other hand, when working with the real leaching solutions the results were surprisingly worse than expected. The use of TBP to remove Fe as a first step did not work in any of the schemes, and it had a big impact in the sequential cycles that followed, compromising the selectivity and efficiency of the extractants towards the PGMs.

A further investigation about the removal of Fe in the preliminary stage should be considered, this would enhance the extraction and stripping yields in future experiments. As well as in the leaching step, a broader screening of the interactions of the extractants with other metals, even when they are in low concentrations, should be performed, this to guarantee the understanding of how they would behave and their suitability for the real leaching solutions.

In the solvent extraction field, this work represents one of the few and first attempts to work with solutions coming from the leaching of real ACC samples; therefore, the findings of this work should be taken as a possible basis for future research works. The data obtained can provide a preliminary idea about the complexity of dealing with real automobile catalyst samples.

As an overall conclusion, a bigger screening of process variables should be considered as a priority in the continuity of this work.

BIBLIOGRAPHY

6. BIBLIOGRAPHY

Ahmed, I. M., Nayl, A. A., Daoud, J. A. (2011). Extraction of palladium from nitrate solution by CYANEX 471X. *International Journal of Mineral Processing*, *101*, 89–93.

Anastas, P. (2010). Ionic Liquids. In P. W. A. Stark (Ed.), *Green Solvents* (pp. 1–1344). Weinheim, Germany. Retrieved from https://www.wiley.com/en-us/Green+Solvents%2C+3+Volume+Set-p-9783527315741

Atomistry. (n.d.). Platinum Alloys. Retrieved October 31, 2018, from http://platinum.atomistry.com/alloys.html

Autocosmos. (2017). Patente N° 37435, el génesis automovilístico. Retrieved October 13, 2018, from https://noticias.autocosmos.com.ar/2017/02/08/patente-n°-37435-el-genesis-automovilistico

Balance, T. (2017). Platinum Group Metals (PGMs). Retrieved November 9, 2018, from https://www.thebalance.com/platinum-group-metals-pgms-2340166

Baghalha, M., Gh, H.K., Mortaheb, H.R. (2009). Kinetics of platinum extraction from spent reforming catalysts in aqua-regia solutions. *Hydrometallurgy 95*, 247-253.

Basics, A. (2013). How Car Exhaust System Works. US: YouTube. Retrieved from https://www.youtube.com/watch?v=W6dIsC_eGBI

Bombay, I. (2017). IIT Bombay Sophisticated Analytical Instrument Facility. Retrieved December 13, 2018, from http://www.rsic.iitb.ac.in/icp-aes.html

Bonucci, J.A., Parker, P. D., 1984. Recovery of PGM from automobile catalytic converters. In: Kudryk, V., Corrigan, D.A., Liang, W.W. (Eds), Precious Metals: Mining, extraction and processing: Proc. Of Int. Symposium, TMS-AIME, pp. 463481.

Boudesocque, S., Mohamadou, A., Conreux, A., Marin, B., Dupont, L. (2019). The recovery and selective extraction of gold and platinum by novel ionic liquids. *Separation and Purification Technology*, *210*, 824–834.

Chu, H. (2015). Automotive Catalyst (p. 160). Lecture displayed in National University of Tainan, Taiwan. Retrieved November 9, 2018, from http://myweb.ncku.edu.tw/~chuhsin/ppt/Advanced%20Air%20Pollution%20Control%20Engineering/06-Automotive%20Catalyst.ppt

Cieszyñska, A., Regel-rosocka, M., Wisniewski, M. (2007). Extraction of Palladium(II) Ions from Chloride Solutions with Phosphonium Ionic Liquid Cyphos ® IL101. *Polish Journal of Chemical Technology*, *9*(2), 99–101.

Costa, M. C., Almeida, R., Assunção, A., Maria, A., Nogueira, C., Paiva, A. P. (2016). *N,N'*-tetrasubstituted succinamides as new molecules for liquid-liquid extraction of Pt(IV) from chloride media. *Separation and Purification Technology*, 158. 409-416.

Cotton, S. (1997). *Chemistry of Precious Metals* (1st ed.). Netherlands: Springer Netherlands.

Cytec. (2013). Cyanex. Retrieved February 12, 2019, from https://www.solvay.com/en/products/brands/cyanex

Dictionary, C. (2018). What are Hard and Soft Acids and Bases? Retrieved February 12, 2019, from https://www.chemicool.com/definition/hsab.html

DieselNet. (2013a). Emission Standards. Retrieved November 6, 2018, from https://www.dieselnet.com/standards/eu/index.php#vcat

DieselNet. (2013b). Emission Stantards. Retrieved November 1, 2018, from https://www.dieselnet.com/standards/us/ld_ca.php

DieselNet. (2018). Emission Standards. Retrieved November 6, 2018, from https://www.dieselnet.com/standards/eu/ld.php

Duche, S. N., & Dhadke, P. M. (2001). Extraction of Palladium(II) with Cyanex-923 and Cyanex-471X from bromide media and its separation from Pt(IV), Rh(III) and Ir(III). *Journal of the Chinese Chemical Society, 48*, 1115–1122.

European Commission (2017). *Study on the review of the list of Critical Raw Materials*. Brussels. Retrieved January 20, 2019 from https://publications.europa.eu/en/publication-detail/-/publication/08fdab5f-9766-11e7-b92d-01aa75ed71a1

Firmansyah, M. L., Kubota, F., & Goto, M. (2018). Solvent extraction of Pt(IV), Pd(II), and Rh(III) with the ionic liquid trioctyl(dodecyl) phosphonium chloride. *Journal of Chemical Technology and Biotechnology*, *93*(6), 1714-1721.

Fornalczyk, A., Saternus, M. (2009). Removal of platinum group metals from the used auto catalytic converter. *Metalurgija*, *2*, 133–136. Retrieved from http://citeseerx.ist.psu.edu/viewdoc/download?doi=10.1.1.603.2623&rep=rep1&type=pdf

Gao P., Hensley R.I., Zielke, A. (2014). A road map to the future for the auto industry, 13. Retrieved from https://www.mckinsey.com/industries/automotive-and-assembly/our-insights/a-road-map-to-the-future-for-the-auto-industry

Gervasio, A. P. G., Lavorante, A. F., Blassioli-Moraes M.C., Giné, M. F., Saraiva, C. E., Carrilho, E. (2003). Electroforese capilar acoplada á espectrometria com plasmas: uma ferramenta eficiente para a especiação. *Quimica Nova*, *26*(1), 65–74

GROW - Internal Market, D. D. (2017). Communication from the commission to the european parliament, the council, the european economic and social committee and the committee of the regions on the 2017 list of Critical Raw Materials for the EU. Retrieved from https://ec.europa.eu/transparency/regdoc/rep/1/2017/EN/COM-2017-490-F1-EN-MAIN-PART-1.PDF

Gupta, B., Singh, I. (2013). Hydrometallurgy extraction and separation of platinum , palladium and rhodium using Cyanex 923 and their recovery from real samples. *Hydrometallurgy*, *135*, 11–18.

Havlik, T. (2008). *Hydrometallurgy-Principles and Applications* (1st ed.). Woodhead Publishing. Retrieved from https://www.elsevier.com/books/hydrometallurgy/havlik/978-1-84569-407-4

Hepburn, J. S., Patel, K. S., Meneghel, M. G., Gandhi, H. S., Team, E. T. W. C. D., & Team, J. M. T. W. C. D. (1994). Development of Pd-only Three Way Catalyst Technology. *SAE Transactions*, *103*, 727–733. Retrieved from http://www.jstor.org/stable/44612379

Iyer, J. N., Pawar, S. D. (2002). The phosphine oxides Cyanex-921, Cyanex-923 and Cyanex-925 as extractants for Pb(II) from aqueous media. *International Journal of Chemical Technologies*, *9*, 251–255.

Jararifar, D., Daryanavard, M.R., Sheibani, S., (2005) Ultrafast microwave-assisted leaching for recovery of platinum from spent catalyst. *Hydrometallurgy, 78*, 166171.

Jha, M. K., Lee, J. C., Kim, M. S., Jeong, J., Kim, B. S., Kumar, V. (2013). Hydrometallurgical recovery/recycling of platinum by the leaching of spent catalysts: A review. *Hydrometallurgy*, *133*, 22–32.

Leroy, T.; Petit, N. . J. C. G. C. (2007). Three-way catalityc converter. Retrieved October 31, 2018, from https://www.researchgate.net/publication/48416161_Motion_planning_control_of_the_airpath_of_a_SI_engine_with_Valve_Timing_Actuators

Lonmin. (2015). Lonmin. Retrieved November 10, 2018, from http://sd-report.lonmin.com/2015/corporate-profile/

Mason, T. O. (1999). Automotive ceramics. In *ENCYCLOPÆDIA BRITANNICA* (1st ed., p. 3). Encyclopedia Britannica. Retrieved from https://www.britannica.com/technology/automotive-ceramics

Mhaske, A. A., & Dhadke, P. M. (2001). Extraction separation studies of Rh , Pt and Pd using Cyanex 921 in toluene — a possible application to recovery from spent catalysts. *Hydrometallurgy*, *61*, 4–11.

Minerals, J. B.-F. (2016). Cordierite Mineral Data. Retrieved October 20, 2018, from http://webmineral.com/data/Cordierite.shtml#.W9hWOGj7TIV

Mooney, J. J. (2007). The 3-Way Catalytic Converter: a) Invention and Introduction into Commerce - Impacts and Results; b) Barriers Negotiated. In J. J. M. LLC (Ed.), *Chairman Invitational Seminar Series*. California. Retrieved from http://www.arb.ca.gov/research/seminars/mooney/mooney.pdf

Motorfull. (2007). El coche de Leonardo Da Vinci. Retrieved October 12, 2018, from http://motorfull.com/2007/02/el-coche-de-leonardo-da-vinci-1495

Muraki, M., Mitsui, Y. (1986). Method for collecting platinum and palladium from platinum catalyst. Japanese patent: 61110731 A2 (Nippon Magnetic Dressing)

Nesbit, M., Fergusson, M., Colsa, A., Ohlendorf, J., Hayes, C., Paquel, K., Schweitzer, J.-P. (2016). Comparative study on the differences between the EU and US legislation on emissions in the automotive sector. *European Parliament's Comittee*. Retrieved from http://www.europarl.europa.eu/RegData/etudes/STUD/2016/587331/IPOL_STU(2016)587331_EN.pdf

Nguyen, V. T., Lee, J. C., Chagnes, A., Kim, M. S., Jeong, J., & Cote, G. (2016). Highly selective separation of individual platinum group metals (Pd, Pt, Rh) from acidic chloride media using phosphonium-based ionic liquid in aromatic diluent. *RSC Advances*, *6*(67), 62717–62728.

Nogueira, C. A., Paiva, A.P., Oliveira, P.C., Costa, M. C., Rosa da Costa, A. M. (2014). Oxidative leaching process with cupric ion in hydrochloric acid media for recovery of Pd and Rh from spent catalytic converters. *Journal of Hazardous Materials*, *278*, 82–90.

Nriagu, J. O. (1990). The rise and fall of leaded gasolines. *The Science of the Total Environment, 92*, 13–28. Retrieved from http://www.columbia.edu/itc/sipa/envp/louchouarn/courses/env-chem/Pb-Rise&Fall(Nriagu1990).pdf

Paiva, A. P. (2017). Recycling of Palladium from Spent Catalysts Using Solvent Extraction—Some Critical Points. *Metals*, *7*, article 505 (pp 16)

Paiva, A. P., Ortet, O., Carvalho, G. I., Nogueira, C. A. (2017). Recovery of palladium from a spent industrial catalyst through leaching and solvent extraction. *Hydrometallurgy*, *171*, 394–401.

Panda, R., Jha, M. K., & Pathak, D. D. (2018). Commercial processes for the extraction of platinum group metals (PGMs). *Minerals, Metals and Materials Series*, *Part F5*, 119–130.

Papaiconomou, N., Svecova, L., Bonnaud, C., Cathelin, L., Billard, I., Chainet, E. (2015). Possibilities and limitations in separating Pt(IV) from Pd(II) combining imidazolium and phosphonium ionic liquids. *Dalton Transactions*, *44*(46), 20131–20138.

Park, J., Jung, Y., Kusumah, P., Lee, J., Kwon, K., Lee, C. K. (2014). Application of ionic liquids in hydrometallurgy. *International Journal of Molecular Sciences*, *15*(9), 15320–15343.

Peng, Z., Li, Z., Lin, X., Tang, H., Ye, L., Ma, Y., Jiang, T. (2017). Pyrometallurgical Recovery of Platinum Group Metals from Spent Catalysts. *Jom*, *69*(9), 1553–1562.

Regel-rosocka, M., Rzelewska, M., Baczynska, M., Janus, M., Wisniewski, M. (2015). Removal of palladium(II) from aqueous chloride solutions with cyphos phosphonium ionic liquids as metal ion carriers for liquid-liquid extraction and transport across polymer inclusion membranes. *Physicochemical Problems of Mineral Processing*, *51*, 621–631.

Saguru, C., Ndlovu, S., Moropeng, D. (2018). A review of recent studies into hydrometallurgical methods for recovering PGMs from used catalytic converters. *Hydrometallurgy*, *182*, 44–56.

Science, P. (1929). US makes 90 percet of world's automobiles. *US Makes 90 Percet of World's Automobiles*, 84. Retrieved March 4, 2019 from https://www.popsci.com/green-argument-driverless-cars

Shimadzu. (2018). Environmental Solutions. Retrieved March 4, 2019, from https://www.ssi.shimadzu.com/industry/environmental/icp-aes.html

Sigma Aldrich. (2003). CYPHOS® Phosphonium Ionic Liquids. Retrieved February 11, 2019, from https://www.sigmaaldrich.com/technical-documents/articles/chemfiles/cyphos-phosphonium0.html

Sigma Aldrich. (2010). Trioctylphosphine oxide. Retrieved February 12, 2019, from https://www.sigmaaldrich.com/catalog/product/8616?lang=pt&region=PT

Sommer, K. (1986). *Sampling of powders and bulk materials* (1st ed.). Berlin: Springer-Verlag Berlin Heidelberg. https://doi.org/10.1007/978-3-642-82605-4

Sousanis, J. (2011). World Vehicle Population Tops 1 Billion Units. Retrieved October 17, 2018, from https://www.wardsauto.com/news-analysis/world-vehicle-population-tops-1-billion-units

Steinlechner, S., Antrekowitsch, J. (2015). Potential of a Hydrometallurgical Recycling Process for Catalysts to Cover the Demand for Critical Metals, Like PGMs and Cerium. *JOM*, *67*(2), 406–411.

Svecova, L., Papaiconomou, N., Billard, I. (2016). Quantitative extraction of Rh(III) using ionic liquids and its simple separation from Pd(II). *Dalton Transactions*, *45*(38), 15162–15169.

Technology, I. (2018). Particle Size Monitoring. Retrieved November 9, 2018, from https://www.innopharmalabs.com/tech/applications-and-processes/particle-size-monitoring#

Truong, H. T., Lee, M. S. (2018). Separation of Pd(II) and Pt(IV) from hydrochloric acid solutions by solvent extraction with Cyanex 301 and LIX 63. *Minerals Engineering*, *115*, 13–20.

Tyson, D.R., Bautista, R.G. 1987. Leaching kinetics of platinum and palladium from spent automotive catalysts. *Sep. Sci. Technol. 22*, 1149-1167

U.S. Environmental Protection Agency. (1999). The Benefits and Costs of the Clean Air Act 1990 to 2010 - EPA Report to Congress. EPA 410-R-99-001. *Environtal Protection Agency*, *1*, 654.

W.H.O. (2018). World Health Organization. Retrieved November 2, 2018, from http://www.who.int/news-room/fact-sheets/detail/lead-poisoning-and-health

Wei, W., Cho, C., Kim, S., Song, M., Kwame, J., Yun, Y. (2016). Selective recovery of Au(III), Pt(IV), and Pd(II) from aqueous solutions by liquid – liquid extraction using ionic liquid Aliquat-336. *Journal of Molecular Liquids*, *216*, 18–24.

Zhang, C., Huang, K., Yu, P., & Liu, H. (2013). Ionic liquid based three-liquid-phase partitioning and one-step separation of Pt(IV), Pd(II) and Rh(III). *Separation and Purification Technology*, *108*, 166–173.

ANNEXES

ANNEXES

Annex I. Cars and Light-trucks classification inside the EU

The subcategories of the cars and light-trucks classification of the EU in terms of emission of air pollutants is given in Table A1. In terms of this study, only the vehicles classified as M1 are considered.

Table A1. European cars and light-trucks classification

Category	Description
M	Vehicles with at least 4 wheels designed for carrying passengers
M1	Vehicles designed for carrying passengers comprising no more than 8 seats, including the driver's seat.
M2	Vehicles designed for carrying passengers comprising no more than 8 seats, including the driver's seat and not exceeding 5 tonnes in mass
M3	Vehicles designed for carrying passengers comprising more than 8 seats in addition to the driver's seat and exceeding 5 tonnes in mass
N	Motor vehicles with at least 4-wheels designed for the carriage of goods.
N1	Vehicles designed for the carriage of goods and having a mass not exceeding 3.5 tonnes
N2	Vehicles designed for the carriage of goods and having a mass exceeding 3.5 tonnes but less than 12 tonnes
N3	Vehicles designed for the carriage of goods and having a mass exceeding 12 tonnes
O	Trailers (including semi-trailers)
O1	Trailers with a mass not exceeding 0.75 tonnes
O2	Trailers with a mass exceeding 0.75 tonnes but less than 3.5 tonnes
O3	Trailers with a mass exceeding 3.5 tonnes but less than 10 tonnes
O4	Trailers with a mass exceeding 10 tonnes
G*	Off-road vehicles

Annex II. Inductively coupled plasma-atomic emission spectrometry

The ICP-AES technique is a spectrophotometric analysis method, used to determine the concentration of elements in a aqueous sample by analysing the energy emitted at a specific wavelength for the electrons of the chemical element when they return to the basal/ground state after being excited by a high-temperature argon plasma (Bombay, 2017). This energy emission acts as a fingerprint of the element, because it depends directly on the electronic configuration of the atom.

For the analysis, a single wavelength (or a small range of them) is chosen to measure the intensity of the energy emission in the set conditions; this quantity is directly proportional to the concentration of the element in the sample. The determination of the wavelengths and the intensity allows quantifying the concentration of the element by comparing these values to a reference standard.

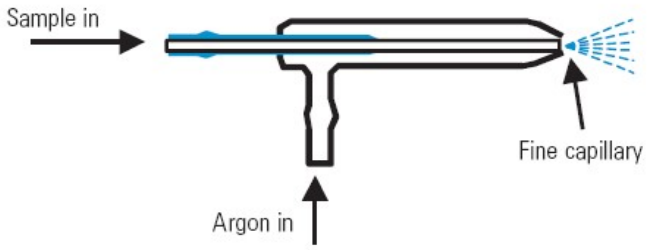

Figure A1. Representation of a nebulizer for ICP tests. Adapted from "Electroforese capilar acoplada á espectrometria com plasmas: uma ferramenta eficiente para a especiação" by Gervasio, A. et. al. 2003.

The methodology of analysis starts with the setting of a liquid sample in a nebulizer to spray it into small and uniform drops that can be transferred to the argon plasma (Figure A1); the nebulizer used will depend on the nature of the sample.

After the nebulization, the sample will enter the spray chamber with the intention to remove the bigger drops and only let the finer drops enter in contact with the plasma. The plasma for this analysis is a defined volume of gas containing argon gas, argon ions, and electrons at an average temperature of 10,000ºC (Shimadzu, 2018). The contact with the plasma will achieve the ionization of the elements in the sample and a determined number of photons will be emitted during this step. The quantification of these photons provides a proportional relationship between photons and the atoms that were contacted with the plasma (concentration of the element).

Plasma torches are usually composed by three different tubes, usually made out of quartz, that are classified as outer tube, middle tube, and sample injector tube. A first stream of argon plasma will pass between the outer and inner tubes and creates a spiral flow, while a second stream of plasma will pass through the middle and

injector tubes to regularize the plasma position towards the injector. The nebulized sample, third stream, will enter in contact with the plasma and the ionization will be carried out. A general representation of this technique is showed in Figure A2.

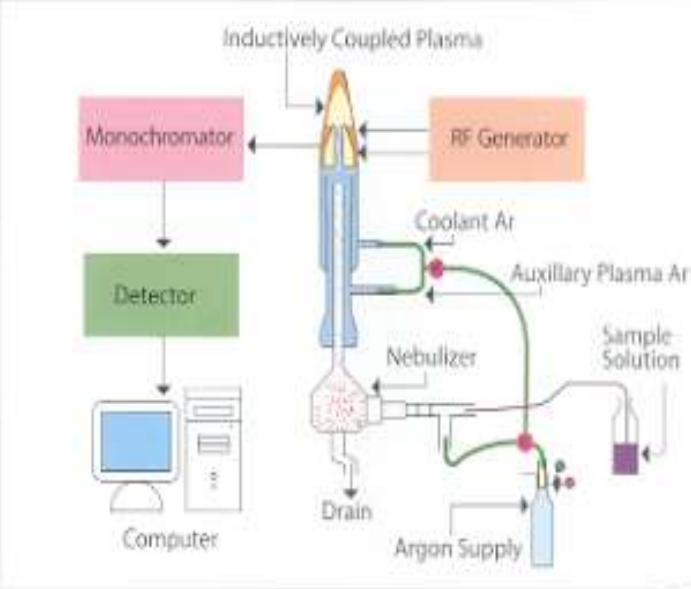

Figure A2. Diagram of an ICP-AES analysis. Adapted from "Electroforese capilar acoplada á espectrometria com plasmas: uma ferramenta eficiente para a especiação" by Gervasio, A. et. al. 2003.

The method described above was used to determine the concentration of metals in the aqueous phase of the leaching experiments, as well as from the solvent extraction experiments. The resulting concentrations set the basis for the calculations of efficiency and selectivity of the methodology developed in the present work.

The values of the limit of detection (LOD) and limit of quantification (LOQ) used in all the ICP analysis are 10 µg/L and 33 µg/L, respectively. With these values the proper calculation of the metal concentration in the samples is assured.

Annex III. Sieving procedure for the particle characterization

Photographs of the sieves taken after 60 min shaking. The particles retained on each sieve can be appreciated, prior to the measurement and determination of the average particle size composition for I95.

Sieve #7 	Sieve #10 	Sieve #14 
Sieve #18 	Sieve #25 	Sieve #35 
Sieve #45 	Sieve #60 	Sieve #80 

Sieve #120	Sieve #170	Sieve #230
		
Sieve #325	**Sieve #330**	
		

Annex IV. Factorial design methodology and ANOVA

A factorial design methodology is an experimental strategy to analyze the relationship between independent variables X_i, known as factors, and the dependent variables, known as responses, *Y.* The mathematical model in its general form has the form of Eq. A1,

$$Y = f(x_1, x_2, \dots, x_i, \dots, x_k,) + \varepsilon \qquad (Eq. A1)$$

where ε is the error of the function and *k* is the number of factors involved. The values of *Y* are called responses, Y_m, where the sub-index *m* indicates each of the experimental conditions evaluated. In the conditions evaluated, the values taken for each factor are called levels, and they assume a high and a low level; with this, the total amount of experiments required, *p*, is given by Eq. A2

$$p = 2^k \qquad (Eq. A2)$$

Eq. A2 points out all the combinations between the factors at the chosen levels. Often, and to simplify the mathematics operations, the use of *codified factors* with unit-values of +1 for the high level and -1 for the low level are used; these factors x_i are defined from the variables V_i through Eq. A3,

$$x_i = \frac{V_i - \frac{V_i^+ + V_i^-}{2}}{\frac{V_i^+ - V_i^-}{2}} \qquad (Eq.A3)$$

where V_i^+ and V_i^- are the high and low levels of V_i, respectively. These experiments are commonly presented in the form of a matrix to facilitate their visualization; the matrix corresponding to the present work, with a 2^3-program implied is presented in Table A2.

Table A2. The matrix of experiments for a 2^3 program

Experiment	Factors x_i and levels			Response Y_m
	x_1	x_2	x_3	
1	-	-	-	Y_1
2	+	-	-	Y_2
3	-	+	-	Y_3
4	+	+	-	Y_4
5	-	-	+	Y_5
6	+	-	+	Y_6
7	-	+	+	Y_7
8	+	+	+	Y_8

The FDM suppose a statistical analysis on the effect of the factors. For this, an estimation of the error should be addressed. Estimating the error can be performed by several ways but the chosen approach in this work was the evaluation of experiments with conditions settled in the central point between the high and low level of the factor, expressed in Eq. A4.

$$V_i^0 = \frac{V_i^+ + V_i^-}{2} \qquad (Eq.A4)$$

The influence of factors over the variables is calculated through the principal effect E(x) as the difference between the mean of Y_m for the high and low level, respectively, as shown in Eq. A5.

$$E(x_i) = \frac{2}{p}\sum_m Y_{m,xi=+1} - \frac{2}{p}\sum_m Y_{m,xi=-1} \qquad (Eq.A5)$$

The application of Eq. A5 to the program of the developed methodology produces equations Eq. A6 to A8:

$$E(x_1) = \frac{1}{4}(Y_2 + Y_4 + Y_6 + Y_8) - \frac{1}{4}(Y_1 + Y_3 + Y_5 + Y_7) \qquad (Eq.A6)$$

$$E(x_2) = \frac{1}{4}(Y_3 + Y_4 + Y_7 + Y_8) - \frac{1}{4}(Y_1 + Y_2 + Y_5 + Y_6) \qquad (Eq.A7)$$

$$E(x_3) = \frac{1}{4}(Y_5 + Y_6 + Y_7 + Y_8) - \frac{1}{4}(Y_1 + Y_2 + Y_3 + Y_4) \qquad (Eq.A8)$$

According to the previous equations, the effects will be positive if the values from the high level of the factor are bigger than the values from the low level of the same factor. Therefore, the effect will be an indication of the direct and individual influence of that factor over the variable of response.

The FDM also provides the evaluation of the interactions between the factors, which are the influence of the variables among each other and help to know when certain factor will affect significantly the value between the levels; these interactions can be calculated through the equation Eq. A9.

$$E(x_i x_j) = \frac{2}{p}\sum_m Y_{m,xi=xj} - \frac{2}{p}\sum_m Y_{m,xi\neq xj} \qquad (Eq.A9)$$

The interaction between factors will result positive when the positive influence of certain factor (x_1) in the response is more accentuated in the high level of another factor (x_2), and it will be negative when the influence of (x_1) is more notorious in the low level of (x_2).

Analysis of Variance

The evaluation of the effects of the factors can be done through a statistical analysis, for which is necessary the analysis of the variance of the factors; for a program of 2^3 and the case of a determined factor (x_1) and its corresponding principal effect E(x_1), the variance represents the dispersion between the mean of the 2 responses for each level of the factor (2 sets of 4 observations each set) and the mean global value of the 8 responses, denominated $\bar{Y}$. The sum of the squares (SS), SS(x) is obtained, after the appropriate mathematical manipulation, with the equation A10.

$$SS(x_i) = \frac{1}{8}\left(\sum_m Y_{m,xi=+1} - \sum_m Y_{m,xi=-1}\right)^2 = \frac{1}{8}(4E(x_i))^2 = 2E(x_i)^2 \qquad (Eq.A10)$$

Eq. A10 provides the relationship between the effect of the variable and the sum of squares and it can be applied for every type of factors (main factors or their interactions). The mean square (MS) or variance of the factor studied will be determined by the product between the SS and the degrees of freedom (DF)

associated. In the case of our study the DF is the unity (corresponding to 2 set of observations, high and low level, therefore DF=2-1=1), leading to Eq. A11.

$$MS(x_i) = SS(x_i) \qquad (Eq.A11)$$

The estimation of the associated error, considering the central points-evaluation approach, will complete the analysis of the variance; n-number of responses will be obtained for Y as $Y_{0j}(j = 1\ to\ n)$, which will lead to the SS and MS of the experimental error, SS_E and MS_E, given by Eq. A12 and A13, respectively.

$$MS_E = \sum_{j=1}^{n} \left(Y_{0,j} - \bar{Y}_0\right)^2, where\ \bar{Y}_0 = \sum_{j=1}^{n} \frac{Y_{0,j}}{n} \qquad (Eq.A12)$$

$$MS_E = \frac{SS_E}{n-1} \qquad (Eq.A13)$$

The evaluation of the variance for the experimental error will validate the significance of the variances associated to the different factors. In fact, this analysis will allow us to know if two independent estimations of variances belong to the same population. When they are significantly different, then the factor will have statistical significance, for this, the Fisher-Snedecor distribution will be applied, with Eq. A14.

$$F_{exp}(x_i) = \frac{MS(x_i)}{MS_E} \qquad (Eq.A14)$$